

University of Massachusetts Medical School

eScholarship@UMMS

GSBS Dissertations and Theses

Graduate School of Biomedical Sciences

2012-06-25


Slow-Cycling Cancer Cells: A Dissertation

Nathan F. Moore

University of Massachusetts Medical School

Let us know how access to this document benefits you.

Follow this and additional works at: https://escholarship.umassmed.edu/gsbs_diss

 Part of the [Cancer Biology Commons](#), [Cells Commons](#), [Neoplasms Commons](#), [Pathological Conditions, Signs and Symptoms Commons](#), [Pharmaceutical Preparations Commons](#), and the [Therapeutics Commons](#)

Repository Citation

Moore NF. (2012). Slow-Cycling Cancer Cells: A Dissertation. GSBS Dissertations and Theses. <https://doi.org/10.13028/0rvq-7r49>. Retrieved from https://escholarship.umassmed.edu/gsbs_diss/620

This material is brought to you by eScholarship@UMMS. It has been accepted for inclusion in GSBS Dissertations and Theses by an authorized administrator of eScholarship@UMMS. For more information, please contact Lisa.Palmer@umassmed.edu.

Slow-cycling Cancer Cells

A Dissertation Presented

By

Nathan F. Moore

Submitted to the Faculty of the
University of Massachusetts Graduate School of Biomedical Sciences, Worcester
in partial fulfillment of the requirements for the degree of

DOCTOR OF PHILOSOPHY

June 25, 2012

Cancer Biology

Slow-cycling Cancer Cells

A Dissertation Presented

By

Nathan F. Moore

The signatures of the Dissertation Defense Committee signifies completion and approval as to the style and content of the Dissertation

Dr. Stephen Lyle, Thesis Advisor

Dr. Junhao Mao

Dr. Leslie Shaw

Dr. Janet Stein

Dr. Sridhar Ramaswamy

The signature of the Chair of the Committee signifies that the written dissertation meets the requirements of the Dissertation Committee

Dr. JeanMarie Houghton, Chair of Committee

The signature of the Dean of the Graduate School of Biomedical Sciences signifies that the student has met all graduation requirements of the school

Anthony Carruthers, Ph.D.,

Cancer Biology
June 25, 2012

Dedication

This thesis is dedicated to my parents Bruce and Sandy Moore and my incredible husband Jay Sage. Mom and Dad, you have been an astounding source of support and love and I would not be writing this thesis without you. Jay, you have been my rock throughout this entire process. I am so glad you are part of my life and I love you so much.

Copyright Notice

Parts of this dissertation have appeared in the following:

Moore, N.F., Houghton, J.M., Lyle, S.R. (2011) Slow-Cycling Therapy Resistant Cancer Cells. *Stem Cells and Development*. Epub ahead of print Nov. 11.

Moore, N.F. and Lyle, S.R. (2012) Quiescent, Slow-Cycling Stem Cell Populations in Cancer: A Review of the Evidence and Discussion of Significance. *Journal of Oncology*. pii396076.

Acknowledgements

I would like to thank my advisor Stephen Lyle. I have grown so much as a scientist over the past five years and it is in no small part to his mentorship. I would also like to thank my committee chair, JeanMarie Houghton, who has always been one of my strongest supporters and a second mentor. Many thanks to my thesis committee: Dr. Junhao Mao, Dr. Leslie Shaw, and Dr. Janet Stein. Without the foundation of their experiences this project would never have progressed beyond its proposal. I would like to give a special thank you to Dr. Sridhar Ramaswamy for participating in my dissertation defense as my external member and taking the time to review my work.

The Lyle lab has been a profound support base for my thesis work. Specifically, I would like to thank Dr. Kyle Draheim for advice and guidance during my early years and Amy Chen for constant support and willingness to help when needed. I would have also never made it through my thesis sane if not for the trouble shooting/venting coffee breaks with Yulian Ellis.

Lastly, I would like to thank my friends and family for helping me become the person I am today. Your love and confidence has gotten me through the dark times and made the good times all that much brighter.

Abstract

Tumor recurrence after chemotherapy is a major cause of patient morbidity and mortality. Recurrences are thought to be due to small subsets of stem-like cancer cells that are able to survive chemotherapy and drive tumor re-growth. A more complete understanding of stem-like cancer cell regulation is required to develop therapies to better target and eliminate these cells.

Slow-cycling stem cells are integral components of adult epithelial tissues and may give rise to cancer stem cell populations that share similar characteristics. These slow-cycling adult stem cells are inherently resistant to traditional forms of chemotherapy and transference of this characteristic may help to explain therapy resistance in cancer stem cell populations. Using a novel application for the proliferation marker CFSE, we have identified populations of slow-cycling cancer cells with tumor initiating capabilities. As predicted, slow-cycling cancer cells exhibit a multi-fold increase in chemotherapy resistance and retain the ability to re-enter the cell cycle. Furthermore, we observed consistent over-expression of the CDK5 activator, p35, in slow-cycling cancer cells. Manipulation of p35 expression in cancer cells affects cell cycle distribution and survival when these cells are treated with traditional forms of chemotherapy. Additionally, we demonstrate that alterations in p35 expression affect BCL2 levels, suggesting a mechanism for the survival phenotype.

Combined, our data suggest a model whereby slow-cycling stem-like cancer cells utilize the p35/CDK5 complex to slow cell cycling speed and promote resistance to chemotherapy. Future p35 targeting, in combination with traditional forms of

chemotherapy, may help eliminate these cells and reduce tumor recurrence rates, increasing long-term patient survival.

Table of Contents

Copyright Notice.....	iv
Acknowledgements.....	v
Abstract.....	vi
Table of Contents.....	viii
List of Figures.....	x
List of Abbreviations.....	xii
Chapter I: Quiescent, Slow-cycling Stem Cell Populations in Cancer.....	1
The Mammalian Cell Cycle and Quiescence.....	1
Adult Stem Cells and Quiescence.....	5
Cancer Induction from Adult Stem Cells.....	12
Quiescence and CSCs.....	17
Quiescence and Resistance to Chemotherapy.....	21
Quiescence Regulators as Potential Therapeutic Targets.....	28
Remaining Questions.....	37
Chapter II: Slow-cycling Therapy Resistant Cancer Cells.....	39
Abstract.....	39
Introduction.....	39
Results.....	41
Discussion.....	56
Chapter III: Regulation of Slow-cycling Cancer Cells by p35.....	62
Abstract.....	62

Introduction.....	62
Results.....	66
Discussion.....	86
Chapter IV: Slow-cycling Cancer Cells and Cancer Stem Cells.....	90
Abstract.....	90
Introduction.....	90
Results.....	94
Discussion.....	102
Chapter V: Discussion and Conclusions.....	109
CFSE Label-retaining Cells.....	110
Slow-cycling Cells and Cancer Stem Cells.....	112
Profiling Slow-cycling Cancer Cells.....	113
Knockdown of p35 in Slow-cycling Cancer Cells.....	114
p35 and the Slow-cycling Cell Phenotype.....	116
p35 and Implications for Metastasis.....	118
Targeting CDKs and p35/CDK5 in Therapeutics.....	119
Conclusions and Model.....	121
Appendix I: BH3 Profiling in Slow-cycling Cancer Cells.....	125
Appendix II: Complete qPCR Array.....	130
Appendix III: Materials and Methods.....	133
Appendix IV: Alternative Experiments and Future Directions.....	140
References.....	143

List of Figures and Tables

Figure 1.1: Mammalian cell cycle.....	2
Figure 1.2: Colon crypt structure.....	9
Figure 1.3: Tissue and tumor cell hierarchy.....	14
Figure 1.4: Cancer stem cells and recurrence.....	24
Table 1.1: Major quiescence regulators.....	33
Figure 2.1: CFSE and label dilution.....	42
Figure 2.2: <i>In vitro</i> identification of label retaining cells.....	45
Figure 2.3: <i>In vivo</i> identification of label retaining cells.....	48
Figure 2.4: Label retaining cells are colony forming and tumorigenic.....	51
Figure 2.5: <i>In vitro</i> label retaining cells demonstrate increase therapy resistance.....	54
Figure 2.6: <i>In vivo</i> label retaining cells demonstrate increased therapy resistance.....	57
Figure 3.1: Identification of slow-cycling cancer cells.....	68
Table 3.1: BCL2 and p35 are up-regulated in slow-cycling cancer cells.....	71
Figure 3.2: p35 slows the cell cycle.....	72
Figure 3.3: p35 regulates chemotherapy resistance.....	75
Figure 3.4: p35 in cancer.....	78
Figure 3.5: p35 target regulation.....	81
Figure 3.6: p35 expression increases post-chemotherapy in rectal cancers.....	84
Table 4.1: Slow-cycling cells are not enriched for CSC mRNA.....	95
Figure 4.1: CSC markers do not enrich for slow-cycling cancer cells.....	97

Figure 4.2: Slow-cycling cancer cells are not enriched in the side population.....	100
Figure 4.3: <i>In vitro</i> slow-cycling cells are sphere forming.....	103
Table 4.2: <i>In vivo</i> limiting dilution analysis.....	105
Figure 5.1: p35 regulation of slow-cycling cells in cancer.....	123
Appendix I Figure 1: BH3 Profiling of slow-cycling cancer cells.....	127
Appendix II: Complete qPCR array.....	130

List of Abbreviations

³ H-TdR	Tritiated thymidine
5-FU	5-Fluorouracil
ALDH	Aldehyde dehydrogenase
AML	Acute myeloid leukemia
APC	Adenomatous polyposis coli
BMP	Bone morphogenic pathway
BrdU	5-bromo-2'-deoxyuridine
CDK	Cyclin-dependent kinase
CFSE	Carboxyfluorescein diacetate succinimidyl ester
CKI	Cyclin-dependent kinase Inhibitor
CSC	Cancer stem cell
DAPI	4',6-diamidino-2-phenylindole
DiI ⁺ /SCC	DiI label-retaining slow-cycling cell
DMSO	Dimethyl sulfoxide
EMT	Epithelial to mesenchymal transition
EpCAM	Epithelial cell adhesion molecule
FACS	Fluorescence activated cell sorting
FOX	Combination of 5-Fluorouracil and Oxaliplatin
FTC	Fumitremorgin C
G1	Gap phase 1
G2	Gap phase 2

H&E	Hematoxylin and eosin
hNMSC	Human normal mammary gland stem cell signature
HSC	Hematopoietic stem cell
IF	Immunofluorescence
IHC	Immunohistochemical
IP	Immunoprecipitation
Lgr5	Leucine-rich G protein coupled receptor
LRC	Label retaining cell
M	Mitosis
Msi1	Musashi-1
Oxali	Oxaliplatin
Rb	Retinoblastoma
S	Synthesis
Sca1	Stem cell antigen-1
shRNA	Small hairpin ribonucleic acid
TA	Transit amplifying
qPCR	Quantitative polymerase chain reaction

Chapter I:

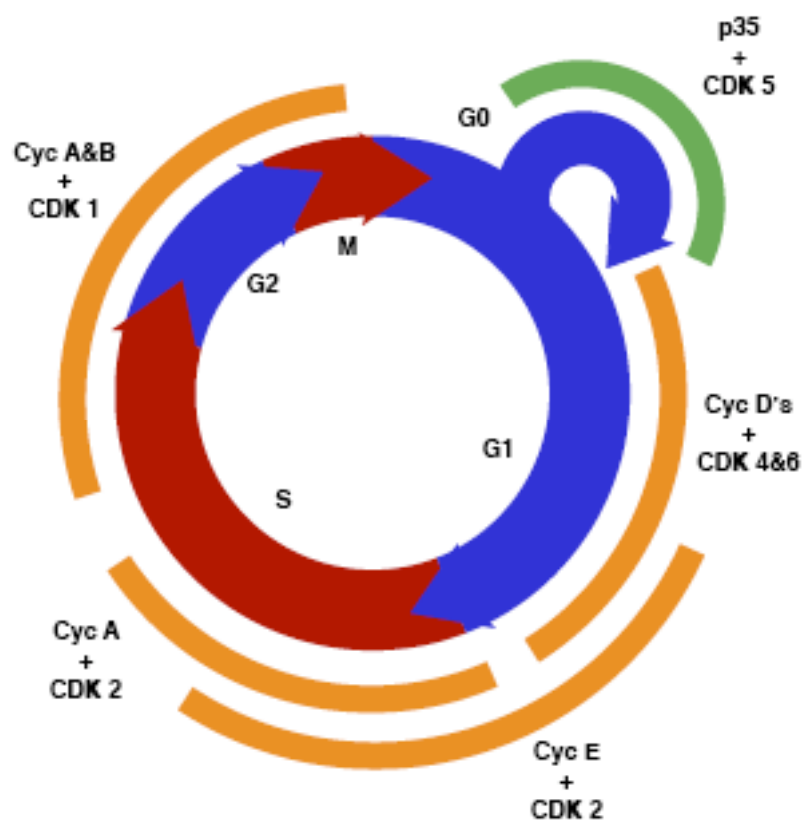
Quiescent, Slow-cycling Stem Cell Populations in Cancer

The Mammalian Cell Cycle and Quiescence

The standard mammalian cell cycle is a tightly controlled process consisting of four major phases: gap 1 (G1), synthesis (S), gap 2 (G2), and mitosis (M) (Figure 1.1). Although thousands of proteins play roles in the cell cycle, the process is primarily regulated by a family of proteins known as the cyclin-dependent kinases (CDKs). Activity of specific CDK family members increases and decreases throughout the cell cycle, phosphorylating proteins that drive major checkpoints of the cell cycle. Activation and context specific activity of the CDK family is dependent on binding to one or more cyclin proteins during the correct phase of the cell cycle. The G1 phase cyclins (cyclin D1, D2, and D3) bind and activate CDKs 4 and 6 in the G1 phase. During this phase, cells begin to increase in size, protein mass, and organelles in preparation for division. Importantly, G1 is also a time for monitoring both external and internal signaling, ensuring proper conditions for cell division (1). When both external and internal signals are appropriate, the cyclin D/CDK4 complex helps initiate activation of the G1/S cyclin E complex, which binds CDK2, allowing for the phosphorylation of the Retinoblastoma (Rb) family of proteins (2). Phosphorylation of Rb deactivates the protein, freeing the cell cycle driver E2F to push cells through the first major regulatory checkpoint known as “Start.” After passing “Start,” a cell becomes committed to completion of the cell cycle and enters S phase, where DNA is duplicated. The S phase

Figure 1.1: Mammalian cell cycle

The cell cycle consists of four major phases: Gap phase 1 (G1), Synthesis (S), Gap phase 2 (G2), and Mitosis (M). Driving progression through these phases are cyclin dependent kinases (CDKs) whose activity is regulated by binding of specific cyclin activators (Cyc). During G1, CDKs 4 and 6 bind Cyc D family members to regulate cell growth and organelle expansion. Transition into S is controlled by the Cyc E and CDK2 complex. S phase is further regulated and sustained by Cyc A binding CDK2. Finally, cells are driven through G2 and M by CDK1 activated by either Cyc A or Cyc B. Stem cell populations temporarily exit the cell cycle into G0. Maintenance and re-entry from G0 is regulated by CDK5 binding its cyclin-like activator p35.



cyclin A binds CDKs 1 or 2 to drive the cell through both S and G2 phases. The G2 phase is an additional time for cell growth and serves as a pause prior to commitment to mitosis, a second major regulatory step (3). The G2/M checkpoint ensures faithful DNA replication and a continued favorable division environment. Finally, the M phase cyclin B binds and activates CDK1, phosphorylating different targets from the cyclin A/CDK1 complex, pushing the cell through the G2/M checkpoint and into mitosis. During the tightly regulated M phase, duplicate chromosomes are segregated and the cytoplasm is divided, completing the formation of two daughter cells.

Not all cells continuously progress through the cell cycle, but instead, may exit the cycle in a state termed G₀ or quiescence. Quiescence is generally achieved through the activity of cyclin dependent kinase inhibitors (CKIs) that primarily block binding of cyclin proteins to CDKs. The INK4/ARF CKI family of proteins (p16, p18, and p19) target CDK4/6, leading to G₁ stage arrest while the Cip/Kip CKI family of proteins (p21, p27, and p57) targets G₁/S phase complexes, leading to late stage G₁, S, and potentially G₂/M arrests (4). In healthy adult tissues, the Cip/Kip family members p21, p27, p57 likely play an important role in controlling self-renewal of neural and hematopoietic stem and progenitor cells (5-7), while INK4/ARF family members may control brain, lung, and pancreatic stem cell proliferation (8-10). These data suggest an important role for quiescence in adult tissue homeostasis and stem cell populations.

Interestingly, the CDK family member, CDK5, may play an important role in the maintenance of cell cycle arrest. Like other CDK family members, CDK5 requires the presence of one of its cyclin-like binding partners (p35 or p39) for activation (11). Little

is known about the functional differences between p35 and p39, but knock out studies in mice suggest at least some functionally independent roles for the two activators (12). The best studied of the two activators, p35, has no sequence homology with the cyclin family, but does appear to share structural homology and is believed to function in a similar manner (13). The activity level and target specificity of CDK5 is dependent on binding either a 35 kD form of p35 or a more stable, highly active 25 kD form. In some cases, binding the 35 kD form may have important differences in functional implications for CDK5 apart from binding the 25 kD form (14). Unlike other CDK family members, the p35/CDK5 complex has no known role in driving the cell cycle forward, but may instead function in tandem with CKIs to block progression of the cell cycle. In the context of developing neurons, p35/CDK5 has been demonstrated to bind to and translocate with p27 into the nucleus where they work in tandem to inhibit cell cycle progression (15). Additionally, loss of p35 has been demonstrated to decrease cell cycle exit in osteosarcoma cells induced to express p16, suggesting a cooperative role between the two proteins (16).

Adult Stem Cells and Quiescence

In tissues like those of the intestine and skin, new cells are continuously required to replace those that are lost to the environment. To facilitate this constant need for new cells, some epithelial tissues are arranged hierarchically with slowly proliferating stem cells that asymmetrically divide to give rise to a new stem cell and a rapidly dividing cell called a transit amplifying (TA) cell (17). TA cells proliferate quickly for a limited

number of divisions, allowing for the high degree of cell proliferation necessary to sustain adult tissues. Adult stem cells are also critical for continued normal tissue homeostasis and in response to wounding for many of the epithelial tissues of the body. Adult stem cells are characterized by their ability to self-renew indefinitely and produce progeny capable of differentiating and repopulating tissue specific lineages (18). Populations of adult stem cells have been identified in tissues throughout the body, including the skin (19-21), mammary glands (22, 23), intestine (24, 25), prostate (26), brain (27), and the hematopoietic system (28, 29). Infrequent division or a quiescent nature is not definitive for adult stem cells, but is suggested to be important for maintenance of many adult stem cell pools. Evidence suggests that quiescence may play an important role in protecting stem cells from exhausting their proliferative capacity, inhibiting differentiation, and limiting accumulation of mutations which may occur during frequent rounds of DNA synthesis (30-32).

Initial efforts to identify and study adult stem cells took advantage of the slow-cycling nature of stem cell populations in studies employing pulse/chase methodology (19, 24). In these studies, DNA in cells was labeled with either tritiated thymidine (^3H -TdR) or 5-bromo-2'-deoxy-uridine (BrdU), repeatedly administered to mice or cultured cells. DNA labeling was followed by a chase period, in which rapidly proliferating TA cells divided the label between daughter cells, consequently diluting the label. In contrast, slow-cycling stem cells underwent fewer divisions and retained detectable quantities of label for much longer periods of time. Cotsarelis *et al.* demonstrated that label retaining cells (LRCs) were exclusively present in the stem cell niche of the mouse

hair follicle known as the “bulge”, located adjacent to the hair follicle and just below the epidermis (19). These cells were found to be relatively stem-like: “primitive” in cytoplasmic contents, structurally similar to other putative stem cell populations, and able to be stimulated to proliferate. Cells present in the bulge region have been experimentally shown to be quiescent for up to 1 year (33), and based on the hair growth cycle of scalp skin can likely remain quiescent for up to 5 years. Under correct stimulation, bulge cells from human skin can differentiate into epidermal, sebaceous and hair follicle lineages *in vitro* (34). These experiments demonstrate the important link between stem cell populations and the slow-cycling phenotype.

Although likely important for the maintenance of the stem cell pool, quiescence may not be a requirement for adult stem cells. Using a *lacZ* construct under a conditional promoter for the stem cell associated protein leucine-rich G protein- coupled receptor 5 (Lgr5), Jaks *et al.* demonstrated a distinct non-label retaining subpopulation of bulge cells that overlap with the CD34⁺/K15⁺ stem cell population at the resting stage (telogen) but not the growth phase (anagen) of the hair growth cycle (35). Lineage tracing techniques confirmed that Lgr5⁺ cells actively cycled during normal homeostasis and had a multipotent phenotype. Jaks *et al.* suggest that the Lgr5⁺ population of cells represents a cycling population of stem cells under normal conditions, whereas the label retaining CD34⁺/K15⁺ stem cells may represent a reserve population that is activated after tissue damage. As yet, a conclusive relationship between these two populations cannot be firmly established.

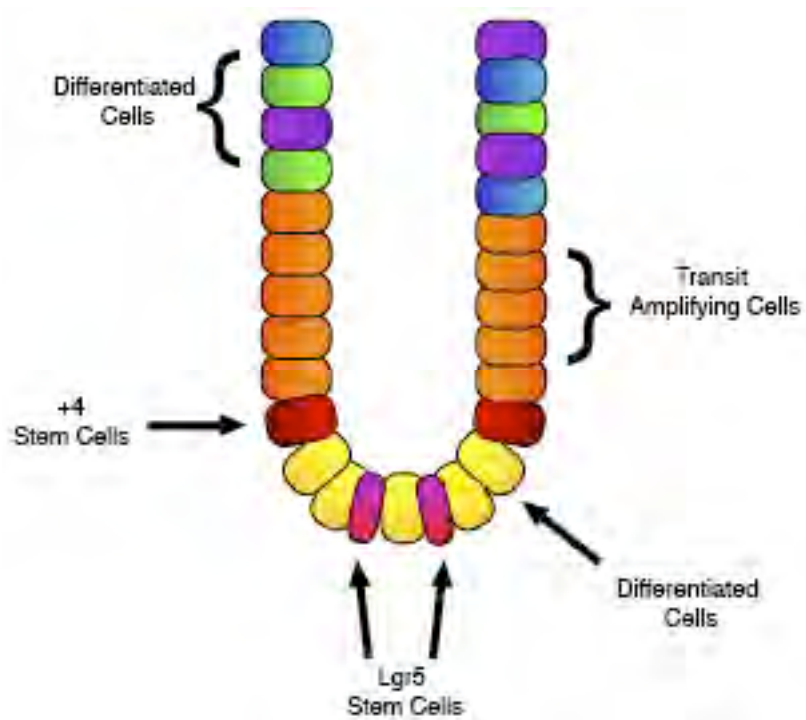
Similar label-retaining methods have been used to study slow-cycling cells in other tissues, such as the small intestine and colon. Work conducted by Potten and colleagues identified slow-cycling LRCs at the +4 position of the colon crypt. These crypt base cells were found to be maintained in a steady state of between four and six cells that go through division approximately once a week (36). Upon irradiation, these cells demonstrated increased expression of the anti-apoptotic protein BCL2, decreased expression of the cell-survival regulator p53, and high activation and involvement in clonogenic regeneration of the crypt, suggesting a stem cell phenotype of crypt base cells. Two additional studies involving the putative stem cell associated RNA binding protein Musashi-1 (Msi1) again demonstrated a link between slow-cycling cells and the stem cell phenotype through co-localization of Msi1 with colon LRCs (37, 38).

From the evidence collected in these studies and others, a model has been proposed in which slow-cycling stem cells, found at the base of the crypt, undergo periodic division to give rise to TA cells (Figure 1.2). TA cells low in the crypt undergo rapid division and eventually lose replicative potential and differentiate as they progress up the crypt. These cells are ultimately lost to the environment (36, 39).

As within the hair follicle, there is convincing evidence for an Lgr5⁺ non-label retaining population of colon stem cells additionally found at the base of the crypt (25). While the LRCs reside at the +4 population, Lgr5 cells are observed as slender wedge shaped cells at the +2 position. Again, the exact relationship between the LRCs and the Lgr5⁺ cells is yet to be fully explored and more data into the lineage potential of both of these cell populations is needed to form a cohesive model.

Figure 1.2: Colon crypt structure

The colon is organized into crypt structures arranged hierarchically. Two stem cell populations, Lrg5 cells at the base (pink) and cells at the +4 position (red), asymmetrically divide to self-renew and produce transit amplifying cells (orange). Located just up the crypt from the stem cells, transit amplifying cells rapidly proliferate to replace cells that are constantly lost to the environment at the top of the crypt. As transit amplifying cells move up the crypt, they differentiate into cell types that take up nutrients, support stem cells, and protect against infection (blue, green, purple, and yellow).



Since the early identification of colon and hair follicle slow-cycling stem cell populations, label-retaining techniques have been used to identify and validate putative stem cell populations in multiple epithelial tissues. In the mammary gland, three separate label-retaining populations have been identified and proposed as possible stem cells. In a study conducted by Welm *et al.*, BrdU LRCs were stem cell antigen-1 positive (Sca1⁺) and enriched for the ability to form both ductal and alveolar cell types (22). In contrast, Shackleton *et al.* identified a BrdU LRC population that was hematopoietic lineage negative and enriched by the marker combination CD29^{hi}CD24⁺ that did not enrich for the Sca1⁺ cells (23). Pece *et al.* used the lipophilic fluorescent dye PKH26 to identify a population of mammary LRCs that demonstrated increased *in vitro* sphere formation efficiency (40). Pece *et al.* used this LRC population to create a human normal mammary gland stem cell signature (hNMSC) consisting of the markers CD49F/DNER/DLL1. These findings may suggest a stem cell hierarchy in which multiple layers of stem cells exist within the mammary gland (41).

In the brain, quiescent cells were able to generate spheres *in vitro* or repopulate the proliferating population *in vivo*, suggesting a stem cell phenotype for these quiescent cells (42). Prostate slow-cycling LRCs located in the proximal ducts demonstrated high proliferative potential and the ability to reconstitute the prostate glandular structure *in vitro*. This ability singles them out as stem cells over more rapidly cycling TA cells located at the distal region of the ducts (43). Finally in the pancreas, characterization of

LRCs around the acini and ducts suggested a stem cell population by demonstrating increased activation in response to damage to form duct-like structures (44).

Combined, these studies demonstrate an important pattern of tissue organization that appears to maintain slow-cycling cells in multiple epithelial tissues. Importantly, the existence of slow-cycling cell populations is linked with the stem cell phenotype.

Cancer Induction from Adult Stem Cells

In the United States, half of all men and a third of women will develop cancer over their lifetime (45). Cancer is essentially a disease of uncontrolled cell growth. Unlike healthy cells, cancer cells bypass death signals and continue to grow, potentially spreading from the tissue of origin to other tissues throughout the body through a process called metastasis. As tumors grow, they disrupt normal tissue function, taking up valuable space and nutrients. Traditional chemotherapeutic treatments of cancer rely on cytotoxic compounds that damage DNA during cell growth, preferentially targeting rapidly proliferating cells with the intention of inducing cell death. In colorectal cancers and other epithelial tumors, as many as 75% of late stage tumors will become resistant to traditional chemotherapies (46). Surviving tumor cells lead to recurrence of tumors that are often more aggressive. Ultimately, tumor cells prevent the healthy organs from functioning and kill the patient.

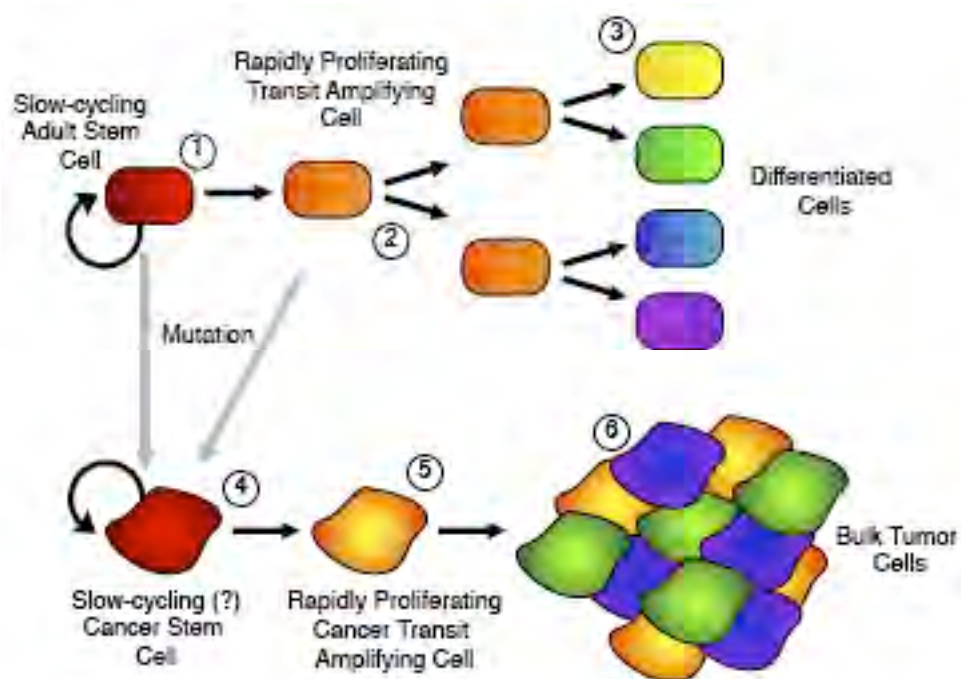
The development of cancer is a complex multi-step process that requires the accumulation of mutations resulting in a cell acquiring the essential hallmarks of cancer: evasion of apoptosis, self-sufficiency in growth signals, insensitivity to anti-growth

signals, invasive and metastatic abilities, limitless replicative potential, and sustained angiogenesis (47). Over years or decades, long-lived stem cells have the opportunity to accumulate oncogenic mutations from common mutagenic sources like inflammation, radiation, chemicals, or infection (48, 49). Combined with inherent limitless replicative potential, it is hypothesized that mutated adult stem cells are transformed into the cells of origin for many cancers (Figure 1.3) (50, 51). Like healthy adult stem cells, transformed stem cells are expected to be able to generate a form of TA cell that unlike healthy TA cells, would be oncogenic and capable of driving tumor heterogeneity (18, 39). Transformed stem cells have been termed cancer stem cells (CSCs) and are defined as the fraction of cells within a tumor that are long lived, possess the potential to proliferate indefinitely, and can generate the heterogeneity of the original tumor (39, 52). CSCs are expected to utilize characteristics commonly found in stem cell populations such as differential metabolic activity, specific signaling pathway activity, and regulation of cell cycling characteristics, albeit with aberrant regulation (18, 53). Importantly, CSCs that survive chemotherapy treatment could account for tumor recurrence as a result of reactivation of proliferation in surviving CSCs (54). Traditional chemotherapy regimes target proliferating cells, potentially missing slower dividing CSCs that must be eradicated to provide long-term disease-free survival (55). A better understanding of CSCs is essential in understanding the biological and clinical consequences of existing regimens and designing new therapies to improve patient outcome (53).

Current methods for isolation and study of CSCs rely on cell surface markers found to be enriched in populations with stem cell-like properties. This technique was

Figure 1.3: Tissue and tumor cell hierarchy

Adult epithelial tissues are organized hierarchically, with slow-cycling stem cell populations located at the top (1). Stem cells asymmetrically divide to give rise to a new stem cell and a rapidly dividing transit amplifying cell. Transit amplifying cells undergo rapid proliferation, required to replace cells that are lost to the environment (2). Transit amplifying cells eventually differentiate into the multiple lineages of the adult tissue (3). Cancer stem cell populations are derived from adult stem cell or early transit amplifying cells that acquire oncogenic mutations over the life of an individual (4). These cancer stem cells likely maintain the slow-cycling phenotype of their adult tissue counterparts and produce rapidly proliferating oncogenic transit amplifying cells that drive tumor growth (5). Tumor transit amplifying cells differentiate into the heterogeneous tumor cells identified in epithelial tumors (6).



first used by Bonnet and Dick in 1997 when they demonstrated that only cells positive for the membrane protein CD34 and negative for the membrane protein CD38 were capable of initiating human acute myeloid leukemia (AML) in immune compromised mouse models (56). Since the work of these two pioneers, CSC populations have been identified in multiple epithelial cancers including the breast (52), prostate (57), pancreas (58), colon (59-61), ovaries (62), and brain (63).

Unfortunately, the use of CSC markers has not been without controversy. One issue centers on inconsistencies and uncertainty of the functional implications of CSC markers. This uncertainty is best exemplified by the use of the stem cell associated membrane protein CD133 in the identification of colon CSCs. Shortly after Ricci-Vitiani *et al.* (2007) demonstrated the use of CD133 to identify CSCs in colon tumors, Shmelkov *et al.* demonstrated that CD133 expression was not restricted to colon CSCs, but that CD133 is expressed on differentiated colonic epithelium in both mice and humans (60, 64). These data suggest CD133 expressing cancer cells may not all be stem-like. Reasons behind these contradictions were explored by Kemper *et al.* who methodically evaluated the differing epitope between the CD133 antibodies used by both groups. Kemper *et al.* reached the conclusion that the CD133 antibody used by Ricci-Vitiani *et al.* recognized a differentially expressed form of CD133 protein (termed AC133) that is not recognized by the antibody used by Shmelkov *et al.* (65). It appears that CD133 protein is expressed in all colon epithelium, but the CD133 antibody used by Ricci-Vitiani *et al.* identifies an undetermined modification of the CD133 protein, specific for the CSC phenotype. Furthermore, Kemper *et al.* were unable to determine the functional

significance of the differentially modified isoforms of CD133, highlighting the disconnection between marker status and functional implication. Very little is known about the function of many of the proposed CSC markers, while even less is understood about how these relate to the CSC phenotype. CD133 is implicated in pluripotency and differentiation, suggesting it may somehow regulate cancer differentiation (66). Other proposed CSC markers like CD44 and aldehyde dehydrogenase (ALDH) are linked with apoptosis resistance and chemoresistance and are less clearly related to the CSC phenotype. At best, markers must be viewed as only tools for stem cell enrichment, suggesting the need for a more functionally significant means of CSC identification (67). Given the similarities between normal adult stem cells and CSCs, regulation of self-renewal and cycling speed is likely central to CSC pathology (53, 54). Targeting pathways that mediate stem cell quiescence is therefore an intriguing alternate method for functional identification of CSC populations.

Quiescence and CSCs

If CSCs do originate from normal adult stem cells, then it is foreseeable that key stem cell regulatory traits are retained through the oncogenic transition; quiescence is potentially one of these traits. Little research has been done to address how quiescence might play a role in CSC biology, but there are some indications that quiescent stem-like populations might contribute to tumor development. In primary ovarian tumors, Gao *et al.* demonstrated that slow-cycling cells expressed stem cell-associated genes like *nestin*, *oct4*, and both *notch1* and *notch4* (62). Low numbers of slowly proliferating cells were

shown to produce tumors in a xenograft model where bulk cells were found to be non-tumorigenic. These data implicate a link between quiescence and ovarian tumor CSCs.

Pece and colleagues also observed a link between CSCs and quiescence in breast tumors (40). Using the hNMSC signature associated with normal slow-cycling mammary cells discussed earlier, Pece *et al.* turned their attention to the analysis of primary breast tumors. They found that the hNMSC signature was more commonly found in grade 3 tumors over that of grade 1. When grade 1 and grade 3 mammospheres were analyzed for PKH26 label retaining cells, both populations were found to retain label, with grade 3 tumors demonstrating a higher percentage. These data suggest an increase in slow-cycling stem-like cells as tumors progress. When evaluated for tumorigenicity, breast tumor cells positive for the hNMSC signature were more efficient at forming *in vitro* spheres and *in vivo* xenograft tumors than those cells lacking the hNMSC signature.

Cultured cancer cell lines are often used to study signaling pathways, invasion, migration and apoptosis, but are rarely thought of as candidates for CSC studies. Many of the most widely used cell lines have been in passage for years, are perceived to be homogeneous, and change characteristics based on alterations in culture conditions. Therefore, cultured cell line studies assessing CSC characteristics must be evaluated critically, data interpreted within the context of the experimental parameters, and results confirmed under biologically relevant conditions. Still, interesting work in the cultured breast tumor lines like MCF10A, MCF7, SUM149, SUM159, SUM1315 and MDA.MB.231 suggests that these lines may not be as homogenous as once thought. Cells expressing the marker combination $CD44^+/CD24^-/ESA^+$ within these lines were

found to contain the ability to self-renew, to reconstitute the parental line, and to be up to 90% label retaining (68). Additionally, the $CD44^+/CD24^-/ESA^+$ cells within these cultures were found to consistently produce tumors with as few as 1,000 cells, compared to unsorted cell lines that only consistently produced tumors with ten times as many cells. While these data appear to support a CSC phenotype, other researchers have demonstrated that single cell cloning some of these cell lines resulted in varied metastatic potential and protein expression within clone outgrowths, suggesting that tumor propagating cells within these cell lines may not be uniform in outgrowth potential (69, 70). Combined, these data suggest that while tumor-initiating potential may be restricted to a subset of cells, the tumor propagating phenotype may not be the result of a single CSC population atop a tumor cell hierarchy. Future work will need to determine if these differences are the result of a single population responding to stimuli in multiple ways, or truly different cell types. Importantly, these data demonstrate that popular cell lines are not homogeneous and add validity to future study of quiescent cells and their relationship to potential CSCs within these lines.

Additional connections between quiescence and CSCs was explored in the work conducted by Roesch *et al.* in melanoma (71). This group found that primary melanoma cell lines contained a PKH26 label retaining population that was almost specifically identified by the H3K4 demethylase JARID1B. This population of cells was found to incorporate BrdU more slowly, retain it for a longer period of time, lack staining for the proliferation marker Ki67, and have a doubling time of up to 4 weeks *in vitro*. When EGFP was placed under the control of the JARID1B promoter, GFP^+ cells demonstrated

increased sphere forming ability *in vitro*, suggesting increased CSC properties within these cells. Interestingly, *in vivo* GFP⁺ cells did not show increased tumor initiating abilities over GFP⁻ cells. These contrasting data highlight disparities between *in vitro* and *in vivo* culture systems and their ability to conclusively delineate the CSC phenotype. While these data may indicate that quiescent cells within an *in vivo* environment may not be enriched for the CSC phenotype, it is also possible that Roesch and colleagues are correct when they propose that the xenograft growth assays may better measure reaction to host-derived environments and the loss of tumor growth rather than tumor initiation potential.

The most direct evidence to date for quiescence playing a role in CSCs came from a study conducted by Dembinski and Krauss (72). In this study Vybrant[®] DiI cell-labeling solution was used to label pancreatic adenocarcinoma cells and conduct cancer stem cell studies on label-retaining cells that had been sorted by flow cytometry. DiI label-retaining slow-cycling cells (DiI⁺/SCCs) comprised ~3% of total cell number. Interestingly, LRCs also exhibited an elongated fibroblast shape and an increase in the epithelial-mesenchymal transition (EMT) markers vimentin, snail, and twist. A fibroblast-like CSC is consistent with evidence demonstrating an increase in stem-like properties in cells that have undergone an EMT (73). Importantly, this EMT has implications for progression towards metastatic abilities, allowing for tumor cell dissemination throughout the body. Furthermore, sorted DiI⁺/SCCs demonstrated a 2.5-10-fold increase in soft agar colony forming ability, two-fold increase in invasive potential, and more than a ten-fold increase in xenograft formation over non-label

retaining cells. Combined, these data suggest that DiI⁺/SCCs represent an enriched slow-cycling CSC population. When assessed for common CSC marker status, DiI⁺/SCCs only partially overlapped with CD24⁺/CD44⁺ and CD133⁺ populations. These data suggest the slow-cycling phenotype may not be associated with traditional CSC markers and highlight the critical importance for functional identification and characterization.

Like the melanoma study by Roesch *et al.* (71), Dembinski and Krauss's study also indicated the ability for LRCs to produce non-LRCs and surprisingly also for non-LRCs to produce LRCs, suggesting two possibilities: 1) that the true unknown CSC population is favored in the LRCs, but also found in the non-LRCs and can therefore give rise to both populations, or 2) that there exists a dynamic relationship in LRC-CSC populations that is context dependent and allows for inter-conversion between the two states. The Dembinski and Krauss study argues a dynamic population of CSCs that might coincide with an EMT. EMT plays a central role in embryogenesis and mesoderm differentiation into multiple tissue types during development while also having important implications for metastasis in the cancer setting (73). The emergence of embryonic stem cell-associated genes like *nanog*, *oct4*, *sox2*, and *c-myc* in high grade undifferentiated cancers suggests that aberrant regulation of EMT and other early development pathways might be playing a role in CSC characteristics (74). These data provide further evidence to support a dynamic slow-cycling stem-like model for many types of cancer.

Quiescence and Resistance to Chemotherapy

Tumors from different patients in the same organ are likely to have undergone different oncogenic transitions, leading to a diversity of possible regulatory mechanisms and pathway activities that might be contributing to the survival of a specific cancer. While broad patterns like the dysregulation of the stem-cell associated Wnt pathway in colon carcinomas are commonly observed, the secondary mutations that may accompany these cancers could be vastly different and contribute to survival in different ways (75). Even within the same tumor, different CSCs accumulate unique mutations that provide added resistance to chemotherapy, and pass these mutations on to daughter cells. Considering the vast differences in tumorigenesis and heterogeneity within a tumor, it is not surprising that the exact contributors to chemotherapy resistance and consequently which patients will respond optimally to chemotherapy are not well understood. It has been proposed that variations in cell cycle-control, anti-apoptotic proteins, increased DNA damage repair capacity, up-regulation of cellular pumps, and increased metabolic activity may all play important roles in chemotherapy resistance (39, 76-79).

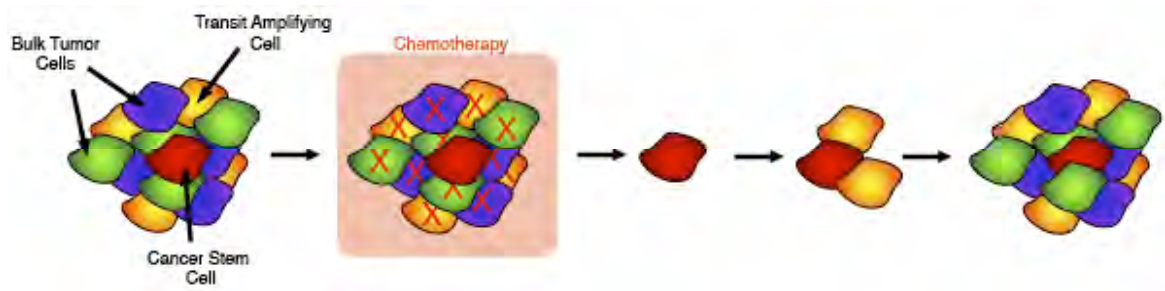
Conventional chemotherapies and radiotherapies target proliferating cells and require active cycling for induction of apoptosis. The slow-cycling nature of many adult stem cell pools is therefore an inherent mechanism for resistance and cell survival in response to conventional therapies. In the hematopoietic system, normal hematopoietic stem cells (HSCs) contain high levels of the CKI p21 (5). When treated with the commonly used pyrimidine synthesis inhibitor 5-fluorouracil (5-FU), mice that were p21 deficient had a significant decrease in cobblestone area-forming stem cells compared to normal p21 expressing wild type mice. In the brain, Morshead *et al.* demonstrated that

high doses of tritiated thymidine ($^3\text{H-TdR}$) killed the constitutively proliferating cells in the adult mouse forebrain, but had no effect on quiescent stem cell ability to survive and generate spheres when plated *in vitro* following treatment (42). These data support a model in which slow-cycling mouse forebrain stem cells are able to survive and re-enter the cell cycle to allow for regeneration of the damaged tissue. A similar pattern of stem cell survival and regeneration was observed following treatment with the DNA intercalator doxorubicin in mouse intestine. In this experiment, mice epithelial intestinal crypts demonstrated increased amounts of cell death via apoptosis in the +3-6 positions stem cell compartment and a parallel disappearance of mitotic activity (80). This period of relatively non-existent mitotic activity was followed by stem cell re-entry into the cell cycle and tissue regeneration in the stem cell compartment. Furthermore, colon stem cell survival during chemotherapy is aided by increased expression of BCL2 family members that inhibit apoptosis (81). In chemotherapy-induced alopecia, the rapidly dividing TA cells in the hair matrix undergo apoptosis, while the stem cells in the bulge region survive to regenerate the follicle after chemotherapy is withdrawn. These data suggest a relationship between slow-cycling cell populations and the resistance phenotype.

Similar mechanisms for survival and self-renewal for CSCs are plausible in instances of tumor recurrence in human patients where cytotoxic agents kill proliferative cancer cells, leaving slow-cycling cells (39). CSCs that survive chemotherapy would have the ability to re-enter the cell cycle and produce highly proliferative, rapidly dividing progenitor cells that can re-establish the tumor (Figure 1.4). It is probable that successive cycles of chemotherapy would further promote tumor progression by inducing

Figure 1.4: Cancer stem cells and recurrence

Epithelial tumors are believed to be hierarchically arranged with slow-cycling stem-like cell populations (red), rapidly proliferating transit amplifying cells (yellow), and more differentiated bulk tumor cells (blue and green). Traditional forms of chemotherapy preferentially proliferating tumor cells, killing transit amplifying cells and more differentiated cells while leaving stem-like cell populations alone. At the cessation of chemotherapy treatment, stem-like cells re-enter the cell cycle and produce transit amplifying cells that continue to divide and differentiate, leading to tumor recurrence.



further mutation and eliminating lesser resistant adult stem cells, thereby creating the opportunity for transformation into therapy resistant CSCs that give rise to resistant offspring (53).

CSC populations in the colon, breast, ovaries, and pancreas have been shown to demonstrate the ability to survive double the level of therapies that kill rapidly proliferating bulk tumor cells (62, 72, 79, 82). These data demonstrate how ineffective conventional therapies can be on slow-cycling cell populations and help to explain why tumors that seem to fully regress during treatment can recur. Furthermore, they suggest a model in which single CSCs, undetectable with current diagnostic technology, survive chemotherapy or radiation and are able to re-enter the cell cycle and re-establish tumors (68, 83). Even more devastating to the survival of patients may be the CSC response to stress from chemotherapy and radiotherapy. Mouse ovarian CSCs have been demonstrated to undergo symmetric division during radiotherapy regimens, expanding the CSC pool and driving development of a more aggressive secondary tumor (84). Furthermore, these CSCs may be positively selected to produce chemotherapy resistant offspring, rendering the tumor unaffected by later rounds of treatment.

While quiescence is likely to contribute to the survival of CSCs in response to chemotherapy and radiation, slow cycling is likely to work in parallel with other systems to increase survival. $Msi1^+$ colon cancer cells are less sensitive to cytotoxic drugs due to increased expression and orchestration of anti-apoptotic mechanisms (85). The expression of anti-apoptotic BCL2 family members is frequently seen in stem cell and CSC populations and contribute to cell survival during radiation and chemotherapy (76,

77). BCL2 family members are divided into three groups: the multi-domain pro-apoptotic group, the pro-apoptotic BH3-only group, and the anti-apoptotic group. The multi-domain pro-apoptotic group (BAX and BAK) is localized to the mitochondrial membrane and contains three conserved α -helical domains (BH1, BH2, BH3) (86). In response to death stimuli, these family members oligomerize and form pores that release pro-apoptotic factors like cytochrome c from the mitochondrial intermembrane space, driving apoptosis (87). The anti-apoptotic group (Bcl-2, Bcl-X, Bcl-w) is also primarily localized to the mitochondrial membrane and contains an additional conserved α -helical domain (BH4) (86). These anti-apoptotic family members inhibit apoptosis in response to cytotoxic insults by sequestering BAX and BAK and preventing pore formation, thus stabilizing the mitochondrial membrane and preventing release of cytochrome C (88). In contrast, the BH3-only pro-apoptotic members are initially localized to the cytosol or cytoskeleton and contain only the BH3 conserved domain. In response to death signaling, BH3-only family members localize to the mitochondrial membrane and interact with anti-apoptotic family members to inhibit their function (86). This inhibition of function allows for BAX and BAK to oligomerize, driving pore formation and apoptosis. In this manner, sensitivity and resistance to apoptosis is determined by the ratio of pro-apoptotic and anti-apoptotic family members. By increasing expression of anti-apoptotic family members like BCL2, cells are more able to resist the apoptotic signaling induced by standard chemotherapy and radiation. Combining increased BCL2 anti-apoptotic signaling and a reduction in cytotoxic stress from slower cycling, may

provide a mechanism for CSC populations to achieve multi-fold resistance capabilities over bulk tumor cells.

Additional mechanisms for CSC survival include increased DNA damage repair, up-regulation of cellular pumps, and increased metabolic activity through proteins like ALDH (78, 79). Although the quiescence contribution to these mechanisms of resistance is unclear, it is likely that reduced proliferative rate only adds to their effectiveness. Additional time in S or G2 phase of the cell cycle coupled with increased DNA repair protein activity may afford a survival advantage over bulk cells that continuously accrue DNA damage and ultimately are forced to undergo apoptosis. Reduced cycling speed together with increased cellular pump activity would facilitate drug removal from CSCs, limiting overall cytotoxic effects. Additionally, slower cycling would allow for increased metabolic activity of ALDH and other metabolic proteins over that of bulk cells. Importantly, there is no reason why combinations or all of these resistance mechanisms could not be playing a role in CSC survival. Future therapies may need to address all these issues to be successful in complete tumor eradication.

Quiescence Regulators as Potential Therapeutic Targets

Given the importance of quiescence in the CSC contribution to tumor progression and survival, understanding the mechanisms that govern quiescence will lead to the identification of novel targets to better eliminate slow-cycling CSC populations. Much of our current understanding of the mechanisms controlling quiescence comes from studies using conditional induction of quiescence in normal adult fibroblasts. The induction of

quiescence in fibroblasts is generally accomplished in one of three ways: mitogen deprivation, contact inhibition, or loss of adhesion. Each method of inducing quiescence in fibroblasts appears to yield a different quiescent transcriptional program (30). The three transcription programs overlap in differential expression of 131 genes that Collier *et al.* have designated as a “quiescence signature.” This signature is comprised of genes that regulate cell growth and division, suppress apoptosis and differentiation, and govern intercellular communication. Down-regulated elements in the quiescence signature consist of genes associated with cell cycle progression including cyclin B1, cdc20, cul-1, and myc. Up-regulated genes included important cell cycle regulators like p53 and cyclin D2. Also up-regulated in this signature are regulators of key stem cell associated pathways including the Wnt pathway, the BMP pathway, and the Notch pathway. Notch activation of the stem cell associated transcription regulator Hes1 is of particular interest as it has been shown to control reversibility of fibroblast quiescence by blocking differentiation and entry into irreversible cell cycle arrest (31). Notch pathway activity is important in mammary gland development as well as the mammary CSC response immediately following irradiation, suggesting that the Notch pathway may be a potential target in CSCs (49, 89). Importantly, each one of these dysregulated factors and pathways represents a potential therapeutic target that may help in elimination of CSC populations. Inducing expression of down-regulated targets or decreasing activity of up-regulated targets may prove an effective means of increasing susceptibility of slow-cycling cancer cells. Future studies evaluating the role and importance of each of these

factors will play an important part in the development of next generation drugs aimed at eliminating the CSC population.

Interestingly, there exists a fourth transcriptional program in fibroblasts induced by over-expression of CKIs like p21 and p16 (30). The CKI p21 has been found to control entry into quiescence and maintenance of the quiescent state, allowing cells to activate a DNA damage-like response (90). Additionally, maintenance of fibroblast quiescence has also been shown to be highly regulated by the Rb family members (91). Loss of Rb family members did not affect the ability of fibroblasts to enter G₀, but these cells were unable to maintain the quiescent state. While Rb loss is generally associated with the progression of cancer, retention of Rb in CSCs or contribution of other Rb family members may be important in CSC maintenance of quiescence and a potential target.

Developing and studying a quiescence signature in fibroblasts may be important in understanding regulation of the cell cycle, but the exact relevance to slow-cycling stem cell populations is not clear. Primarily, quiescence fibroblast studies are conducted on large populations of fibroblasts under biologically stressful conditions like contact inhibition or serum starvation. In contrast, individual stem cells and CSCs maintain quiescence while in contact with daughter cells and stromal layers and in the presence of normal mitogenic signals. Additionally, sphere-forming assays commonly used for the identification of stem cells and CSCs rely specifically on proliferation under non-adherent conditions. If mitogen deprivation, loss of adhesion, and contact inhibition truly activate three different transcriptional programs in quiescent fibroblast populations, it is

possible that the transcriptional program facilitated by slow-cycling stem cells and CSCs may be very different.

Quiescence regulation of a stem cell population is most comprehensively understood in the hematopoietic system. When compared to differentiated or cycling HSCs, quiescent HSCs were found to have up-regulated genes associated with cell cycle regulation, translation, RNA processing, and metabolic processes (92). Down-regulated genes were generally associated with transcription factors, signaling proteins, cell cycle proteins, and inhibitors of cell cycle progression. In line with these findings, the CKIs p21 and p57 were found to be necessary for quiescence and maintenance of the HSC pool. Mice that are p21 null demonstrate an increase in the number of stem cells present and lose the ability to repopulate the bone marrow in serial transplant experiments, suggesting uncontrolled expansion and eventual exhaustion of the stem cell pool (5). Similar results were obtained in p57 knockout mice that demonstrated a loss of the HSC population and a reduction in self-renewal potential associated with a loss of quiescent cells (7). Deregulation of the stem cell pool is likely due to p21 and p57 downstream effects on Rb family members, which play important roles in regulating E2F activity and G1/S transition. Knockout of these Rb proteins resulted in hematopoietic progenitor G1/S transition and proliferation, leading to exhaustion of the proliferative potential, similar to that seen in p21 loss (32). Importantly, if Rb family members play a similar role in tumors, combining drugs that target these proteins may push slow-cycling cancer cells into the proliferative pool, making them more susceptible to traditional chemotherapeutics.

While p21 appears to play a role in adult neural stem cell regulation and maintenance, other factors have been shown to be important contributors to quiescent stem cell activation (Table 1.1) (6). Occasional exit of neural stem cells from the quiescent state is important for proper tissue maintenance and may be controlled through Notch signaling via Hes1 oscillations (93). Down-regulation of Hes1 in neural progenitor cells during G1 phase reduced repression of cyclin D, *ngn2*, and *Dll1*, activating Notch signaling and driving cell cycle progression and generation of neural progenitors. Neural progenitors and neurons continue to retain low levels of Hes1 as they proliferate and differentiate. In neural stem cells, Hes1 expression and control of cyclin D and Notch signaling increase until subsequent G1 entry. These data suggest that it may be possible or necessary to target specific pathways like Notch signaling in combination with chemotherapeutics to better target slow-cycling cell populations.

Signaling pathways with interactions to other CKIs also play important roles in quiescent adult stem cell regulation. In mammary glands, the Hedgehog pathway component *Bmi1* has been demonstrated to regulate stem cell self-renewal (94). When injected into cleared mammary fat pads, *Bmi1* over-expressing mammospheres were able to produce substantially more outgrowths than control mammospheres. *Bmi1* has been demonstrated to transcriptionally repress the p16 and p19, suggesting a role for *Bmi1* in mammary stem cell cycle control and revealing *Bmi1* activation as a potential tool during chemotherapy treatment.

Additional signaling pathways have been demonstrated to play important roles in stem cell quiescence, specifically the bone morphogenic pathway (BMP) in skin. BMP

Table 1.1: Major Quiescence Regulators

Pathway	Regulator
Cell cycle	p21, p16, p57, Rb, p35/CDK5
Wnt	B-catenin, APC
Notch	Hes1, Jagged 1
BMP	NFAT1c
Hedghog	Bmi1

and calcineurin signaling up-regulate the transcription factor NFAT1c that has been found to highly co-localize with stem cells in the hair follicle (95). NFAT1c represses transcription of CDK4, stalling cells in G1/S phase and maintaining quiescence. Loss of NFAT1c permits entry into the cell cycle, shortening the telogen phase and prompting aberrant entry into the anagen phase. If expressed in tumors, targeting NFAT1c may increase CSC susceptibility to chemotherapy.

Combined, these data suggest important roles for various pathways in quiescence regulation and subsequently potential therapeutic targets. Understanding the contribution of each of these pathways in regulating the slow-cycling cell phenotype in cancers will be important in determining which pathways and potentially individual substrates can be targeted to better eliminate these cells.

Interestingly, it may be possible to target multiple pathways and downstream signaling components all at once by targeting key regulators at the intersections of many of these pathways. The p35/CDK5 complex appears to have functions related to many quiescence associated pathways and factors. Besides interactions with p27 and p16, p35/CDK5 may further regulate the cell cycle through interactions with E2F and the Rb family. The CDK5/p35 complex is able to bind the cell cycle driver E2F and sequester it, inhibiting activation of cell cycle gene promoters (14). Additionally, phosphorylation of the Rb family of proteins may inhibit release from E2F with similar results (15).

Furthermore, the roles of p35/CDK5 in therapy resistance may go beyond the cell cycle to promote cell survival and cell metastasis. Activation of the Erk pathway or direct binding of BCL2 family members by p35 has been demonstrated to stabilize BCL2

protein and increase anti-apoptotic signaling and cell survival (96, 97). At the cell membrane, p35/CDK5 is able to regulate E-cadherin and β -catenin signaling, down-regulating E-cadherin and freeing β -catenin to relocate into the nucleus to drive Wnt signaling and quiescent associated signaling (98, 99). Consequently, the down-regulation of E-cadherin ties p35/CDK5 to cytoskeletal turnover, suggesting implications for increased migratory abilities and the EMT transition, further linking p35/CDK5 to the quiescent stem-cell phenotype (73, 100, 101).

Combined, these data suggest that p35/CDK5 has multiple links to control of slow-cycling cells in normal tissues. Therapeutic targeting of p35/CDK5 in combination with chemotherapeutics is therefore likely to push slow-cycling cells into a more proliferative state by decreasing CKI activity or increasing E2F activity, making cells more susceptible to DNA damage. Additionally, p35/CDK5 inhibition is likely to lead to increased BCL2 degradation and decrease anti-apoptotic signaling, reducing quiescent slow-cycling cell ability to resist apoptotic stimuli.

While significant advances are being made in understanding quiescence control in normal adult stem cell populations, much less is known about control of quiescent CSC populations. Very few studies have been conducted specifically addressing control of quiescent CSCs, mostly likely due to the difficulty of isolating and analyzing pure CSC populations. If CSCs are truly derived from adult stem cells, then it is possible that CDK5/p35, Hes1, p21, p16, p57, Rb family members, and NFAT1c play significant roles in CSC regulation.

Cancers frequently have aberrant signaling in the Wnt and Notch self-renewal pathways that likely contribute to cell cycle control and differentiation. Increased expression of Hes1 has been observed in ovarian, breast, and non-small cell lung carcinomas, suggesting active regulation of Notch signaling (31). In melanoma, the slow-cycling cells identified by Roesch *et al.*, repress notch signaling directly through JARID1B interaction with the Notch ligand Jagged 1 promoter, consequently reducing intracellular Notch and controlling proliferation (71). Hes1 and Jagged1 may therefore be potential targets in future cancer treatments designed to target CSCs. Targeted reduction of Hes1 would increase Notch signaling, driving CSCs to proliferate and exhaust their proliferative potential, making them more susceptible to conventional therapy.

In colon cancers, mutations in Adenomatous polyposis coli (APC) and β -catenin are considered to be a driving force behind transformation (39). In the presence of Wnt signaling, β -catenin is no longer taken up by the APC-dependent degradation complex and translocates to the nucleus where it binds transcription factors to control expression of cell cycle target genes. Loss of APC in crypt cells has been demonstrated to be an important step towards initiation of intestinal adenomas (102). Interestingly, cells expressing high Wnt downstream transcription factors in primary sphere cultures demonstrated increased clonogenicity and the generation of both cycling and non-cycling cells (103). In tumors, these high Wnt expressing cells were located near stromal fibroblasts that provided signals to activate β -catenin dependent transcription. Furthermore, p35/CDK5 activity was linked to β -catenin and activation of Wnt signaling.

Similar p35/CDK5 activity may contribute to response to androgen signaling in prostate cancers in response to apoptotic stimuli (104, 105). These data suggest targeting Wnt pathway regulators may represent a potential mechanism for limiting CSC expansion and preventing recurrence.

While p35/CDK5, p21, Notch, and Wnt signaling may provide tempting targets for the removal of CSCs, disruption of these pathways would require meticulous targeting of CSC or titration of inhibitors to act on CSCs but not normal stem cell populations. Such treatments could severely weaken patients. Additionally, improper application of cell cycle inhibitors may fuel tumor growth and aggressiveness. The CDK inhibitor p21 acts as a tumor suppressor in dividing cells by protecting against genome instability and working with other tumor suppressors to subdue oncogenes (106, 107). Loss of p21 combined with chemical induction of carcinogenesis has demonstrated increased induction of tumors and increased aggressiveness in resulting tumors (108, 109). Combining widespread targeting of p21 or CKI regulators like p35/CDK5 with chemotherapy may have similar effects on tumors. These data highlight the necessity to be able to target CSCs selectively when using CDK inhibitors and add to the challenges ahead in developing treatments to better eradicate CSCs.

Remaining Questions

The limited data available on the regulation of slow-cycling cells equates to a poor understanding of the role that these cells may be playing in tumor progression and recurrence. What little evidence there is suggests that the slow-cycling phenotype might

be an important factor in tumor cell survival after conventional therapy. Our work focuses on the utilization of novel pulse chase techniques to verify the existence of slow-cycling cancer cells. Mechanistically, slow-cycling cancer cells suggest an inherent population of therapy resistant cells that, when coupled with increased DNA repair or anti-apoptosis signaling could explain the patterns of recurrence and acquired resistance currently observed in post-therapy cancer patients. We evaluate the tumor initiating capabilities and therapy susceptibility of these slow-cycling cell populations to determine if this proposed mechanism is scientifically supported. Additionally, we begin to profile differences between slow-cycling cells and rapidly proliferating cells and evaluate the differentially regulated protein p35 for contribution to the therapy resistance phenotype.

Chapter II:

Slow-cycling Therapy Resistant Cancer Cells

Abstract

Tumor recurrence after chemotherapy is a major cause of patient morbidity and mortality. Recurrences are thought to be secondary to small subsets of cancer cells that are better able to survive traditional forms of chemotherapy and thus drive tumor re-growth. The ability to isolate and better characterize these therapy resistant cells is critical for the future development of targeted therapies aimed at achieving more robust and long-lasting responses. Using a novel application for the proliferation marker CFSE, we have identified a population of slow-cycling, label-retaining tumor cells in both *in vitro* sphere cultures and *in vivo* xenograft models. Strikingly, label-retaining cells exhibit a multi-fold increase in ability to survive traditional forms of chemotherapy and re-enter the cell cycle. Furthermore, we demonstrate the innovative application of CFSE to live sort slow-cycling tumor cells and validate their chemoresistance and tumorigenic potential.

Introduction

The incidence of recurrence after treatment in patients with epithelial tumors is a major obstacle in developing truly curative treatments. Although many Stage II colon cancer patients show initial responses to standard chemotherapies, five-year recurrence

rates can be as high as 25% (110). In breast cancer patients, 15-year recurrence rates are as high as 20% (111). While factors associated with recurrence (sizes, grade, etc.) can suggest which tumors are likely to recur, the inability to accurately predict recurrence risk can lead to both unnecessary and insufficient treatment. It appears likely that subsets of tumor cells evade initial chemotherapy and survive to re-propagate the tumor (79, 112)

Traditional chemotherapies like 5-fluorouracil (5-FU) and Oxaliplatin require active cycling cells to trigger cell death (112, 113). Cells that are quiescent or cycling slowly are therefore less likely to be susceptible to these drugs, suggesting an inherent recurrence mechanism in which slow-cycling cells evade therapeutic agents and re-propagate tumors. Evidence for such chemo-resistance abilities is observed in normal skin tissue where more slowly dividing cells in the bulge survive chemotherapy to regenerate the hair follicle (114). In the mouse forebrain, high doses of tritiated thymidine ($^3\text{H-TdR}$) kill constitutively proliferating cells, but have no effect on quiescent cells (42).

Similar to adult tissues, slow-cycling populations of cells have been identified in cancer tissues. Roesch *et al.* demonstrated that primary melanoma cell lines contain a PKH26 label retaining population that has a doubling time of four weeks (71). Using the same PKH dye, Kusumbe and Bapat demonstrated the existence of a slow-cycling population of cells in ovarian cancer (115). Dembinski and Krauss used Vybrant[®] DiI to demonstrate a pancreatic adenocarcinoma slow-cycling cell population (72). Even cell lines grown for years *in vitro*, like MDA.MB.231, have been found to contain label-retaining cell populations (68). The contribution that slow-cycling populations play in

chemotherapy resistance is not well studied and it is unclear if this characteristic may be a significant factor in tumor recurrence.

In this study, we use an innovative application for the cell tracing dye CFSE (carboxyfluorescein diacetate succinimidyl ester) to identify and isolate slow-cycling label retaining cells in both commonly used colon and breast tumor cell lines, as well as a primary human breast tumor. We demonstrate that these slow-cycling cells are tumorigenic and more resistant to traditional chemotherapies than rapidly dividing cells. Importantly, slow-cycling cells survive treatment and demonstrate active DNA synthesis after the removal of chemotherapy drugs, suggesting that they may drive recurrence in the clinical setting.

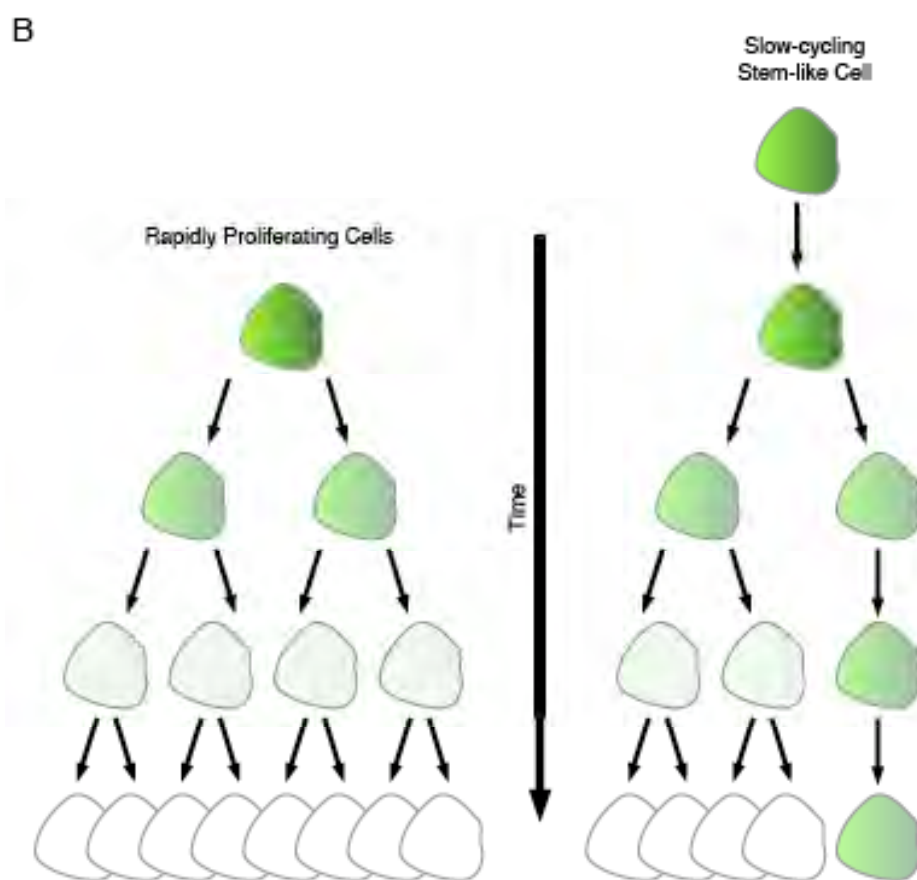
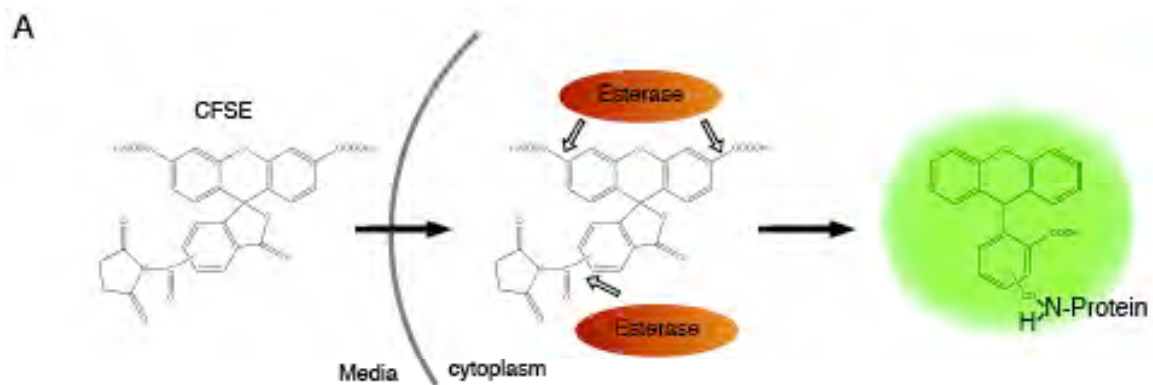
Results

Detection of *In vitro* and *In vivo* Label Retaining Cells

To identify slow-cycling cancer cells, we developed a novel pulse/chase protocol utilizing the cell trace compound CFSE. Initially, CFSE is membrane permeable and non-fluorescent (Figure 2.1A). Upon entry into cells, two acetate groups on CFSE are cleaved by endogenous esterases and the compound becomes fluorescent under light stimulation. Cleavage of the acetate groups additionally allows for binding of the compound to amine groups on protein, trapping CFSE within cells. In rapidly proliferating cells, CFSE label is divided evenly between daughter cells, decreasing label intensity over successive divisions (Figure 2.1B). In contrast, slow-cycling cells over the

Figure 2.1: CFSE and label dilution

(A) Carboxyfluorescein diacetate succinimidyl ester (CFSE) is initially non-fluorescent and membrane permeable. Upon entry into the cell, the acetate groups are cleaved by endogenous esterases and the compound becomes fluorescent green under stimulation. Cleavage of CFSE allows for binding of the compound to amine groups found on proteins, trapping the compound within the cell. (B) In rapidly proliferating cells, CFSE is divided evenly into daughter cells during division. Over multiple divisions, CFSE is diluted out to low or undetectable levels. In contrast, slow-cycling cells over the same period do not divide as frequently. When they do divide, asymmetric divisions create one daughter cell that maintains the slow-cycling phenotype and one daughter cell that rapidly proliferates to dilute out the label. Over time, populations of mixed slow-cycling label retaining cells and dark rapidly proliferating cells are established.

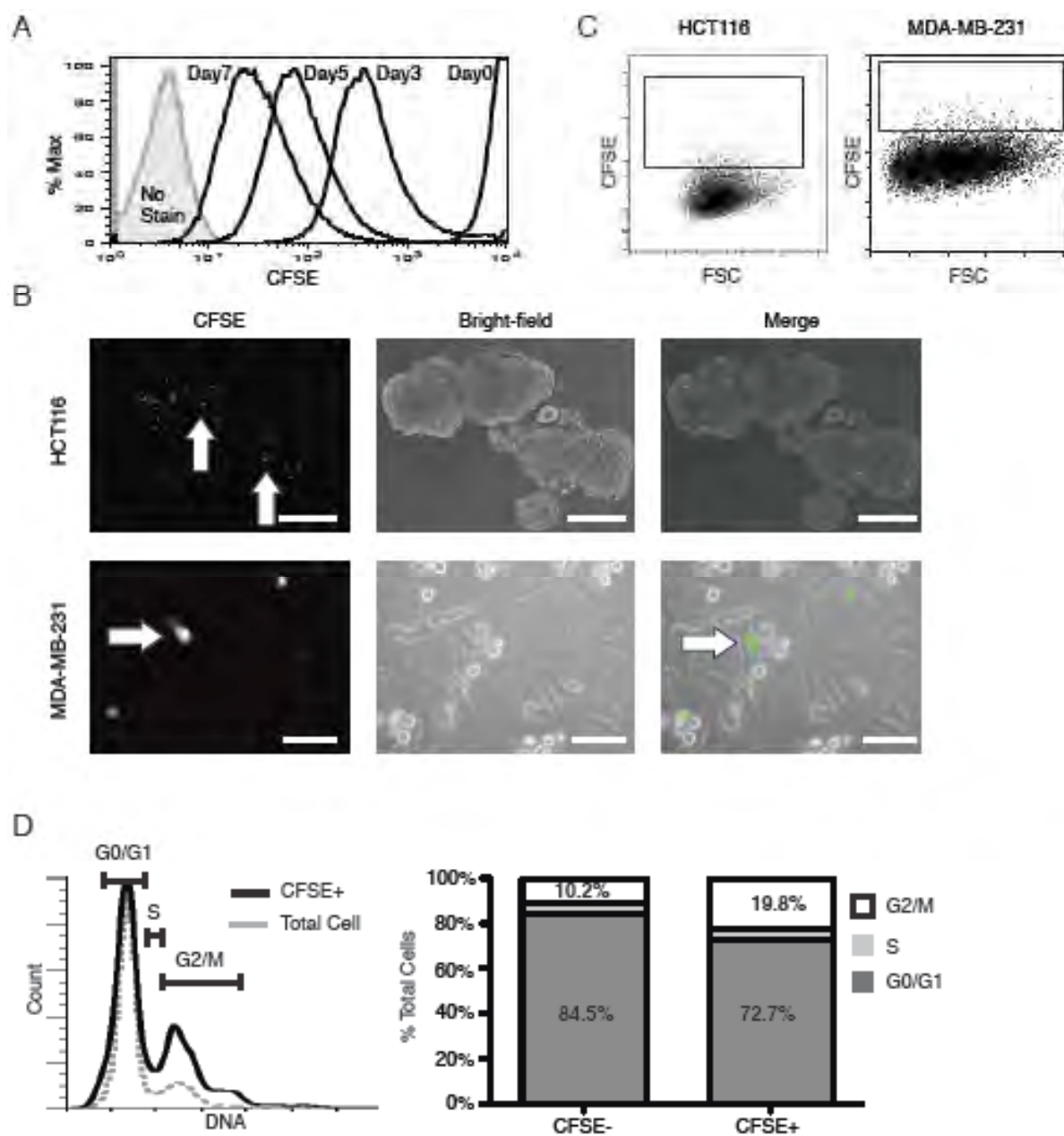


same period of time undergo fewer divisions, retaining higher CFSE intensity, therefore distinguishing slow-cycling cells from their rapidly proliferating counterparts.

Because sphere cultures are considered to better retain properties of stem-like tumor cells, we used this system to determine if slow-cycling cells were present in the colon tumor line HCT116. Like other groups, we found that in sphere media MDA-MB-231 (MDA231) cells formed poorly proliferative, loosely associated clumps of cells that made pulse/chase growth assays impractical (116). Therefore, MDA231 cells were grown as adherent cultures during evaluation for *in vitro* label-retaining cells (LRCs). MDA231 cultures or HCT116 spheres were digested into single cells and labeled with the fluorescent cell tracing dye CFSE. Over the course of one week, dividing cells plated in media progressively dilute CFSE label between daughter cells, decreasing fluorescence intensity (Figure 2.2A). At one week, a CFSE-high cell population was distinguishable from non/CFSE-low bulk cells by microscopy under both conditions (Figure 2.2B). When single cells were analyzed by flow cytometry, an average CFSE-high LRC population of $4.2 \pm 2.1\%$ was detected in HCT116 spheres and $0.99 \pm 0.14\%$ in MDA231 adherent cultures (Figure 2.2C). Using the mean CFSE intensity to compare CFSE-low cells (mean CFSE = 26.8) to CFSE-high cells (black box, mean CFSE = 227), HCT116 CFSE-high cells were approximately 3 cell divisions behind non/low-labeled bulk cells (Figure 2.2C) indicating a distinct population of slowly dividing cells. Cell cycle analysis of HCT116 CFSE-high spheres revealed a 2-fold increase in G2/M phase cells when compared to total cells (Figure 2.2D) suggesting an extended G2/M phase or arrest.

Figure 2.2: *In vitro* identification of label retaining cells

(A) Flow cytometry plot demonstrating HCT116 sphere dilution of CFSE over seven days. All HCT116 cells are intensely positive directly after labeling. Over time, label is lost in rapidly proliferating cells, with a tail of more slowly cycling label-retaining cells visible after only three days. (B) Fluorescent and bright-field image overlay of HCT116 sphere cultures and MDA231 adherent cultures one week after CFSE labeling (scale bar = 100 μm) CFSE-high slow-cycling cells are identifiable in green within fields of dark bulk tumor cells. (C) Representative flow cytometry plot of digested HCT116 sphere cultures and MDA231 adherent cultures after seven days. Black box depicts the approximate collection gate around the highest CFSE intense cells. (D) Representative cell cycle profile of total HCT116 sphere cultures. CFSE-low cells (Grey) and CFSE-high label retaining cells (Black) after one week and adjacent quantification bar graphs.



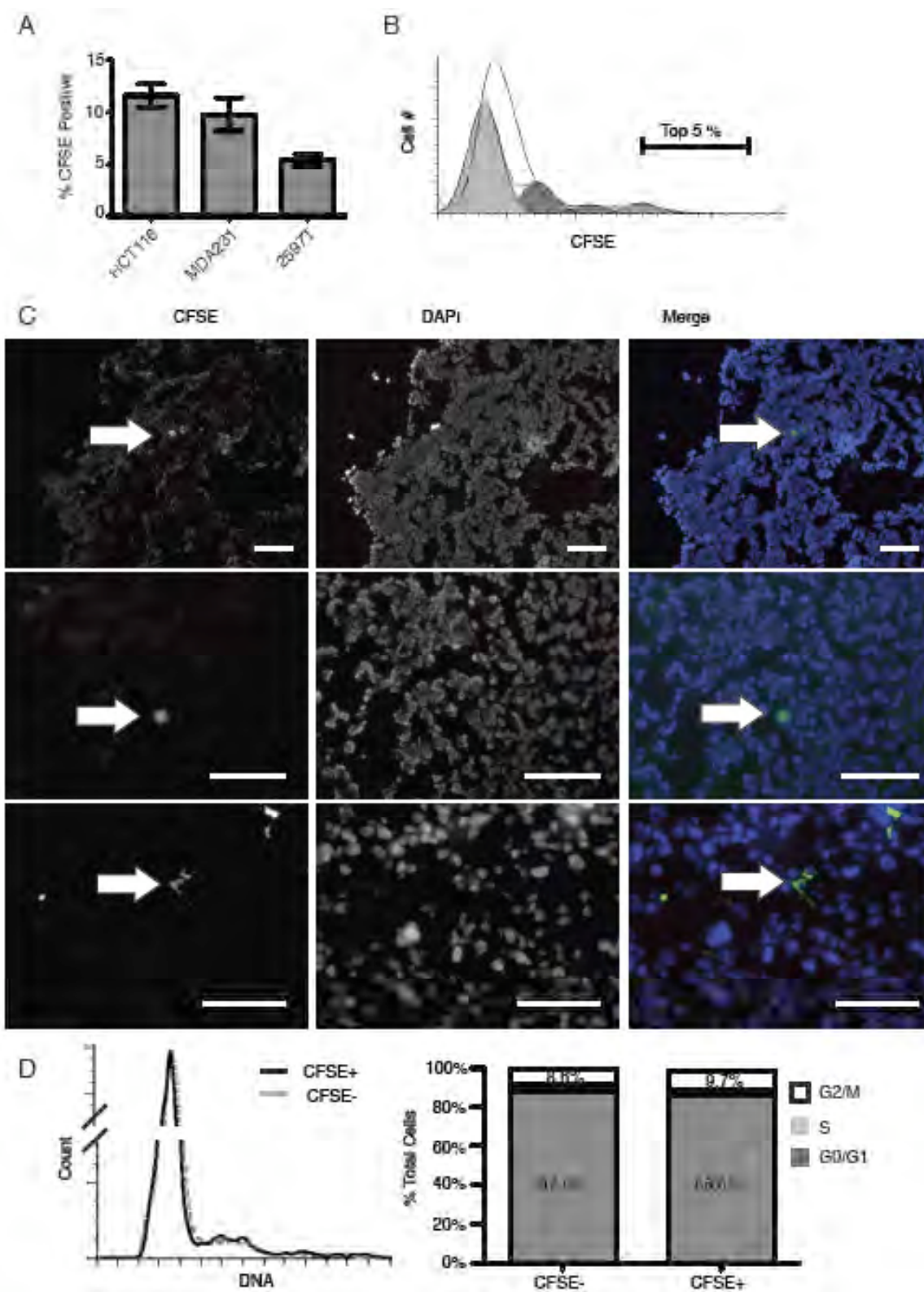
We next used CFSE labeling to determine if slow-cycling cells were detectable in an *in vivo* system. HCT116 and MDA231 cells were labeled with CFSE and injected sub-cutaneously or into the mammary fat pads, respectfully, of NOD/SCID mice. After two weeks of growth, flow cytometry indicated a population of CFSE-high cells distinguishable from the bulk tumor cells: HCT116 with $11.6 \pm 2.9\%$ and MDA231 with $9.7\% \pm 3.5\%$ CFSE-high cells (Figure 2.3). To demonstrate that this was not limited to cell lines, we performed similar *in vivo* studies with a patient-derived primary breast tumor (2597T) that was serially passed in xenografts and digested to single cells before labeling and injection. This primary breast tumor demonstrated an LRC content of $5.3 \pm 0.8\%$ (Figure 2.3A). Using the proliferation wizard from the Modfit software package, we calculated that the top 5% CFSE intense cells have undergone at least 3-5 fewer cell divisions than the bulk tumors cells in HCT116 xenografts (Figure 2.3B). On frozen tissue sections of tumor xenografts, only a small number of scattered CFSE-high cells were detectable (Figure 2.3C), demonstrating the sensitivity of flow cytometric analysis over immunofluorescence microscopy for this system. When analyzed for cell cycle stage, *in vivo* CFSE-high cell cycle profiles were similar to bulk tumor cells with only a slight enrichment for the G2/M phase (Figure 2.3D).

Label Retaining Cells are Tumorigenic and Not Senescent

To assess the capacity of LRCs to contribute to tumor growth, we live-sorted pulse-chased HCT116 spheres (Figure 2.4A, Row1) and replated the CFSE-high cells.

Figure 2.3: *In vivo* identification of label retaining cells

(A) Composition of CFSE positive cells after 2 weeks of tumor growth in HCT116 colon tumors, MDA231 breast tumors, and the primary breast sample 2597T tumors. (B) Representative flow cytometry plot of CFSE cell intensities for HCT116 tumor xenografts after two weeks growth. White peak is the unanalyzed data according to CFSE intensity and cell number. Grey peaks represent predicted dilution populations calculated by the proliferation wizard of the Modfit software package. Six separate division peaks were calculated, with two small peaks of greatest CFSE intensity not visible. Black bar approximates the gate used during live sorting to collect the highest 5% intense cells. (C) Fluorescent staining of HCT116, MDA231, and 2597T xenograft tumors counter stained with DAPI (blue). Only rare cells retain a visible intensity of CFSE (green) while less intense cells are still detectable by flow cytometry (scale bar = 100 μ m). (D) Cell cycle profiles for HCT116 xenografts. CFSE-low cells (Grey) and CFSE-high label retaining cells (Black) after two weeks and adjacent quantification bar graphs.



After one week, approximately 75% of CFSE-high cells had divided to form spheres (Figure 2.4A Row 2). It is interesting to note that 25% of cells did not appear to divide and retained high levels of the CFSE label, suggesting that a population of LRCs may exhibit long-term cell cycle arrests.

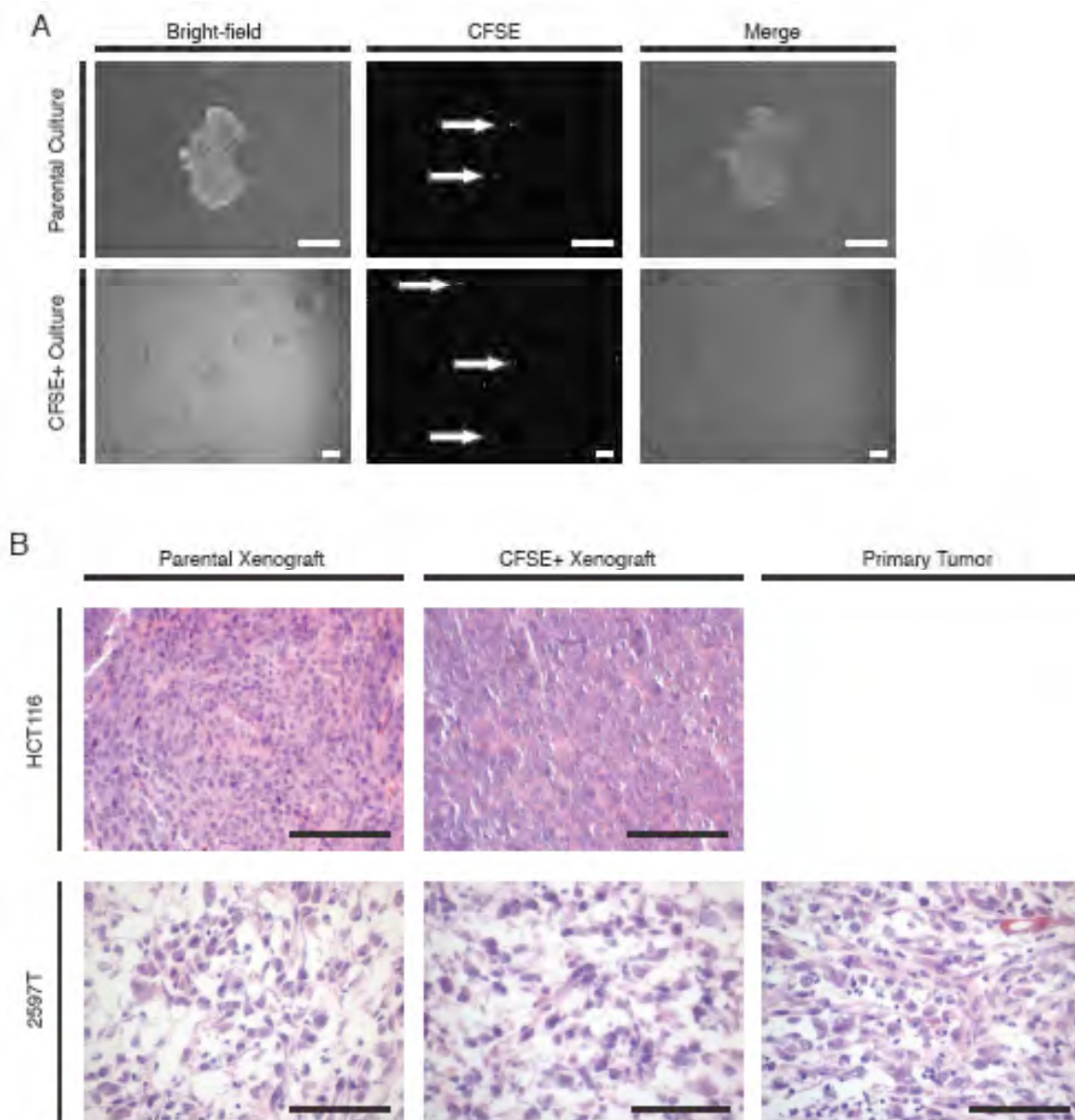
To determine if *in vivo* derived LRCs are tumorigenic, CFSE pulse-chased HCT116 and 2597T primary breast tumors were digested after two weeks to single cells and live sorted for a maximum of 5% of the top CFSE-high cells. When 5,000 HCT116 or 50,000 2597T CFSE-high cells were re-injected into 2 mice, large tumors were formed within two months. Histologically, CFSE-high tumors were similar to tumors formed from the established parental cell line (Figure 2.4B). Tumors were poorly differentiated, had little structure or organization, were densely packed with cuboidal tumor cells, had poor stromal or vascular presence, and had large necrotic centers. Cells from both tumors contained large nuclei with little cytoplasmic content and no cell polarity. In the primary 2597T breast line, CFSE-high tumors were also similar to the histology of the primary patient sample. All tumors were poorly differentiated and contained loosely associated elongated spindle type cells as well as pockets of more densely packed cuboidal cells. Cells had irregularly shaped nuclei that were occasionally enlarged. These tumors contained little vascular invasion or fibrotic scarring.

LRCs are Enriched Following Chemotherapy

Slow-cycling label retaining cells in adult tissues have been demonstrated to survive chemotherapy better than other cells within the tissue (5, 80, 114). To investigate

Figure 2.4: Label retaining cells are colony forming and tumorigenic

(A) HCT116 labeled spheres were digested after one-week growth (Row1) and live sorted for CFSE-high cells. Fluorescent and bright-field imaging of representative HCT116 CFSE-high cells (green) after one-week (Row2). (B) HCT116 or 2597T CFSE labeled tumors (Column1) were digested into single cells and live sorted for CFSE-high cells (EpCAM⁺ and Lin⁻). H&E images of CFSE-high xenograft growth (Column2). CFSE-high tumors are histologically similar to both parental tumor xenografts, and in the case of 2597T, similar to the primary patient tumor as well (Column3) (scale bar = 100 μ m).

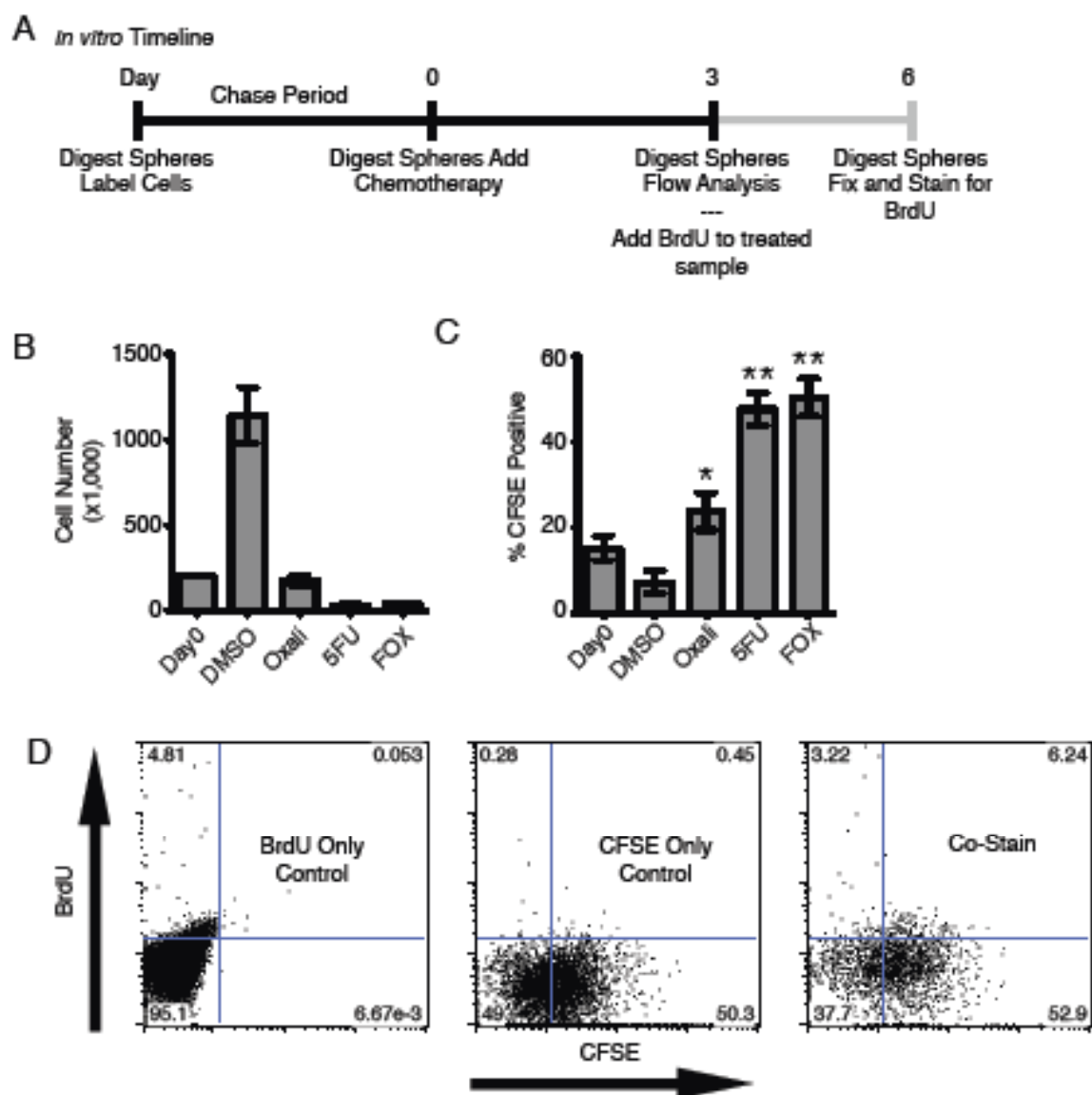


if chemotherapy resistance is also a characteristic of our slow-cycling tumor cells, we CFSE labeled HCT116 cells and chased for one week in sphere media. Single cell digests were then either plated in DMSO (vehicle control) or a chemotherapy reagent at a combined concentration to kill between 75% and 90% of cells and discern more resistant cells (Figure 2.5A). After three days in culture, DMSO treated cells had expanded by 5-fold, while Oxali (15%), 5FU (2.8%), and FOX (3.3%) treated cultures expectedly contained only a fraction of viable cells compared to DMSO controls (Figure 2.5B). When analyzed for CFSE, DMSO control samples demonstrated an expected decrease in CFSE content (15.2% to 7.1%) as these cells continued to proliferate. Strikingly, Oxali, 5FU, and FOX treated cells demonstrated 3.4, 6.7, and 7.1 fold increase in CFSE-high cell content respectively (Figure 2.5C). To determine if LRCs are capable of dividing after treatment, HCT116-FOX treated cultures were replated in sphere media containing BrdU. After three days, 6.2% of total cells were BrdU⁺/CFSE-high cells suggesting approximately 10% of CFSE-high cells (6.2% of 59.1%) had undergone DNA replication and re-entered the cell cycle during this early post-chemotherapy recovery period (Figure 2.5D). Similar levels of CFSE-low cells were found to be BrdU⁺ as well, suggesting that surviving rapidly proliferating cells continued to proliferate following chemotherapy treatment.

To elucidate whether slow-cycling LRCs are chemo-resistant *in vivo*, CFSE labeled HCT116 cells were injected into NOD/SCID mice and allowed a 12 day chase before being placed on a FOX treatment regime (Figure 2.6A). At the end of treatment, FOX treated tumors were significantly smaller in size (541mg) compared to DMSO

Figure 2.5: *In vitro* label retaining cells demonstrate increased therapy resistance

(A) Timeline for *in vitro* HCT116 chemotherapy treatment experiments. (B) Number of surviving cells after three days in the presence of DMSO, 2 μ M Oxaliplatin (Oxali), 250 μ M 5FU (5-Fluorouracil), or the combination of Oxali and 5FU “FOX”. (C) Percent CFSE positive cells after three days in the presence of drug. Oxali, 5FU, and FOX treated samples are significantly enriched over DMSO treated samples (n = 3, *p = 0.01, **p < 0.0001). (D) Representative BrdU incorporation flow cytometry plots for FOX treated sphere cultures with single color controls.



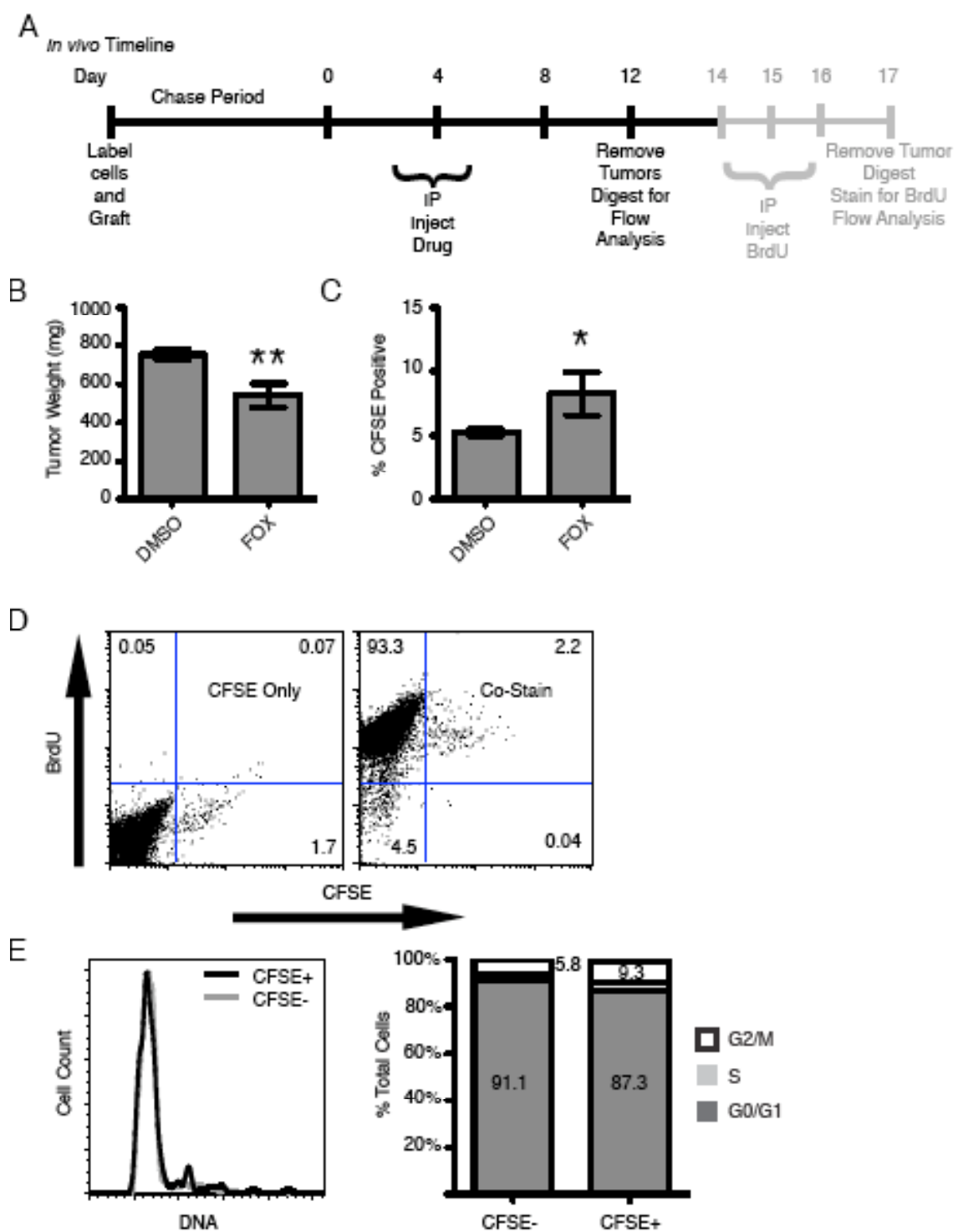
treated controls (753 mg) (Figure 2.6B). When analyzed for CFSE content, DMSO treated tumors averaged 5.3% CFSE-high cells while FOX treated tumors had a statistically significant increase in CFSE-high cells at 8.3% (Figure 2.6C). When FOX treated tumors were pulsed with BrdU for four days, LRCs demonstrated the ability to cycle at least once over the time period through BrdU incorporation (Figure 2.6D) and a cell fraction within all stages of the cell cycle via DAPI stain (Figure 2.6E). Combined, these data demonstrate the ability for LRCs to re-enter the cell cycle and actively proliferate shortly after chemotherapy treatment.

Discussion

The use of CFSE to demonstrate the existence of slow-cycling label-retaining cell populations in cancer is divergent from the dye's general use of short-term lineage tracing. CFSE offers the distinctive ability to isolate and further characterize live, slow-cycling cells apart from other label retaining methods, like BrdU, that require cell permeabilization. Furthermore, CFSE dilution and retention relies on a functional cellular phenotype and is independent of protein markers with poorly understood functional contribution to cell dynamics. We demonstrate the existence of a CFSE label-retaining cell population in two epithelial tumors lines and one primary patient-derived tumor xenograft. Slow-cycling populations of cells have been found in the normal colon (36) and normal breast tissues (22, 23, 40), suggesting that this characteristic may be carried over from their tissues of origin and serve an important functional role in tissue longevity.

Figure 2.6: *In vivo* label retaining cells demonstrate increased therapy resistance

(A) Timeline for *in vivo* HCT116 xenograft treatment regime. (B) Tumor masses at the end of treatment for DMSO (n=12) and FOX (n=8) (** $p < 0.01$) (C) CFSE composition for DMSO and FOX treated tumors (* $p = 0.045$) (D) Representative BrdU incorporation flow cytometry plots for FOX treated tumors pulsed with BrdU. CFSE-high cells incorporated approximately equal amounts of BrdU as CFSE-low. (E) Representative DAPI derived cell cycle profiles for FOX.



Importantly, the populations of LRCs that we identified both *in vitro* and *in vivo* are capable of re-activation. While it is conceivable that a population of cells that enter a senescent state post-labeling would retain label, the identified LRCs are capable of division when live sorted and replated in sphere media and can regenerate tumors *in vivo*. Taken together, these data suggest that CFSE-high LRCs are capable of driving tumor formation and re-growth in a clinical setting.

The observed enrichment of LRCs after chemotherapy requires either the preferential expansion of the LRC pool or a reduction of the non-label retaining bulk cells. Back calculations of the *in vitro* treated DMSO population suggests an increase in absolute LRC number from ~30,000 to ~80,000, due to LRC proliferation which generates partially-labeled daughters. However, this expansion alone cannot account for the significant increase in overall LRC composition. In addition, the significant difference in survival between Oxaliplatin-treated samples and 5FU/FOX-treated samples further supports the concept of LRC enrichment due to increased chemotherapy resistance. Oxaliplatin had an insignificant overall kill rate and only modest LRC enrichment, while 5FU killed a majority of cells and demonstrated a more profound LRC enrichment (Figure 2.5). These data indicate that LRCs are better able to survive standard chemotherapy treatments and their enrichment is related to chemotherapeutic efficiency of killing non-label retaining bulk cells.

In vivo, we see a similar pattern where treatment with clinically relevant concentrations of FOX resulted in modest de-bulking of tumors, corresponding with only modest LRC enrichment (Figure 2.6). Unfortunately, increasing drug concentrations or

decreasing time between injections proved fatal for a high percentage of mice and hampered our ability to determine if a more profound de-bulking of tumor cells would lead to greater fold LRC enrichment.

In *in vitro* spheres, HCT116 LRCs were enriched for cells in the G2/M phases of the cell cycle (Figure 2.2C). Other groups have associated a G2/M phase arrest with increased resistance to multiple forms of chemotherapy and a propensity to evade apoptosis (117, 118). It is therefore likely that the G2/M arrest observed in our LRCs is a contributing factor to the observed enrichment; perhaps by extending the time for repair or providing the means to evade apoptotic signals. It is also possible that simply arresting in the G2/M state primes LRCs to better respond to cellular stresses and apoptotic signaling that results from therapeutic treatment.

While the ability of cancer cells to survive chemotherapy is important, clinically significant cells must also be capable of proliferation to stimulate tumor recurrence. Therefore, it is important to establish that CFSE-high LRCs are not avoiding the cytotoxic effects of FOX treatment by entering a permanently non-dividing state. Both *in vitro* and *in vivo*, a subset of FOX treated LRCs were able to incorporate BrdU shortly after removal of FOX (Figure 2.5D & 2.6D), demonstrating the capacity of LRCs to actively proliferate and conceivably contribute to tumor recurrence after treatment. This suggests that slow-cycling cells are activated after chemotherapy withdrawal to re-propagate the tumor.

Given the therapy resistant and tumorigenic properties of label retaining cells, it is conceivable to conclude an association between slow-cycling cells and cancer stem cells

(CSCs). The concept that subsets of tumor cells have increased capacity for tumor propagation in mice is still evolving. For instance, in some models of cancer stem cells (such as melanoma) most if not all cells are tumorigenic (119), while in other system (such as in colon cancer) surface markers have been shown to be non-specific, with marker positive and negative cells showing tumorigenicity (60, 64). Evidence from other groups in ovarian tumors, mammary tumors, and melanoma cell lines has demonstrated a connection between the slow-cycling phenotype and identified CSCs populations (40, 62, 71). However, we believe our findings to be biologically and clinically significant, independent of a cancer stem cell model. Given the possibility that most or all cancer cells could be tumorigenic, we identify a subset of slow-cycling cells that is better able to survive treatment, and thus more capable of leading to tumor recurrence.

In summary, we propose a model in which a subset of slow-cycling tumor cells have enhanced chemo-resistance and proliferate after chemotherapy withdrawal to allow for tumor recurrence in a clinical setting. Furthermore, this study details an innovative method to isolate, enrich, and better characterize a population of live therapy resistant cells in both *in vitro* cultures and *in vivo* xenografts. This work should allow for future live enrichment and better characterization of chemotherapy resistant populations in order to develop more targeted therapies.

Chapter III:

Regulation of Slow-cycling Cancer Cells by p35

Abstract

The existence of chemotherapy-resistant slow-cycling cancer cells is a major challenge in limiting tumor recurrence and ultimately improving patient survival. A better understanding of the mechanisms that regulate the slow-cycling therapy-resistant phenotype will allow for the development of drugs that better target these cells. We identify the CDK5 activator, p35, as differentially regulated in slow-cycling cancer cells. Over-expression of p35 leads to increased chemotherapy resistance and increased staining for the anti-apoptotic factor BCL2. Additionally, increased expression of p35 was observed following chemotherapy in rectal cancer samples. These data suggest a model in which slow-cycling cancer cells utilize increased expression of p35 to regulate cycling speed and stabilize BCL2 expression, thus increasing chemotherapy resistance and promoting tumor recurrence.

Introduction

Tumor recurrence in epithelial tumors like those of the colon and breast is a major obstacle to achieving complete remissions in cancer patients. In its most advanced stages of progression, colorectal cancers can have recurrence rates as high as 75% (46). Compounding the issue, recurrent tumors are often more aggressive and resistant to previously successful chemotherapeutic treatments. A better understanding of slow-

cycling cancer cells is critical for targeting these therapy resistant populations and achieving better patient outcomes.

It is believed that small populations of stem-like cancer cells evade the cytotoxic effects of traditional forms of chemotherapy and drive tumor recurrence. These stem-like cancer cells are thought to originally develop from adult tissue stem/progenitor cells given similar characteristics between the two populations (50, 51). If this is true, the chemotherapy resistance and regulatory mechanisms found in adult stem cells may be carried over to stem-like cancer cells.

Control of cell cycling speed is one likely mechanism found in both adult stem cells and stem-like cancer cells. Traditional forms of chemotherapy target actively proliferating cells by inducing DNA damage and apoptotic signaling. Therefore, cells with reduced cycling speeds or infrequent divisions would have an inherent mechanism of resistance to these types of therapies. This concept is supported by experiments that demonstrate populations of slow-cycling adult stem cells with greater resistance to cytotoxic effects of chemotherapy compared to more rapidly proliferating cells (5, 42).

Previous work from our lab has demonstrated that the slow-cycling phenotype of normal adult epithelial stem cells may be present in slow-cycling cancer cells. We have demonstrated the existence of colony-forming slow-cycling populations within *in vitro* sphere cultures and *in vivo* xenografts (120). Furthermore, these slow-cycling cells are more resistant than rapidly proliferating cells to traditional forms of chemotherapy, and are able to re-enter the cell cycle following the cessation of treatment. This work suggests slow-cycling cells may be better able to resist chemotherapy and ultimately

provide a means for tumor recurrence. Identifying and understanding genes that control cycling speed and regulate resistance should lead to the development of drugs to better eliminate these cells.

Interestingly, evidence suggests that the poorly understood CDK5 regulator, p35 (CDK5R1), may be one of these therapeutic targets. Most intensively studied in neuron progenitor cells, p35 acts in a similar manner to other cyclins by binding and activating a member of the CDK family, specifically CDK5 (121). Binding affinity, protein stability, and even protein targets of CDK5 are dependent on binding either a 35 kD form of p35 or the cleaved 25 kD form (14). Unlike other cyclin/CDK complexes, the p35/CDK5 complex does not play an active role in driving the cell cycle forward, but instead may have broad alternate functions related to suppressing cell cycling, migration, and survival as well as the development of Alzheimer's disease (11).

In patients with Alzheimer's disease, dysregulation of p35/CDK5 levels leads to the development of neurofibrillary tangles that are believed to be a major factor in disease progression (122). Knockout studies of p35 in mice produce neurons that fail to arrange cortical lamination correctly and migrate away from the niche, leading to seizures and adult lethality (123). These studies suggest that regulation of migration is an important function of the p35/CDK5 complex. Cellular migration is regulated by the p35/CDK complex through phosphorylation of the cytoskeletal protein Tau at the PHF-1 sites. PHF-1 phosphorylation leads to release of Tau from microtubules and cytoskeletal destabilization, allowing for microtubule turnover and cell migration (100, 101). Migration activity is further regulated by a CDK5-independent function of p35 that can

bind and target E-cadherin to lysosomes, increasing cell migration (98). In complex, p35 functions to phosphorylate β -catenin, altering binding to cadherins and other cell-to-cell interacting proteins, regulating cell adhesions, and opening the door for β -catenin to translocate into the nucleus and drive stem cell-associated Wnt signaling (99, 124). These functions help to regulate migration and stem cell activity in developing neurons and could play an important role in regulating similar functions in slow-cycling cancer cells. Increases in p35 expression have been associated with meningioma progression with possible links to β -catenin localization and activation of Wnt signaling (125).

At present, the basic understanding about expression patterns and the role of p35/CDK5 in epithelial cancers remains unclear. In prostate cancers, increased p35/CDK5 expression is linked to increased androgen receptor signaling and survival in response to certain forms of apoptotic stimuli (104, 105). Apart from these tumors, p35/CDK activity has been demonstrated in other cancers including pancreatic (126), breast (127), and lung (128), although with the impact of this activation is yet to be fully explored.

Importantly, the p35/CDK5 complex may play a protective role in cellular responses to certain forms of apoptotic stimuli that signal through the mitochondrial apoptotic pathway. Activation of p35/CDK5 by the mitochondrial apoptotic pathway has been demonstrated to increase signaling through the ERK pathway, leading to the phosphorylation and stabilization of BCL2 and increasing cell survival (96, 97). Additionally, Erb phosphorylation by p35/CDK5 may mediate neuronal survival by inducing Akt/PI3-kinase signaling (129). Similar responses elicited in tumor cells

expressing p35/CDK5, may represent an important survival mechanism mediated by BCL2 stabilization.

Other protective functions of p35/CDK5 may relate to the ability of the complex to suppress cell cycle progression. When bound to the 35 kD form of p35, CDK5 is able to complex with the cell cycle driver E2F. This interaction inhibits the ability of E2F to bind and activate cell cycle gene promoters, providing neuronal protection from cell stress (14). Additionally, evidence suggests that the p35/CDK5 complex can associate with the cycling dependent kinase inhibitor, p27 and the retinoblastoma protein (Rb) to suppress the cell cycle (15). If p35/CDK5 retains the ability to regulate the cell cycle in tumor cells, it may provide a mechanism to resist synthesis-dependent DNA damage and apoptotic signaling during chemotherapy.

Here we demonstrate that the CDK5 regulator, p35, is consistently up-regulated in slow-cycling cancer cells grown in culture or as tumor xenografts. Strikingly, manipulations of p35 levels correlate with cell survival following treatment with traditional chemotherapy drugs. Immunofluorescence imaging suggests this therapy resistance may be due in part to interactions between p35 and the pro-survival protein BCL2. Finally, we demonstrate clinical evidence for a protective role of p35 by examining pre-chemotherapy and post-chemotherapy matched patient samples of rectal cancer for p35 expression.

Results

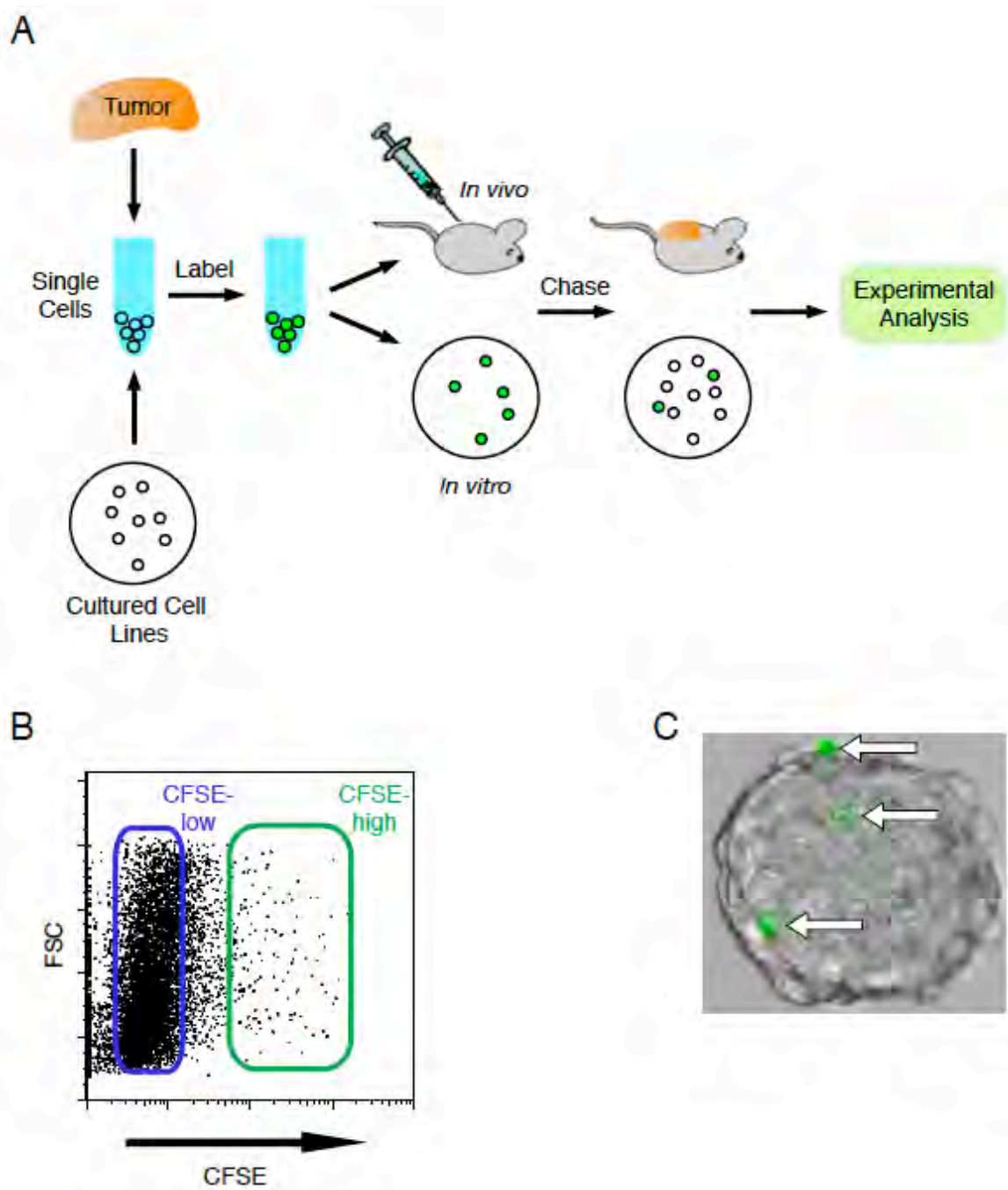
Bcl2 and p35 are Up-regulated in Slow-cycling Cancer Cells

A deeper understanding of the mechanisms that lead to therapy resistance in slow-cycling cancer cell populations will lead to the development of better treatments and increased patient survival. To identify slow-cycling cancer cells, our lab utilizes a CFSE based pulse/chase technique to identify slow-cycling tumor cells (Figure 3.1). Cells were labeled with CFSE and plated in an *in vitro* B27 based non-adherent sphere media or injected *in vivo* into the mammary fat pads of immune compromised mice (Figure 3.1 A). After a growth period in which rapidly proliferating cells dilute label among daughter cells, spheres or tumors are digested into single cells and live sorted into CFSE-high and CFSE-low cells for characterization and further analysis (Figure 3.1B). Under fluorescent microscopy, single CFSE label retaining cells are visible within spheres (Figure 3.1 C).

Previous work from our laboratory has demonstrated increased resistance to traditional forms of chemotherapy in CFSE-high slow-cycling cancer cells (Chapter 2) (120). To determine important signaling pathway regulators that allow slow-cycling cancer cells to better evade the cytotoxicity of chemotherapy, we designed a quantitative PCR (qPCR) array to assess differences in mRNA expression for 93 cell cycle regulators, stem cell related genes, and survival associated genes. Using Fluorescence Activated Cell Sorting (FACS) we live sorted CFSE-high and CFSE-low cells from the colon tumor line HCT116 (*in vitro* n=2, *in vivo* n=3), the breast tumor line MDA-MB-231(n=3), two primary patient derived colon tumors (designated 48116 and 2953T, n=1 for each), and one primary patient derived breast tumor (designated 2597T, n=1), isolated mRNA, and used the subsequent cDNA to perform the qPCR array. Although tumor material limited

Figure 3.1: Identification of slow-cycling cancer cells

(A) To identify slow-cycling cancer cells, cultured cell lines or tumors are digested into single cells and then label CFSE. *In vitro* analysis is performed by replating cells in sphere media while *in vivo* analysis is done by mixing cells with matrigel and injecting into the mammary fat pads of mice. During a chase period, cell populations expand with rapidly proliferating cells diluting label and slow-cycling cells retaining label. At the end of the chase period, spheres and tumors are for ready assay to characterize slow-cycling cancer cells. (B) Representative flow cytometry plot for HCT116 *in vitro* sphere cultures after seven days of chase. CFSE-high cells (green box) are identified as the cell population that is approximately ten-fold higher in CFSE intensity than CFSE-low cells (blue box). (C) Representative bright-field and fluorescent overlay of an HCT116 sphere after seven days pulse/chase with CFSE. Individual CFSE retaining cells (white arrows) are visible within the sphere.



primary tumor data to a single array, when comparing label-retaining cells to bulk tumor cells, label-retaining cells did consistently demonstrate greater than 2-fold increase in expression of the anti-apoptotic factor BCL2 and the CDK5 activator p35. These differences were observed within not only tumors of the same tissue of origin, but for both tumor types (Table 3.1). Interestingly, the array results did not suggest activation of any specific pathways like Notch or Wnt that might be tied with stem-ness, cycling speed, or cell survival (Table 3.1 and Appendix II). Additionally, the array analysis did not suggest consistent differential regulation of known quiescence regulators such as CDKN1A (p21), CDKN2A (p16), or NFAT1c.

Expression of p35 Regulates Cell Cycle Progression

Given the ability for p35 to slow the cell cycle of neuronal cells (14, 16), we explored what role p35 might play in the context of slow-cycling cancer cells. First, we created puromycin selected HCT116 cell lines stably expressing small hairpin RNAs (shRNAs) targeting p35 (constructs identified as shp35-G6 and shp35-G8). We additionally created HCT116 cells transiently transfected with a p35 expression construct driven by the CMV promoter (identified as CMV-p35). Analysis of p35 expression by qPCR indicated that with either clone of the p35-shRNA construct, transduced cells expressed approximately half the p35 transcripts as the control (Figure 3.2A). After transfection with the over-expression construct, p35 was increased ~ 20 fold more transcript than empty vector transfected cells. It is important to note that array data indicate a range of over-expression in slow-cycling cells from ~2-7 fold, suggesting that

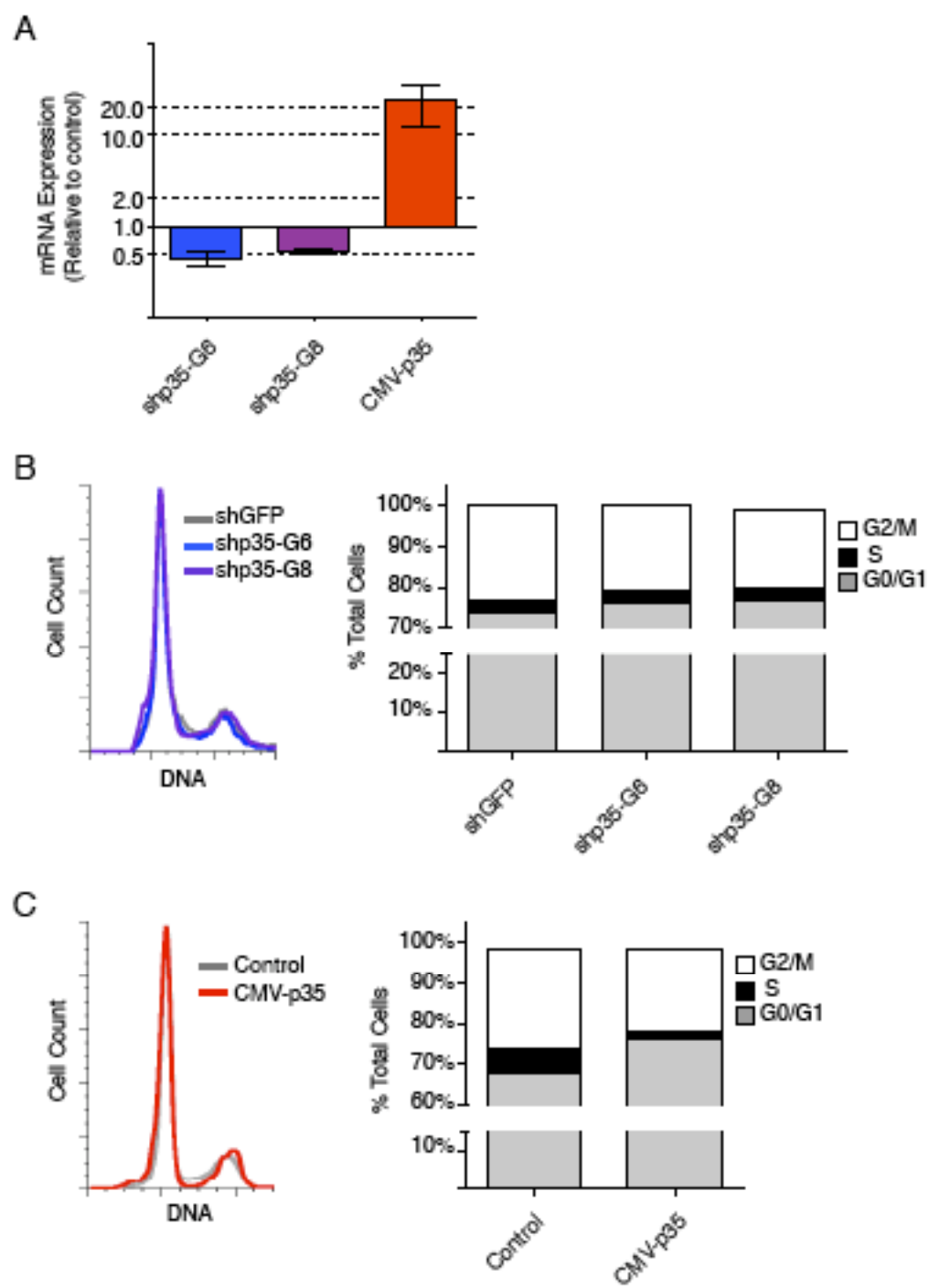
Table 3.1: BCL2 and p35 are up-regulated in slow-cycling cancer cells

	HCT116 <i>in vitro</i>	HCT116 <i>in vivo</i>	2953T	48116	MDA231	2597T
BCL2	3.05	3.67	1.89	2.38	5.74	3.43
CDKN1A	2.65	2.45	1.00	0.77	1.49	2.56
CDKN2A	2.52	1.18	0.97	0.79	2.37	1.36
NFAT1c	3.70	1.97	0.94	0.63	1.22	2.29
NOTCH1	3.89	1.43	0.74	0.54	2.00	-
NOTCH2	1.15	3.93	0.78	0.70	1.02	1.07
p35	2.63	2.39	7.09	3.81	1.79	6.57
WNT1	3.18	1.13	0.62	0.36	0.82	1.48

Value indicate fold CFSE-high expression relative to CFSE-low

Figure 3.2: p35 slows the cell cycle

(A) HCT116 colon tumor cells were transduced with shRNA vectors targeting p35 (two different constructs G6 and G8) or transfected with a vector a CMV promoter driving p35 over-expression. shp35 clones had approximately half the p35 transcript expression of shGFP controls. CMV-p35 HCT116 cells had approximately 20-fold the p35 transcript expression as empty vector transfected cells. (B) Representative cell cycle analysis of shp35 HCT116 clones (blue and purple) compared to shGFP control cells (grey). No difference was observed between the clones (n=2). (C) Representative cell cycle analysis of CMV-p35 transfected cells (red) and untransfected controls (grey). CMV-p35 expressing clones had fewer cells within S phase compared to controls (n=3).



a 20 fold increase in expression may be above physiological relevance and that potential off target effects may be possible.

When cell cycle analysis was performed on these populations, relative to the shGFP control, the loss of p35 did not significantly change the cell cycle profile (Figure 3.2B). In contrast, over expression of p35 shifted cells out of the S phase of the cell cycle and into the G0/G1 phase (Figure 3.2C).

Expression of p35 Regulates Survival after Chemotherapy

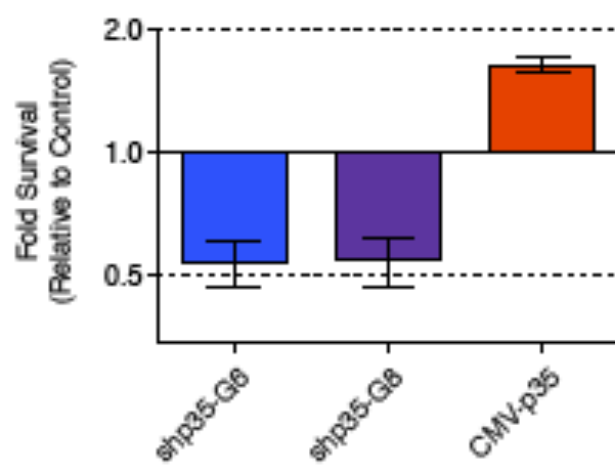
We next explored the effect of p35 levels on the ability of cells to resist the cytotoxic effects of chemotherapy. Using shp35 and CMV-p35 HCT116 clones, we plated single-cell suspensions in either DMSO or the drug combination of 250 μ M 5-Fluorouracil and 2 μ M Oxaliplatin (FOX). This drug combination is consistent with the standard of chemotherapy treatment for patients with colon carcinoma. Compared to the shGFP control, shp35-expressing cells demonstrated increased cell death, with only half the number of cells surviving treatment (Figure 3.3). In contrast, almost two-fold more cells survived chemotherapy in p35 over-expressing cells compared to empty vector controls. This data suggests a protective role for p35 in response to traditional a form of chemotherapy in HCT116 colon tumor cells.

Expression of p35 and Pathway Activity

Understanding the pathways controlled by p35 in slow-cycling cells is an important step to determine how p35 might lead to increased therapy resistance and cell

Figure 3.3: p35 regulates chemotherapy resistance

HCT116 shp35 clone spheres and adherent CMV-35 clones were treated with DMSO control or FOX drug combination (250 μ M 5FU and 2 μ M Oxaliplatin) for three days. At the end of treatment, cultures were digested to single cells and counted for live cells via trypan blue staining. Relative to shGFP control, both shp35 construct expressing cell lines had approximately half the surviving cells. In contrast, CMV-p35 transfected cells had almost two-fold more surviving cells than CMV-empty control cells.

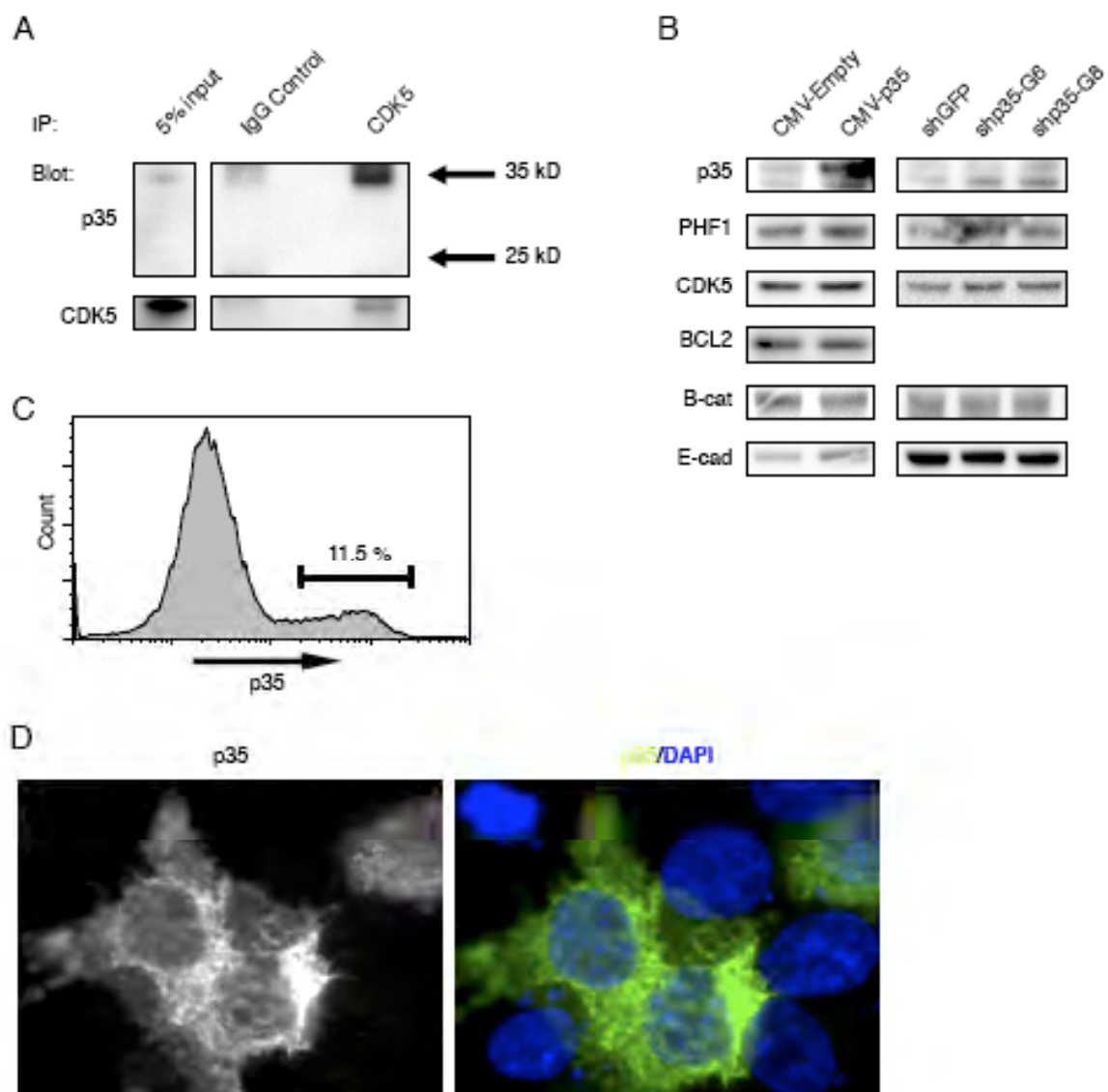


cycle control. We first wanted to determine if p35 is binding to activate CDK5 or if it could be functioning independently of this complex. To confirm that p35 does in fact bind to CDK5 in HCT116 tumor cells, we performed an immunoprecipitation (IP) with an antibody against CDK5 and probed for p35 by western blot (Figure 3.4A). Compared to IgG controls, the full-length form of p35 was successfully pulled down. This data confirms complex interaction between CDK5 and p35 and suggests that interaction is primarily with the full-length 35 kD form.

We next wanted to determine if we could detect differences in the presence and activation of p35/CDK5 targets when levels of p35 were altered. Phosphorylation of Tau at both Ser-396 and Ser-404 are well established targets of p35/CDK5 and are recognized by the PHF-1 antibody (100). When knockdown and over-expression clones were analyzed by western blot to look for changes in PHF-1 levels, we were unable to detect any significant change between the clones and relevant controls. These data suggest that p35 may not act significantly on Tau in slow-cycling cancer cells (Figure 3.4B). p35 is also known to play an important role in β -catenin phosphorylation and E-cadherin endocytosis, allowing for differentiating neuronal cell migration away from the niche (98). Western blots revealed that levels of β -catenin and E-cadherin did not change between shp35 and CMV-p35 expression clones on a global scale. These data suggest that p35 may not play a significant role in the regulation of β -catenin and E-cadherin protein levels within cancer cells. Lastly, we looked for changes in BCL2 levels within our p35 clones. As with Tau, β -catenin, and E-cadherin, we did not see any significant change in total protein level by western blot.

Figure 3.4: p35 in cancer

(A) Western blot probing for p35 following immunoprecipitation with anti-CDK5 antibody in HCT116 cells. CDK5 is able to pull down the 35 kD form of p35 but not the p25 kD form. (B) Western blot of HCT116 shp35 and CMV-p35 clones evaluating protein expression of potential p35 binding partners and targets. No significant changes were observed in phosphorylation of PHF1 (p-tau), CDK5, BCL2, β -catenin, or E-cadherin across all clones in relation to controls. (C) Representative flow cytometry expression profile for HCT116 CMV-p35 transfected cell lines. Expression of p35 is only highly up-regulated in 11.5 % of cells. (D) p35 localization in transfected cells. Staining is in a lattice-like pattern consistent with cytoskeletal association.



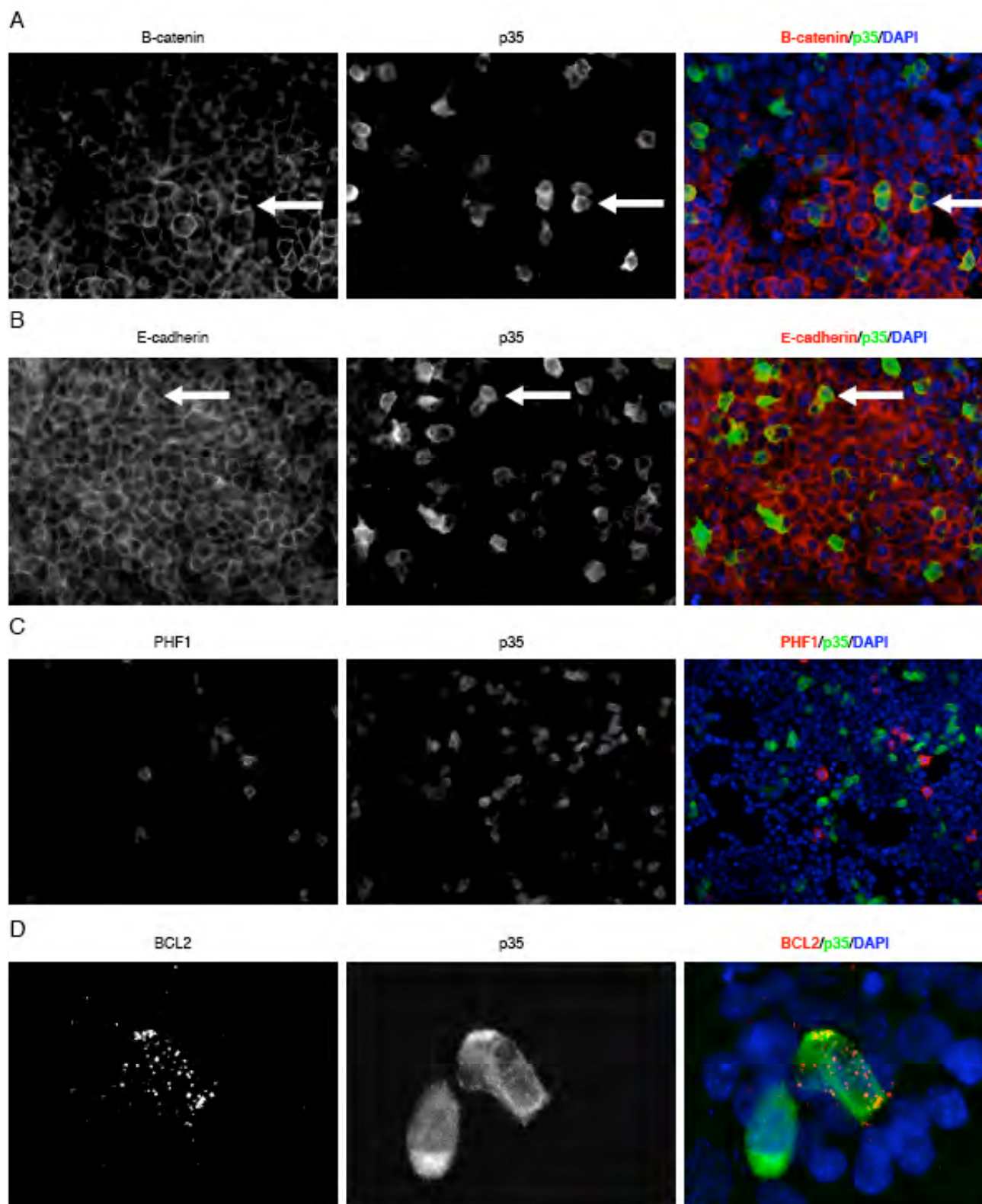
In contrast to the puromycin selected shRNA clones, low transfection efficiencies of our CMV-p35 vector (~10%) may not sufficiently change p35 target levels on a culture wide scale (Figure 3.4C). By immunofluorescent staining, CMV-p35 expressing cells appeared to have p35 localized to both the cytoplasm and nucleus of the cell in patterns consistent with findings by other groups (Figure 3.4D) (96, 99, 128, 130). Staining for p35 within the cytoplasm was very intense, with lattice-like staining features that suggest association with the cytoskeleton. Modest p35 nuclear staining was present, but was less intense than cytoplasmic staining, suggesting localization to the nucleus and the potential to regulate cell cycle progression as observed in our cell cycle profiles.

To evaluate the effect of p35 over-expression on potential p35 targets on a single cell scale, we performed immunofluorescent (IF) co-stains on CMV-p35 cells with anti-p35 antibody and antibodies against β -catenin, E-cadherin, PHF-1, or BCL2. IF staining did not result in any observable differences in the expression level or localization of the β -catenin or E-cadherin proteins when compared to adjacent non-transfected cells (Figure 3.5 A and B). These data support the western blot data and suggest that p35 may not have significant roles in β -catenin and E-cadherin localization or expression levels in slow-cycling cancer cells and may function in a context dependent manner unique from established functions in neuronal precursor cells.

To evaluate changes in phosphorylation of Tau Ser-396 and Ser-404 in p35 over-expressing cells, we co-stained with both p35 and PHF-1 targeting antibodies. Surprisingly, PHF-1 positive staining cells were exclusively negative for p35 staining, suggesting that p35 may not act on Tau in slow-cycling cells (Figure 3.5 C).

Figure 3.5: p35 target regulation

Immunofluorescent staining of HCT116 CMV-p35 clones for p35 (green) and potential p35 targets (red) counterstained with DAPI (blue). Cells expressing p35 (white arrows) did not demonstrate altered β -catenin (A) or E-cadherin (B) expression compared to untransfected cells. (C) Expression of p35 also did not overlap with PHF1 staining (p-tau). (D) Cells positive for p35 staining have increased BCL2 puncta compared to adjacent untransfected cells.



Most importantly, we co-stained CMV-p35 transfected cells with antibodies against BCL2 and p35. In contrast to our western blot data, we observed increased punctal staining of BCL2 in a high percentage of cells over-expressing p35 (Figure 3.5 D). These data suggest that p35 may act through one of the mechanism reported by other groups to localize or stabilize BCL2 protein levels in slow-cycling cancer cells (15, 97). These findings also help to explain why western blots did not detect significant increase in BCL2 expression in CMV-p35 clones. The increased expression of p35 in the relatively low percentage of transfected cells is likely not substantial enough to increase BCL2 protein expression in total culture lysates.

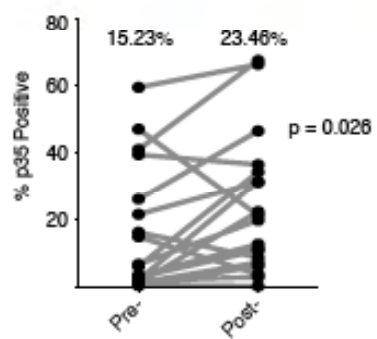
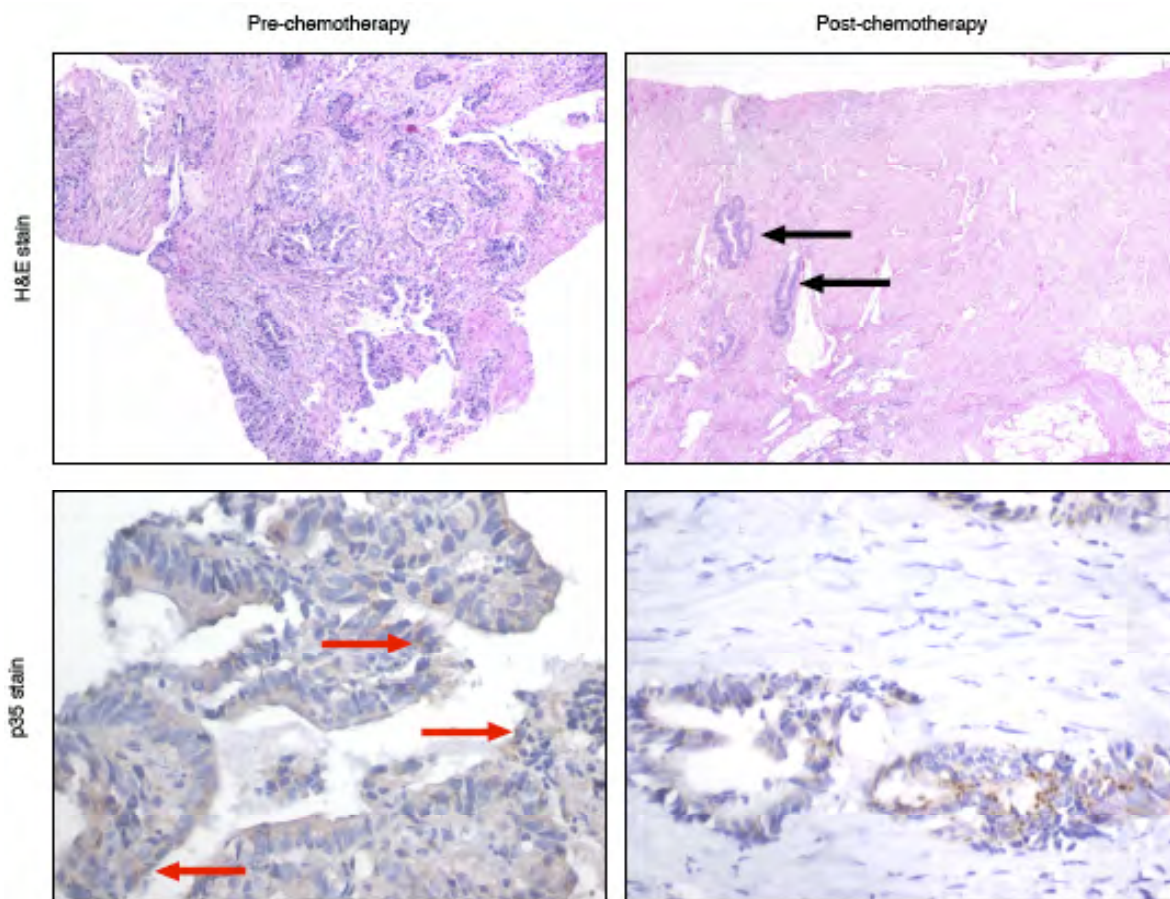
Expression of p35 Increases after Chemotherapy in Primary Tumors

To determine whether p35 may play a role in therapy resistance in cancer patients, we obtained pre-chemotherapy treatment biopsies and post-chemotherapy treatment surgical samples from 20 patients with rectal tumors. Rectal cancer patients receive very consistent therapeutic treatments, limiting potential discrepancies caused by differences in treatment protocols. Additionally, the tissue structure of the rectum is similar to that of the colon and likely to utilize similar regulatory patterns that may be carried over into tumors.

Epithelial tumor glands and high nuclear to cytoplasmic ratio cells was readily apparent on pre-treatment biopsies (Row 1, Figure 3.6). In contrast, post-chemotherapy epithelial tumor gland staining was greatly reduced, leaving isolated outgrowths of resistant tumor cells surrounded by fibrotic scar tissue (Black arrows, Figure 3.6). When

Figure 3.6: p35 expression increases post-chemotherapy in rectal cancers

Pre-chemotherapy tumor biopsies and post-chemotherapy surgical samples were collected from 20 patients with rectal tumors. H&E staining (Row 1) of pre-chemotherapy tumors (Column 1) demonstrates that tumors have a high quotient of epithelial cells (purple). Post-chemotherapy (Column 2), samples were primarily fibrotic (pink) due to scarring from treatment with only few outgrowths of surviving epithelial cells (black arrows). Immunohistochemical staining for p35 (Row 2) revealed the presence of rare p35 expressing cells (red arrows) in pre-chemotherapy samples. Prevalence of p35 positive cells increased in post-chemotherapy samples. When counted and quantified across all samples, expression of p35 significantly increased post-chemotherapy (15.23 % to 23.46 %, $p = 0.026$).



tumor sections were immunohistochemically stained for p35, rare cells were positive for cytoplasmic p35 puncta pre-chemotherapy (Red arrows, Figure 3.6) while more cells were positive for p35 staining post-chemotherapy. When all tumor samples were analyzed, there was a statistically significant increase in p35 staining ($p = 0.026$) across all 20 samples. Interestingly, staining for p35 primarily appeared to be localized to the cellular surface of the plasma membrane in puncta, suggesting localization to an undetermined cellular structure (Figure 3.6).

Discussion

Previous work from our laboratory has demonstrated the existence of therapy resistant, slow-cycling cancer cells. Our efforts to identify differentially regulated transcripts between slow-cycling cells and rapidly proliferation cells using a qPCR array revealed consistent over-expression of the CDK5 activator p35, a relatively poorly studied protein in cancer. The observation that p35 was over-expressed in not only tumors from an individual tissue of origin, but from tumors derived from multiple tissues, suggests that p35 activity may be a broadly used regulatory factor in maintaining slow-cycling cancer populations (Table 3.1).

Consistent with the idea that p35 helps to maintain the slow-cycling phenotype of cancer cells, we observed a decline in S phase cells when p35 was over-expressed (Figure 3.2C). Interestingly, observations for the role of p35 on the cell cycle are not consistent throughout the literature. The ability for p35/CDK5 to regulate E2F or p27 and suppress the cell cycle is inline with our observations of a decline of cells in S phase (14, 15). In

contrast, other studies suggest a much different role, with p35 acting to push cells out of the G1 phase and into S phase and a G2/M arrest (131, 132). It is likely that the localization and activity of p35/CDK5 may act as a gatekeeper into S and G2/M, with nuclear localization slowing the cell cycle and cytoplasmic localization and degradation allowing passage into S phase. In neurons, Zhang *et al.* determined that CDK5 must be ubiquitinated and degraded in order for cells to progress into S phase (133). This ubiquitinylation can be inhibited by p35 and suggests a mechanism within slow-cycling cancer cells that could explain the loss of cells actively progressing through S phase and their retention in the G1 phase of the cell cycle.

The broad range of proposed targets and functions of p35/CDK5 suggests a number of possibilities for the role of p35 over-expression in slow-cycling cancer cells. Curiously, we did not see evidence that p35/CDK5 may be acting on some of the more strongly associated targets like Tau, E-cadherin, and β -catenin (Figure 3.4 B and D). In migrating neurons, p35 is demonstrated to free β -catenin from adhesion complexes, resulting in a re-localization away from the plasma membrane and potential endocytosis and degradation of E-cadherin (98, 124). No change in localization pattern of either protein was observed during IF staining. Several possibilities exist that may explain these observations including differences in CDK5 dependent and independent functions of p35 or differences in targets of full length p35 versus the cleaved form. Western blot and immunoprecipitation experiments in cancer cells suggest that p35 is present primarily in the full-length form and that only a modest portion of this exists in complex with CDK5 (Figure 3.4A). This data would suggest that the CDK5 independent functions of

p35 like E-cadherin down-regulation could be favored (98). Nevertheless, we see little evidence for this type of activity. Alternately, these observations may represent a context dependent functional shift in p35/CDK5 activity, unique to the tissue or cancer environment and availability of upstream and downstream signaling partners. Future work will further clarify and address these questions.

Perhaps the most interesting and relevant finding is the association with p35 and cancer cell survival when treated with chemotherapy. Expression of p35 increased cell survival after chemotherapy treatment, suggesting a protective role for p35 (Figure 3.3). Mechanistically, p35 protection may be due to interaction and stabilization with BCL2. Our striking IF data suggests a link between p35 expression and an increase in BCL2 protein (Figure 3.4E, Row 4). The clear puncta staining of BCL2 may indicate subcompartmental localization, likely to the mitochondria. Curiously, p35 IHC staining of rectal cancer samples also resulted in cytoplasmic puncta staining and may suggest localization of p35 and subsequent stabilization of BCL2 at the mitochondria of rectal cancer cells (Figure 3.6). Stabilization and activation of BCL2 by the p35/CDK5 complex has been demonstrated through BCL2-p35 direct interaction and indirect interaction via the Erk pathway, suggesting that such protein interactions could be active in cancer cells (96, 97). Slow-cycling tumor cells with increased p35 expression may elicit the opposite response, increasing resistance to apoptotic stimuli and ultimately protecting from cell death. This data suggests that p35 may be an important factor in the BCL2 regulation in slow-cycling cancer cells.

Initial profiling arrays between CFSE-high and CFSE-low cells identified p35 and BCL2 as the only two mRNA transcripts up-regulated throughout all the samples tested. While a connection between p35 and BCL2 is well established on the protein level, to date there is little evidence linking p35 activity to BCL2 transcription. It is unclear if a link exists, or if this signature represents yet another layer of uncovered regulatory programming.

In conclusion, this work identifies the CDK5 regulator p35 as up-regulated in slow-cycling tumor cells. We find that expression of p35 in HCT116 colon cells is linked to increased chemotherapy resistance and expression of the anti-apoptotic protein BCL2. Based on these findings, future work targeting p35 in combination with chemotherapy is worth exploring. Ultimately, our work indicates future targeting of p35 via small molecule inhibition during and after chemotherapy may provide the means to target and eliminate therapy resistant cells, improving treatment efficacy and saving the lives of cancer patients.

Chapter IV:

Slow-cycling Cancer Cells and Cancer Stem Cells

Abstract

Cancer stem cell populations have been identified in epithelial tumors from the colon, breast, brain, prostate, and other cancer types. Generally, these cell populations are identified using membrane markers such as CD133 and CD44; or functional assays such as cellular pump activity that have been associated with increased tumor-initiating capabilities. We have determined that subsets of slow-cycling cells exhibited tumor-reactivating abilities when live sorted and regrown as spheres or as tumors in mice. Despite these findings, slow-cycling CFSE label retaining cell populations are not enriched for expression of some of the most commonly used cancer stem cell markers. Our work suggests that slow-cycling cells, while not enriched for classical CSC markers, retain the ability to promote tumor formation and re-growth.

Introduction

The existence of cancer stem cells (CSCs) was first demonstrated in leukemia by Bonnet and Dick in 1997 (56). Since that discovery, CSC populations have been discovered in a multitude of other cancers from tissues including the colon (59-61), breast (52), brain (63), prostate (57), pancreas (58), and ovaries (62). All cancer stem cell populations share three defining traits: first, they are long lived and self-renew throughout the existence of the tumor; second, they possess the potential to proliferate

indefinitely; and third, they can generate daughter cells with the ability to differentiate into any of the heterogeneous cell types found within the initial tumor. Given these necessary traits, it is possible that CSCs are a result of the oncogenic transition of healthy adult stem cell populations. Over time, mutations from inflammation, free radicals, and radiation/chemical exposure can accumulate to transform healthy adult stem cells into CSCs (48, 102).

Similar to the role that adult stem cells play in maintenance of tissue homeostasis, CSCs are thought to be important for tumor homeostasis and longevity. Under the CSC model, as rapidly proliferating transit amplifying tumor cells drive tumor growth they eventually exhaust proliferative potential. CSCs, with the ability to self-renew, undergo asymmetric division, produce new transit amplifying cells that continue to drive tumor expansion (54). This importance in tumor homeostasis identifies CSCs as ideal therapeutic targets. By better targeting CSCs or blocking CSC proliferation, the major driving force behind tumor growth and expansion could be eliminated. Therefore, the identification and isolation of CSCs for further study is incredibly important in the fight against cancer.

One standard method of CSC identification involves isolating the cell population of interest from the tumor and looking for tumor initiating capability in immune-compromised mice. Traditionally, CSCs in these populations are identified using membrane markers that appear to be enriched for tumor initiating capability. Bonnet and Dick discovered that the marker combination $CD34^+CD38^-$ identified leukemia stem cells with the unique ability to initiate leukemia (56). In some epithelial tumors like

those from the brain and colon, CD133⁺ cells are identified as enriched for the tumor initiating phenotype (60, 63). In other epithelial tumors like the breast and pancreas, varying CD44 and CD24 combinations appear to enrich for CSC (52, 58). In recent years however, markers for potential CSC populations have become increasingly numerous. For example, potential colon CSC markers have expanded to including CD44, EpCAM, ALDH, CD166, Lgr5, Bmi1, and others (134-136). However in many cases, it is unclear how and if these populations overlap, obscuring the importance and significance of any one marker. Additionally, the functional significance of many of these markers is unclear, with limited data suggesting these markers may have roles in self-renewal and proliferation, chemoresistance, migration, and engraftment potential (66). For example, the frequently used CD44 marker is regulated by stem cell associated Wnt and Notch signaling (137-139). Functionally, CD44 expression may support migration and chemotherapy resistance; both important characteristics for CSC associated populations. Additionally, CD133 appears to have connections with asymmetric cell division and multipotency, classic stem cell traits that promote tissue homeostasis and longevity (140, 141). Finally, ALDH is linked to cellular responses to stress and drug metabolism, suggesting roles in therapy resistance and survival (142, 143). ALDH may serve to protect CSC populations from cell stress associated with rapidly expanding tumor environments or cytotoxic chemotherapeutic agents.

Unfortunately, none of these markers have been conclusively demonstrated to induce the CSC phenotype. Like other CSC markers, CD133 colon tumor cells may be

enriched for the CSC phenotype but does not uniquely identify CSCs. To date, no individual marker has been demonstrated to confer tumor-initiating capabilities.

Apart from membrane-associated markers, functional readouts like cellular pump analyses have also been reasonably successful at identifying CSC populations in tumors from the brain, breast, prostate, intestine, and ovaries (144-147). By staining populations of cells with fluorescent dyes like Hoechst 33342, subsets of cells with increased cellular pump activity (such as ATP binding cassette transporters) pump out the dye and move away from the “main populations” towards the negative field on a flow cytometry plot, into a “side population”. Functionally defining CSCs in this way may provide critical insight into how these cells respond to various therapeutic approaches. For example, increased pump activity is likely to effect chemotherapy uptake and retention, thus decreasing DNA damage and the subsequent apoptosis caused by these drugs (148). Further study of these populations is therefore important in battling therapy resistance and tumor recurrence.

In this study, we characterize CFSE retaining, slow-cycling cancer cells in the context of a number of classic CSC markers using gene expression analysis. Additionally, we assay CFSE pulse/chased cells in relation to the side population because of the strong links to chemotherapy efflux. Finally, we assay for the CSC phenotype by live sorting *in vitro* and *in vivo* CFSE-high and CFSE-low populations and directly assessing tumor initiating capabilities with limiting dilution assays. While previous functional characterization of CFSE retaining cells and therapy resistance are relevant regardless of the marker status of the cells themselves, understanding how slow-cycling

cells fit into previously identified CSC populations is important in understanding their overall significance in the context of CSC biology.

Results

Slow-cycling cells are not enriched for common CSC markers

To place slow-cycling CFSE-retaining cells in context of other CSC markers, we performed quantitative PCR (qPCR) to detect variations in marker mRNA expression. CFSE pulse/chased samples from either *in vitro* spheres from the colon tumor line HCT116 or *in vivo* tumors from the tumor line HCT116, breast line MDA.MB.321, primary colon cancer samples 48116 and 2953T, or primary breast cancer sample 2597T were live sorted into CFSE-high and CFSE-low populations. RNA and subsequent cDNA extracts from the resulting cells were used to conduct qPCR assays to analyze for differences in expression of potential CSC markers CD133, CD44, and the colon stem cell markers Lgr5 and Bmi1. Most tumors demonstrated increased expression of many markers in CFSE-high cells, however, we did not observe consistent differences of greater than two-fold for any of the markers analyzed (Table 4.1). This data suggests that there is no clear pattern of surface marker expression linked with the slow-cycling phenotype.

To confirm these findings on the protein level, CFSE pulse/chased HCT116 *in vitro* spheres and *in vivo* tumors were digested to single cells and stained with antibodies against CD133, CD44, and ALDH. It is worth noting that the standard assay for measuring ALDH activity is actually a fluorescent substrate-based metabolism assay, but

Table 4.1: Slow-cycling cells are not enriched for CSC mRNA

	HCT116 <i>in vitro</i>	HCT116 <i>in vivo</i>	2953T	48116	MDA231	2597T
BMI1	1.52	1.16	0.82	1.03	2.39	1.59
CD133	1.94	1.04	0.84	1.16	0.89	2.69
CD44	2.25	1.22	0.91	1.21	2.05	1.74
LGR5	3.16	1.33	0.91	1.10	1.91	3.07

Values indicate fold CFSE-high expression relative to CFSE-low

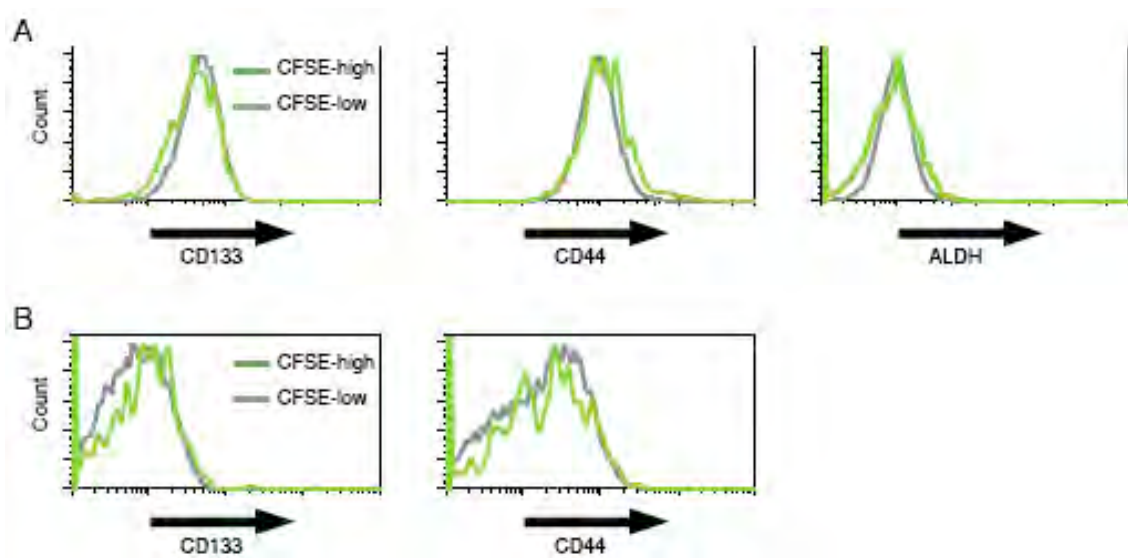
the only commercially available dye for this assay conflicts with the CFSE label. When CFSE-high and CFSE-low cells were separated by fluorescent analysis and the two populations were examined for marker intensity, we did not see any reproducible significant difference for either the *in vitro* (Figure 4.1A) or *in vivo* (Figure 4.1B) populations. This data confirms the initial array data and further suggests that there is no difference in expression of these CSC markers between slow-cycling cells and rapidly proliferating cells for the HCT116 colon line.

Slow-cycling cells are not enriched in the side population

Given the chemotherapy resistance phenotype of slow-cycling cells observed in earlier studies (120), we next asked if slow-cycling cells demonstrate increased pump activity as part of the side population phenotype. To identify the side population in these cells, we stained CFSE pulse/chased *in vitro* and *in vivo* populations with Hoechst 33342 and analyzed for dye efflux by flow cytometry. For cells found within the side population, cellular pumps remove dye from the cytoplasm, and cells become less fluorescent and move away from the labeled main population (Figure 4.2A). To confirm that the cells identified as the side population are a result of cellular pump activity, control cells were treated with the pump inhibitor Fumitremorgin C (FTC), and the loss of the side population was observed (Figure 4.2A). When the main population and side population were analyzed for CFSE levels, we observed that the side population was comprised of approximately one-half the percentage of CFSE-high cells relative to the main population. These results were consistent for both *in vitro* and *in vivo* HCT116

Figure 4.1: CSC markers do not enrich for slow-cycling cancer cells

HCT116 CFSE pulse/chased spheres and tumors were stained for common CSC markers and evaluated by flow cytometry for marker expression. (A) Representative expression profiles of CD133, CD44, and ALDH marker expression in CFSE-high (green) and CFSE-low (grey) cells *in vitro*. No consistent significant difference was observed between CFSE-high (green) and CFSE-low (grey) cells. (B) Representative expression profiles for *in vivo* CFSE-high and CFSE-low cells for the markers CD133 and CD44. No consistent significant difference was observed.



cells (Figure 4.2 B&C) as well as *in vivo* MDA.MB.231 cells (Figure 4.2D). These data suggest that the side population does not enrich for slow-cycling cells and, in fact, may select against slow-cycling cells. Furthermore, it suggests that the therapy resistant phenotype associated with slow-cycling cells is not due to increased pump activity.

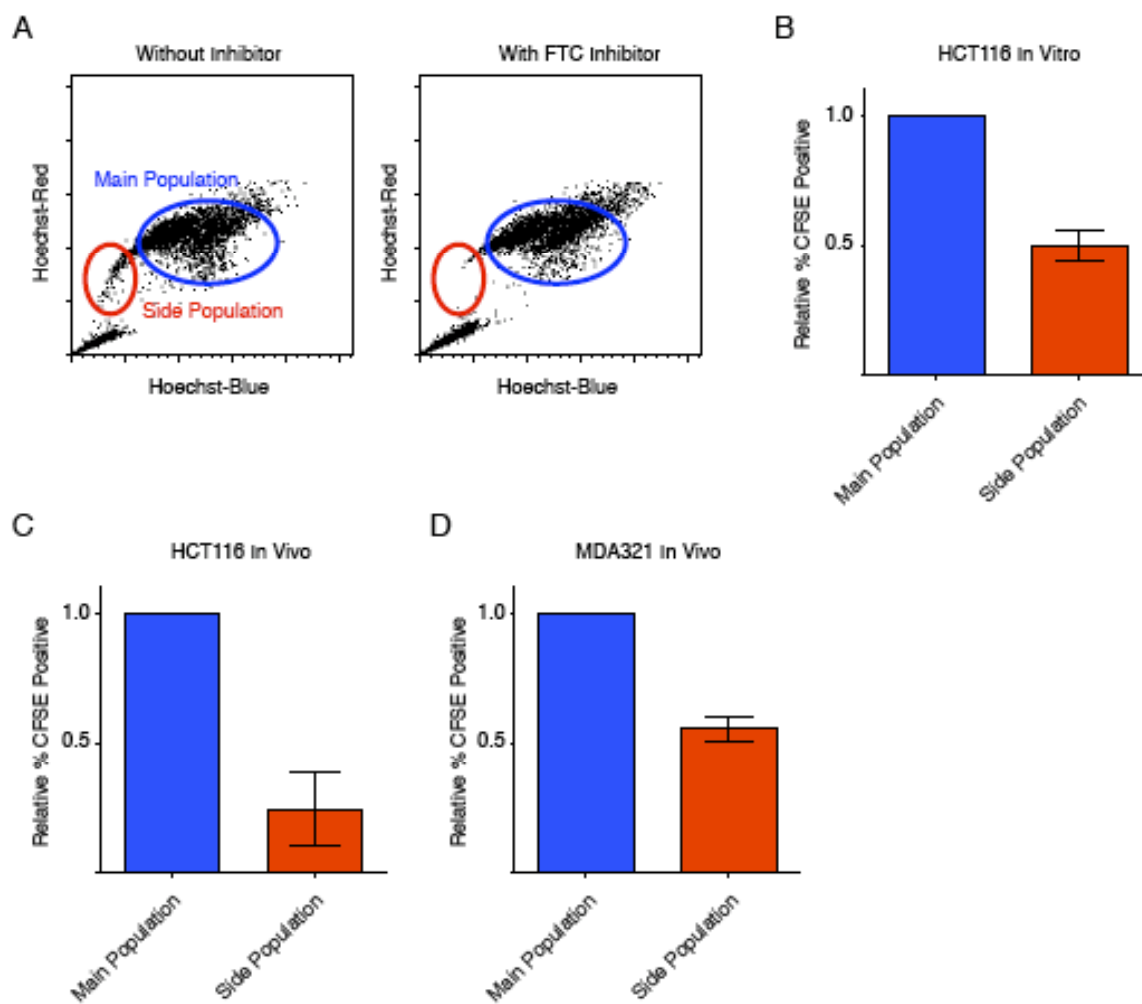
Slow-cycling cells are not enriched for tumor initiating capabilities

While markers and cellular pump activity may enrich for some populations with the CSC phenotype, the defining assay of a CSC is the ability to initiate tumor regrowth. To determine if *in vitro* slow-cycling sphere cells would enrich for the tumor initiating phenotype, we pulse/chased HCT116 spheres with CFSE and live sorted into CFSE-high and CFSE-low populations. Equal numbers of CFSE-high and CFSE-low cells were replated at multiple dilutions in sphere media and incubated under standard conditions. After one week, spheres were counted and analyzed for size by longest dimension. CFSE-high and CFSE-low cells produced equal numbers of spheres at all dilutions (Figure 4.3A). Interestingly, CFSE-high spheres were approximately half the size of CFSE-low cells (Figure 4.3B). These data suggest that slow-cycling and rapidly proliferating tumor cells possess approximately equal tumor initiating potential, although unsurprisingly, slow-cycling, CFSE-high cells proceeded through the cell cycle fewer times over the given period.

To determine if slow-cycling cells were enriched for tumor forming ability *in vivo*, HCT116 tumors and 2597T primary breast tumors were pulse/chased with CFSE, live sorted into CFSE-high and CFSE-low groups, and then reinjected back into immune-

Figure 4.2: Slow-cycling cells are not enriched in the side population

(A) Representative flow cytometry plots of Hoechst stained samples. Cells within the main population (blue) maintain dye while cells with increased cellular pump activity pump out dye and become the side population (red). Population validation is achieved by culturing cells with the pump inhibitor Fumitremorgin C (FTC) and the disappearance of the side population. For all samples (*in vitro* colon HCT116 (B), *in vivo* HCT116 (C) and *in vivo* breast MDA231 (D)), CFSE-high cells were not enriched for the side population. The percentage of CFSE-high cells in the side population was approximately half of the CFSE-high percentage in the main population.



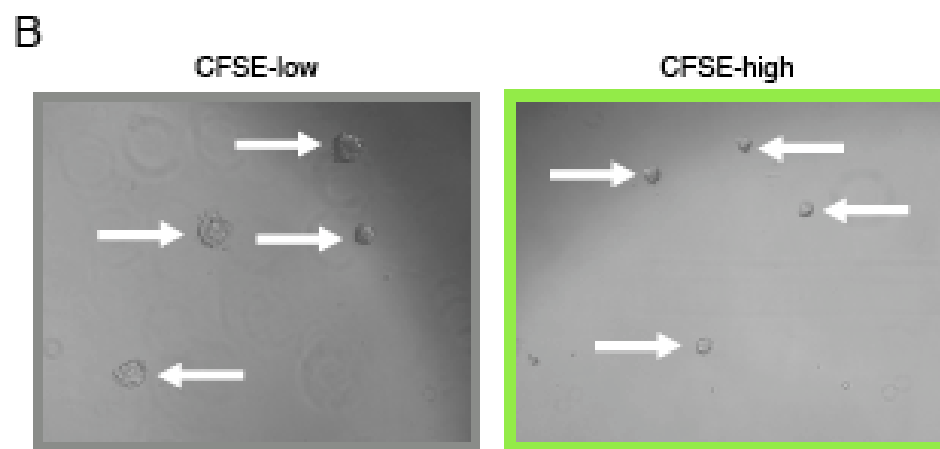
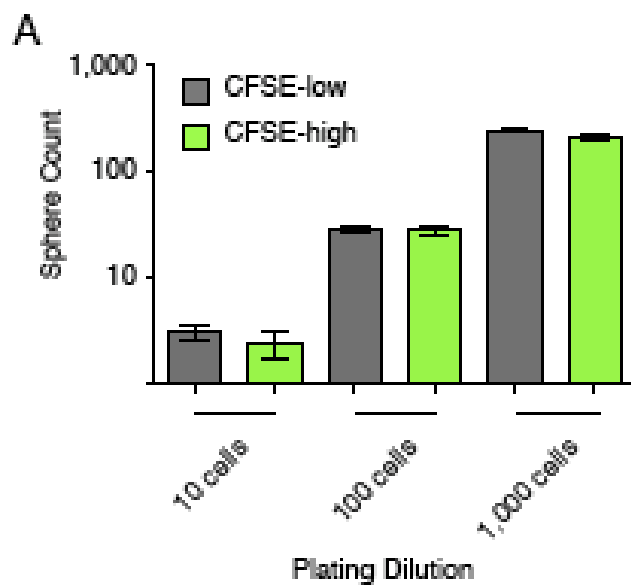
compromised mice for dilution analysis. All tumors for a specific dilution were isolated when the first tumor from the dilution reached 1000 mM³ or three months after injection. HCT116 CFSE-low cells demonstrated the ability to consistently produce tumors with as few as 500 cells (3/3 mice) (Table 4.2). In contrast, HCT116 CFSE-high cells were only able to consistently produce tumors when at least 5,000 cells were injected (3/3 mice), and demonstrated limited ability to initiate tumor growth at 1,000 cells per injections (1/3 mice). When the primary breast tumor 2597T was evaluated for tumor-initiating capability, CFSE-high cells produced a single tumor with 50,000 injected cells, but CFSE-low cells were unable to initiate tumor growth even at 100,000 cell injections (Table 4.2). These data suggest that slow-cycling cells demonstrate tumor initiating ability in at least a subset of cells, but that this initiating ability may not be enriched over that of bulk tumor cells.

Discussion

The relationship between cancer stem cells markers and slow-cycling cells is likely complex and multivariable. CSC surface markers are expressed in slow-cycling cells, but the available evidence from the literature and our data collected in this work does not suggest an exclusive relationship between the two populations (149). It is possible then, that cells moving in and out of the proliferative state may oscillate expression of CSC markers depending on the functional role of the specific marker. For example, the role of CD133 in asymmetric division may suggest increased expression in preparation for cell division, while returning to a baseline expression level during gap and

Figure 4.3: *In vitro* slow-cycling are sphere forming

Live sorted CFSE-high and CFSE-low cells were replated in sphere media at multiple dilutions. (A) After one week, CFSE-high (green) and CFSE-low (grey) cell populations were able to form equal numbers of spheres at all dilutions assessed. (B) CFSE-high sphere diameters (green box) were approximately half the size of CFSE-low sphere diameters (grey box) (81.71 units to 45.43 units, $p < 0.001$).



Avg CFSE-low colony diameter: 81.71
Avg CFSE-high colony diameter: 45.43
CFSE-hi/CFSE-low: 0.56
 $p < 0.001$

Table 4.2: *In vivo* limiting dilution analysis

HCT116		
Dilution	CFSE-high	CFSE-low
5,000	3/3	3/3
1,000	1/3	3/3
500	0/3	3/3
100	0/3	0/3

2597T Breast		
Dilution	CFSE-high	CFSE-low
100,000	-	0/2
50,000	1/2	0/2

synthesis phases. In this way, tumor initiating slow-cycling cells would move into the CD133 positive population just before division in preparation for asymmetric division and return to the CD133 negative population during the rest of the cell cycle and the cell cycle stall. With only a fraction of slow-cycling cells positive for CD133 at any one time, they may not enrich for marker expression at detectable levels.

The HCT116 cells primarily utilized in these studies may not conform to a stem cell model hierarchy associated with any present CSC marker, but may maintain themselves via a stochastic model with no functionally meaningful marker variations (150). Under such a model, slow-cycling cells may then be a dynamic population in which cells transition in and out of the slow-cycling state depending on environmental and cellular cues and independent of CSC marker expression. The HCT116 line highlights the independence of slow-cycling cells from the CSC marker model and suggests that the slow-cycling phenotype may not be as closely linked with the CSC as originally hypothesized.

In contrast, other cell lines do appear to be hierarchically arranged, with stem-like cell populations identified by specific markers. It may then be possible that CSC marker expression within these cells is more functionally relevant. Repeating the analysis from this study in some of these cell lines may be more apt to address how slow-cycling cells definitively relate to CSC markers (68, 151).

Identifying slow-cycling cells as enriched within the side population would associate slow-cycling cells with other CSC populations and suggested a potential mechanism to explain previous data demonstrating increased therapy resistance in slow-

cycling cancer cells. Unfortunately, slow-cycling cells were less frequently found in the side population in relation to the main population (Figure 4.2). While this data indicates that slow-cycling cells do not coincide with previously described CSC populations, it also suggests that cellular pump activity is not contributing to the increased therapy resistance phenotype observed in this cell population.

Combining tumor-initiating potential from both the *in vitro* and *in vivo* data does not present a clear picture of slow-cycling cell tumor-initiating potential. *In vitro* evidence would suggest that both CFSE-high and CFSE-low cells are tumor forming with approximately equal tumor-initiating potential (Figure 4.3). On the other hand, *in vivo* evidence suggests two different answers, with slow-cycling cells both enriching for tumor-initiating cells in the primary breast sample and selecting against tumor-initiating cells in the HCT116 line (Table 4.2). Results from other groups indicate similar patterns to that seen with the 2597T primary breast tumor sample, mainly that slow-cycling cell populations were enriched for the tumor-initiating phenotype over more rapidly proliferating cells (40, 62, 68). Curiously, our *in vitro* data would suggest that slow-cycling HCT116 cells are highly tumor-initiating, leading us only to speculate why *in vivo* cells demonstrated less tumor-initiating potential. While not clearly understood, we suspect that relatively harsh dissociation techniques required to generate single cell suspensions from tumors is likely contributing to the poor tumor-initiating frequency *in vivo*. In comparison to sphere-forming assays that only require rapid and light trypsinization, tumors are first excised from mice then digested for hours in protease, before being heavily mechanically and enzymatically dissociated. These factors are

stressful to cells and likely contribute to a distressed state that may favor poor grafting and proliferation. Isolation of relatively few numbers of slow-cycling cells during live sorts may further affect cell health and grafting ability. Future experiments will need to be aimed at addressing this question in more depth.

In conclusion, our data does not suggest enrichment of slow-cycling cancer cells by any of the popular CSC markers. Additionally, slow-cycling cancer cells do not demonstrate increased cellular pump activity and enrichment within the side population. Regardless of the CSC marker status of CFSE retaining cells, our data demonstrates that at least a sub-population of slow-cycling cells are able to lead to the formation and potential regrowth of tumors.

Chapter V:

Discussion and Conclusions

The existence of slow-cycling adult stem cell populations is important for long-term maintenance of adult tissues. Adult stem cell populations, like those in the breast and colon, have been demonstrated as the cells of origin for many CSC populations that drive tumor growth. As a result of this oncogenic transition, adult stem cell characteristics, like slow-cycling and inherent therapy resistance, are likely retained in CSC populations. Regulation of the slow-cycling phenotype is a complex process that relies on signaling from various stem cell-associated pathways as well as precise interaction between CDKs and their inhibitors, all of which may provide novel targets for cancer therapeutics.

This work utilizes a novel application for the cell proliferation marker CFSE to identify, isolate, and characterize live slow-cycling cancer cells. We demonstrate that slow-cycling cancer cells are present in both cultured cell lines and primary tumors. Additionally, slow-cycling tumor cells were found to have a multi-fold resistance to traditional forms of chemotherapy when compared to bulk tumor cells. Regulation of this resistance phenotype may be due to increased expression of the CDK5 activator p35 and the ability for this protein to interact with anti-apoptotic BCL2. We demonstrate that changes in expression of p35 are associated with similar changes in cell survival in response to chemotherapy treatment. Furthermore, increased expression of p35 was demonstrated to increase BCL2 staining and suggests stabilization of BCL2 by p35.

Immunohistochemical staining of pre- and post-chemotherapy rectal tumors suggest that expression of p35 may have clinical relevance in helping cells survive chemotherapy and potentially lead to recurrence. Finally, we observed that slow-cycling tumor cells did not enrich for commonly used CSC markers, but did demonstrate limited ability to initiate tumor growth independent.

Combined, our work demonstrates the existence of a slow-cycling cancer cell population with limited tumor initiating capabilities and increased resistance to traditional forms of chemotherapy. Importantly, this work identifies a population of cells with the potential to drive tumor recurrence in patients and beings to explore future ways to better target these cells.

CFSE Label Retaining Cells

The use of the fluorescent label CFSE is central to the identification of slow-cycling cancer cells in this body of work. At the onset of this project, the use of CFSE to identify slow-cycling cancer cells was a novel application that offered important differences in previously attempted pulse chase methods: first, CFSE is fluorescent in live cells; second, CFSE binds to internal proteins within the cell and is not subject to asymmetric segregation; and third, CFSE is detectable for up to ten passages after initial staining. Early identification of slow-cycling cells often utilized nucleic acid analogues like BrdU. Identification of these compounds requires the utilization of both antibodies and denaturation of DNA, which kills the cells. Any form of tumor-initiating assay or characterization requiring live cells is not possible using these methods. In contrast, the

fluorescent nature of CFSE provides a means of sorting live cells, allowing for assay and characterization without their destruction.

Interestingly, recent findings suggest that the use of nucleic acid analogues may not always identify cells based on their slow-cycling characteristics. In fact, these labels often identify continuously proliferating cells that asymmetrically segregate DNA, to preserve the original (replication error free) “template strand” (152, 153). The use of DNA analogues in such a cell population would not assay for the slow-cycling phenotype as intended. In comparison, CFSE would still be expected to identify a more slow-cycling cell population regardless of the “template strand” retention phenotype. In light of these discoveries, it may be important to revisit previously identified nucleotide analogue label-retaining cell populations and re-evaluate the mechanisms of label retention and implications.

More recent attempts to study slow-cycling cells have utilized lipophilic fluorescent dyes like the PKH dyes (PKH2, PKH26, PKH67). Membrane fluorescent labels solve many of the problems associated with nucleotide analogues, specifically the ability to track label in live cells. Notably, CFSE offers advantages over these dyes in the method of labeling and processing options. In contrast to the covalent labeling of CFSE to amine groups, PKH dyes are non-covalently bonded (154). These non-covalent bonds are sensitive to solvents and fixatives that may be required in further cell staining or molecular biology techniques. Additionally, these dyes label less homogeneously, potential masking slow-cycling cells.

Slow-cycling Cells and Cancer Stem Cells

The association between slow-cycling cancer cells and cancer stem cell populations has been demonstrated by multiple groups in various tumor types (40, 68, 72). Through limiting dilution analysis, our work demonstrated the ability of *in vitro* slow-cycling cells to efficiently form spheres at rates equal to more rapidly proliferating cells. In contrast, *in vivo* slow-cycling cells were able to initiate tumor growth, but required much higher quantities of cells relative to more rapidly proliferating cells. These findings suggest that unlike a CSC population, slow-cycling cells have equal or diminished tumor initiating abilities compared to bulk tumor cells. Further validating these findings, our slow-cycling cells were not enriched for three of the most commonly used markers for identifying CSC populations.

We conclude that slow-cycling cells are not more stem-like in nature than unsorted or bulk tumor cells. Our data demonstrates that a sub-population of slow-cycling cells is tumor propagating, and suggest that this ability is dependent on cell environment and context. Interestingly, these data imply that the slow-cycling phenotype may not be related to retention of the slow-cycling characteristic from adult stem cells to transformed cancer stem cells during oncogenic transition. Instead, this phenotype may be a naturally occurring process regulated by cell-cell communications and environmental cues with yet undefined purposes. Alternatively, the generation of slow-cycling cells may be a secondary effect of other tumor processes such as moving in and out of a proliferative state due to EMT as described by Dembinski and Krauss (72).

Whether the slow-cycling cell phenotype remains important for long-term tumor maintenance and homeostasis as observed in adult tissues is unclear.

Importantly, the inability to define slow-cycling cells as cancer stem cells is inconsequential to the major biological findings throughout this body of work. We demonstrate a slow-cycling population of cells with increased chemotherapy resistance and the ability to progress through the cell cycle following the cessation of treatment. These traits identify slow-cycling cells as potential drivers of tumor recurrence regardless of marker status and the ability to enrich for tumor initiating cells.

Profiling Slow-cycling Cancer Cells

The qPCR array used to assay transcript differences between CFSE-high and CFSE-low cell populations was focused on identifying potential changes in stem cell associated pathway activities and families of proteins that may regulate slow-cycling and survival. Primarily of interest, this array looked at many of the CDKs including CDK 2,4,and 6, as well as CKIs including CDKN1A (p21), CDKN1B (p27), CDKN2A (p16). Additionally, the array analyzed other cell cycle and quiescence related factors like PCNA, NFAT1c, and Rb. Surprisingly, even factors with strong support in published literature for slow-cycling cell regulation, like p21, did not demonstrate consistently significant differences across all samples, suggesting that different mechanisms of slow-cycling cell regulation may be at work. It is possible that patterns of regulation may exist within specific cell lines or across tumor types. Both *in vitro* and *in vivo* HCT116 colon slow-cycling cells had increases in p21 expression relative to bulk cells, while both breast

tumor derived slow-cycling cells (MDA231 and 2597T) had increases in p16 expression relative to bulk cells. In contrast to these results, the two primary colon tumors did not demonstrate meaningful differences in any CKI or cell cycle related CDKs. These data suggest that regulation of the slow-cycling phenotype may be tumor dependent, with different mechanisms converging to produce slow-cycling cells. These observations imply an important role for slow-cycling cells in cancer homeostasis, while presenting great difficulty in identifying targets and creating applicable therapeutics to eliminate slow-cycling cells. Alternate regulation of slow-cycling cells between tumor types may require identification and implementation of unique drugs for each mechanism for slow-cycling regulation.

Most importantly, the consistent over-expression of p35 (CDK5R1) across all samples suggests that a novel, poorly understood mechanism of cell cycle control may be contributing to the slow-cycling cell phenotype. A single mechanism is further supported by the consistent up-regulation of BCL2 and its established relationship with p35. Conserved p35/CDK5 and BCL2 activity across tumors from multiple subtypes and organs suggests an essential underlying function of this complex. Clinically, a single underlying mechanism for slow-cycling cells may make possible the use of a single therapeutic agent aimed at p35/CDK5 activity that would be applicable across a broad range of tumors.

Knockdown of p35 in Slow-cycling Cancer Cells

Throughout this study, we consistently observed little change in cell cycle profile or effect on p35 target genes in cells with down-regulated p35 signaling. Two likely explanations exist to explain these findings: first, that because the use of shp35 vectors resulted in ~50% loss of mRNA transcripts, the overall p35 protein may still be biologically significant or unchanged, or second, that loss of p35 only affected the small population of slow-cycling cells and that the resulting global changes were undetectable. Both of these hypotheses could explain why western blots failed to detect changes in p35 targets when p35 is down-regulated. If, for example, p35 can lead to the endocytosis and degradation of E-cadherin in cancer cells (98), under the first hypothesis the remaining p35 protein is still sufficient to reduce E-cadherin resulting in equal E-cadherin expression to shGFP controls. Under the second hypothesis, p35 would only be down-regulated in the 2-4% of slow-cycling cells and with the relative insensitivity of western blotting techniques, the resulting minor E-cadherin increase would not be distinguishable.

In support of the second hypothesis, we did observe a difference between shp35 clones and the shGFP control when cultures were treated with chemotherapy. By killing off a large percentage of our cells with chemotherapy we enrich for the slow-cycling (presumably p35 over-expressing) cells. Loss of p35 resulted in reduced total cell number. If p35 mRNA knockdown was not significantly changing p35 protein levels, we would not expect to see a difference in survival between shp35 clones and shGFP controls. Therefore, these data support a hypothesis in which loss of p35 is only affecting a relatively small percentage of cells. By eliminating up to 90% of total cells with

chemotherapy, the further loss of cells reliant on p35 for survival is magnified and would explain the increased death observed in shp35 clones.

p35 and the Slow-cycling Cell Phenotype

Key to the observations and discoveries in this work is the role of p35 in regulation and control of the cell cycle in slow-cycling cells. Interestingly, we observed a major disparity in cell cycle profiles between CFSE-labeled slow-cycling cells and those cells in which p35 is artificially over-expressed. CFSE-labeled slow-cycling cells demonstrated an increase in G2/M phase cells, while CMV-p35 cells demonstrated a diminished number of cells in S phase in favor of the G1 state. A possible explanation for these findings may be due to increased stress levels resulting from artificial over-expression of a protein. This stress may disrupt the cell cycle and provide distorted results.

Alternately, it is likely that simple over-expression of p35 is not a complete replication of the CFSE-labeled slow-cycling cell phenotype. Other factors beyond p35 over-expression are likely differentially regulated between CFSE-high and CFSE-low cell populations, which may further contribute to cell cycle regulation and the disparities observed in cell cycle profiles. These differences are also likely to involve changes in target availability, resulting in differential p35/CDK5 downstream signaling between slow-cycling cells and p35 over-expressing cells. Complete transcript profiling of CFSE-high and CFSE-low cell populations would identify alternately regulated

transcripts between the two cell populations beyond those evaluated here, and help to create a more complete picture for slow-cycling cell regulation.

Additionally, artificial expression of p35 beyond that observed at endogenous levels may lead to over-saturation of CDK5 binding. Without CDK5 as a binding partner, p35 activity may favor an increase in CDK5-independent activity. No studies to date link unbound p35 independent activity directly with regulation of cell cycle control. However, independent functions of p35 do include regulation of E-cadherin and potential release of β -catenin into the nucleus (98). We found E-cadherin and β -catenin localization patterns to be unchanged in p35 expressing cells during our studies, suggesting p35 may not be functioning independently of CDK5 and that other factors may be contributing to differences in cell cycle profiles. Experiments that over-express CDK5 both independently and with p35 would further elucidate the specific role of p35 in cell cycle regulation.

Finally, cell cycle profile differences between slow-cycling cells and p35 over-expressing cells may be a characteristic of localization of p35/CDK5 and the resulting effect on the cell cycle. Cytoplasmic p35/CDK5 may lead to ubiquitylation and degradation, creating a permissive environment for premature entry into S phase, where cells are proposed to stall due to incomplete signaling requirements for completion of mitosis (131, 133). In contrast, the localization of p35/CDK5 into the nucleus has been associated with interactions with both p27 and Rb, contributing to inhibition of the cell cycle (2, 15). Over-expressed p35 protein was primarily located in the cytoplasm, but

nuclear protein was present. Even the low nuclear staining observed must be enough to stall the p35 over-expressing cells in G1 as determined by cell cycle profiles.

From these findings, we conclude that p35 regulates the cell cycle by working with CDK5 to block entry into S phase and stall cells within the G1 phase of the cell cycle. This block is potentially through p35/CDK5 interactions with p27 and E2F, although future experiments will need to validate this relationship experimentally. While this body of work does not explore G0 associated signaling, cell cycle analysis and label dilution experiments suggest that CFSE-high cells are actively cycling. Therefore, it is likely that these cells are not in a more permanent G0 stalled state. Furthermore, there is little background or experimental evidence to suggest that p35 over-expression in slow-cycling cells is directly leading to the G2/M stall observed in CFSE label retaining cells. We propose that this G2/M stall is a side effect of increased apoptosis resistance in this cell population. CFSE LRCs within the G2/M state may be reacting to cell stress or DNA damage by stalling for repairs. While bulk cells may undergo apoptosis during this stall, increased survival proteins like BCL2 may promote repair over apoptosis and lead to a buildup of cells in the G2/M phase of the cell cycle.

p35 and Implications for Metastasis

In the developing brain and postmitotic neurons, p35 plays a key role in regulation of cytoskeletal structures during cell migration (11, 100). Over-expression of p35 demonstrated lattice-like staining patterns consistent with association with cytoskeletal structures. Interestingly, p35 did not appear to alter PHF-1 motif

phosphorylation levels of the microtubule stabilizer Tau, suggesting Tau may not be a target of p35 in slow-cycling cancer cells. Alternatively, the localization of p35 may reflect regulatory activity on other cytoskeletal targets. The functional implications for these findings are unclear, but p35 expression may suggest an increased ability for migration within slow-cycling cancer cells. If validated, these findings would have vast implications for slow-cycling cancer cells as strong candidates for drivers of metastasis. Increased migratory abilities of slow-cycling cells would allow for movement through the matrix and into the blood. At the same time, increased anti-apoptotic abilities in slow-cycling cells via BCL2 would promote survival within the foreign environments of both the blood and metastatic tissues. Finally, slow-cycling cell tumor-initiating abilities would promote establishment and metastatic outgrowth. Future research should look at induction of migration and the effects on metastasis in p35-expressing cells.

Targeting CDKs and p35/CDK5 in Therapeutics

Pathways linked to expression of CDKs are often dysregulated in cancer, making them natural targets for therapeutics. Mutations of CKIs, CDKs, cyclins, and Rb all contribute to aberrant CDK activation and tumor cell proliferation (155). Targeting CDKs with the goal of stopping cell growth and inducing apoptosis is an appealing option when faced with the rapid expansion and mutational diversity characteristic of cancer progression. Targeting CDKs in solid tumors has generated mixed results. Small molecules, such as Flavopiridol, that broadly target CDK activities do not appear to be very effective at tolerated concentrations on a broad scale (156, 157). However, low

percentages of clinically measurable partial and objective responses have been observed with Flavopiridol, suggesting that selecting the right tumors may be important when using CDK inhibitory drugs. Paradoxically, enhanced toxicity of DNA damaging agents like Oxaliplatin and 5-Fluorouracil are observed when used in combination with CDK cell cycle inhibitors (158, 159). The reasons why targeting proliferation activity increases activation of cell cycle dependent drugs is unclear, but may suggest that more than simple cell cycle inhibition is achieved through broad inhibition of CDKs.

Interestingly, drugs more specifically targeting p35/CDK5, like roscovitine and SCH727965, have had few clinically relevant responses in solid tumor xenografts and in patients (160, 161). Primarily, these studies measure response of tumors in the form of changes in tumor size and total cell response, observing little, if any, tumor regression. In contrast, our work identifies a subset of p35 regulated slow-cycling cancer cells that become enriched following treatment with traditional chemotherapies. Manipulations of p35 further increased or decreased survival relative to the amount of p35 expressed. These data indicate that the p35 slow-cycling phenotype contributes to chemotherapy survival in only a subset of cells.

Importantly, inhibition of p35/CDK5 in combination therapy may allow for more direct targeting of therapy resistant cancer cells, limiting damage to normal adult tissues. Unlike other CDKs, Rb, and other cell cycle related drug targets that are critical in adult tissues, p35 activity may be limited to tumor populations. The use of more specific p35/CDK5 inhibitors, like roscovitine and SCH727965, is well tolerated in adult tumor patients without adverse impacts, suggesting that long term loss may have limited side

effects on adult healthy tissues (161, 162). Unfortunately, use of p35/CDK5 inhibitors in pediatric cancers may not be an option. Pre-natal p35 knockout mice fail to develop proper cortical layering, suggesting that p35 inhibition may hinder proper neural development in young children (123).

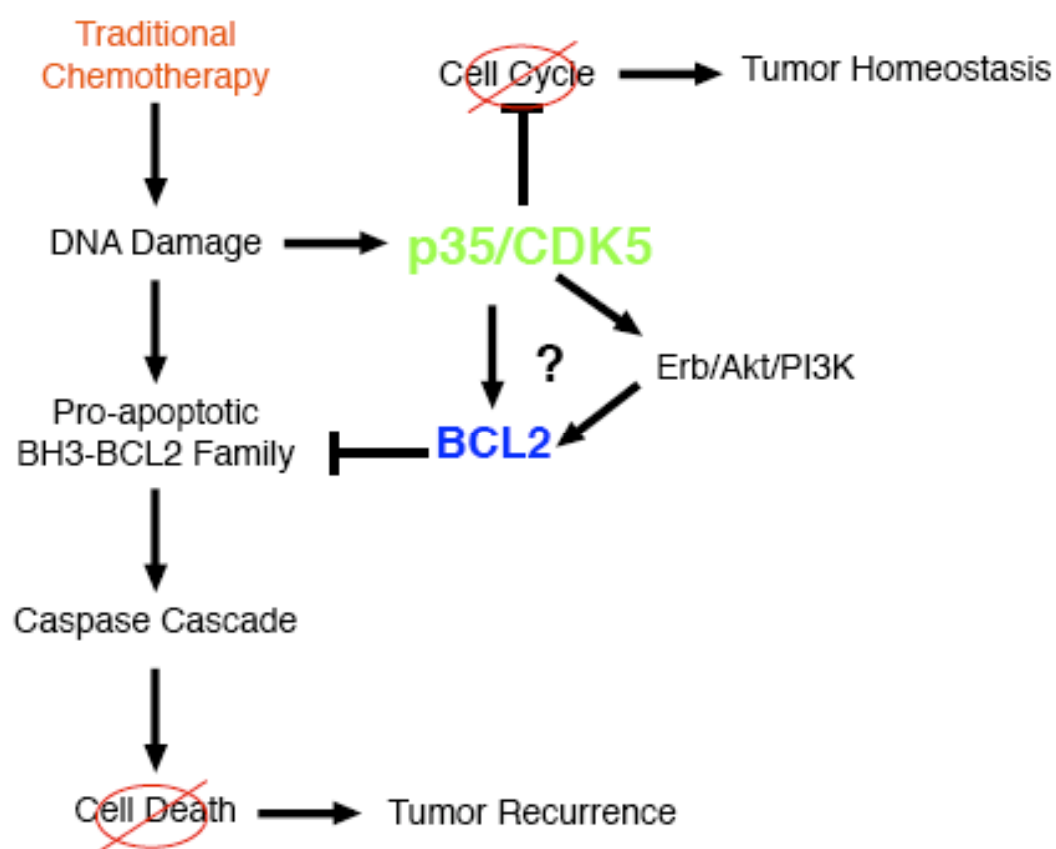
Our data would suggest that drugs like roscovitine and SCH727965 may have the greatest efficacy on the p35 expressing, slow-cycling subset of cells. As a single agent, it therefore is not surprising that a profound response in tumors is not observed if only a small percentage of p35 expressing cells are being targeted. Even in combination with chemotherapeutics, a measurable difference in tumor size may not be expected. A more appropriate measurement of response to these drugs may be changes in recurrence rates and time to recurrence. Our data suggest that p35/CDK5 plays an important role in slowing the cell cycle and increasing anti-apoptotic BCL2 family members. These regulations mitigate DNA damage and mitochondrial-associated apoptotic signaling induced by chemotherapeutics reliant on cycling cells. The use of p35/CDK5 inhibitors before or in combination with chemotherapy will block the anti-proliferative effects of p35/CDK5, pushing slow-cycling cells into the cell cycle and making them more susceptible to DNA damage. At the same time, less active p35/CDK5 will decrease stabilized BCL2, reducing anti-apoptotic signaling and driving cell death. With the elimination of slow-cycling therapy resistant cells, tumor cell survival may be decreased and recurrences should decline.

Conclusions and Model

Based on the findings of this work, we propose a model in which epithelial tumors like those of the breast and colon have an inherent p35/CDK5 regulated slow-cycling cell population that exists to support and replenish rapidly proliferating cells (Figure 5.1). These slow-cycling cell populations further utilize p35 to promote cell survival through stabilization of proteins like BCL2. In response to traditional chemotherapeutic agents, the slow-cycling nature of these cells reduces their overall chemosensitivity; while at the same time, anti-apoptotic BCL2 activity would promote better resistance to death signaling. Finally, following the cessation of treatment, slow-cycling resistant cells are able to re-enter the cell cycle and reactivate tumor growth and expansion. This tumor growth leads to patient recurrences and all too often death.

Figure 5.1: p35 regulation of slow-cycling cells in cancer

Within tumors, sub populations of slow-cycling stem-like cancer cells increase expression of the CDK5 activator p35 to regulate cell cycle and promote tumor homeostasis. Additionally, p35/CDK5 directly or through Erb/Akt/PI3K signaling stabilizes the anti-apoptotic protein BCL2. In response to traditional forms of chemotherapy that induce DNA damage, stabilized BCL2 works to inhibit pro-apoptotic BH3 family members, preventing the activation of caspases and promoting increased cell survival over bulk tumor cells. Following chemotherapy cessation, the stem-like abilities of slow-cycling cancer cells drives tumor reactivation and recurrence.



Appendix I

BH3 Profiling in Slow-cycling Cancer Cells

Treatment of tumors with traditional forms of chemotherapy induces cell stress through DNA damage. This DNA damage ultimately signals for the up-regulation of pro-apoptotic BH3-BCL2 family members that lead to the formation of mitochondrial membrane pores and the release of cytochrome C to drive cell death (86, 88). Anti-apoptotic BCL2 family members, like BCL2, sequester pro-apoptotic BCL2 BH3 family members and inhibit pore formation, promoting survival. Through regulation and interaction of pro-apoptotic and anti-apoptotic BCL2 family members, cells can become more or less primed to undergo apoptosis. Our findings suggest that p35 may function to stabilize BCL2 and increase overall protein, inhibiting formation of mitochondrial membrane pores, and priming slow-cycling cancer cells to be less susceptible to death signaling.

To evaluate the role of p35 and BH3-family interaction, we conducted pilot work with the Letai Lab at Dana-Farber to profile slow-cycling cancer cell apoptotic priming in response to BCL2-BH3 family members (87). *In vitro* spheres pulse/chased with CFSE for one week or *in vivo* labeled tumors pulse/chased with CFSE for two weeks were digested to single cells and cultured with peptides that mimic BCL2-BH3 family members. These BCL2-BH3 peptide mimics are designed to promote apoptotic signaling and induce mitochondrial membrane depolarization. Treated cultures were then stained with a compound (JC-1) that is fluorescent green in healthy mitochondrial matrices, but

changes to fluorescent red when mitochondrial membranes are permeabilized. The JC-1 compound allows for the identification of mitochondria that have undergone membrane depolarization via flow cytometry.

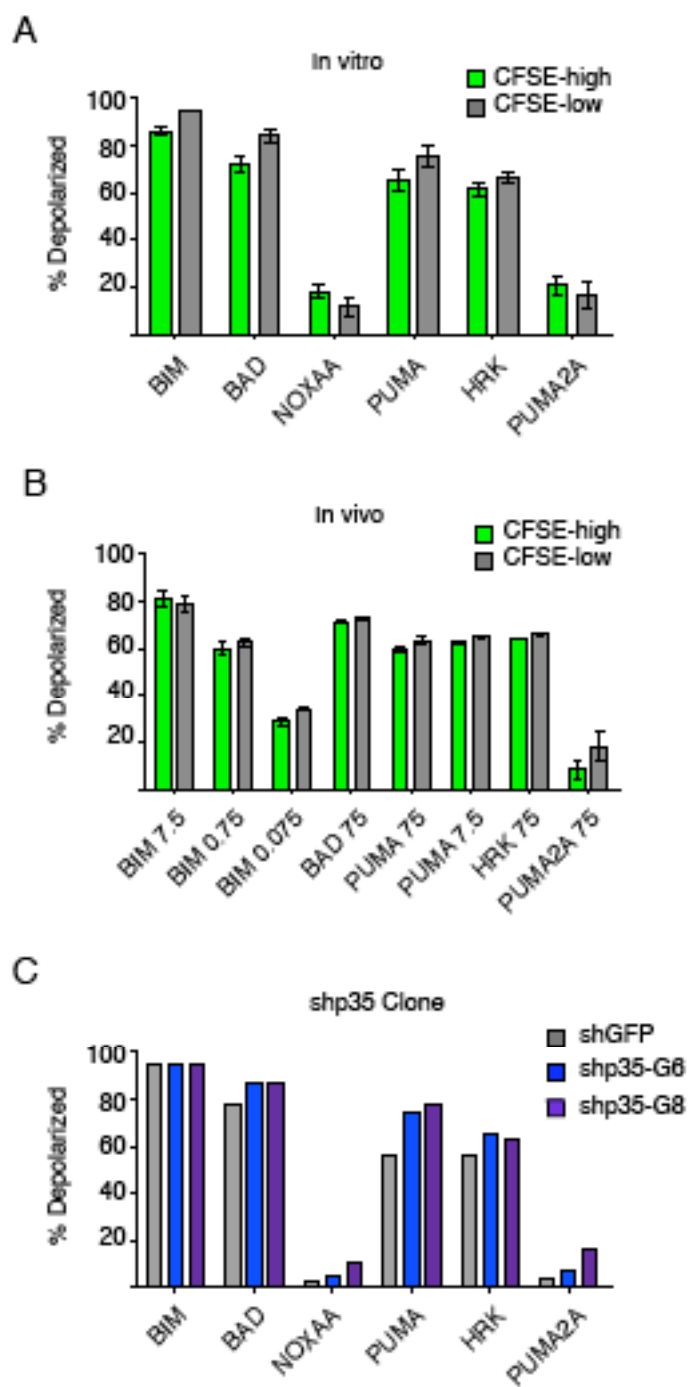
When compared to CFSE-low cell populations, CFSE-high *in vitro* cells demonstrated decreased membrane depolarization in response to several of the BH3 peptides, suggesting less apoptotic priming and more resistance to certain forms of death stimuli (Appendix I Figure 1A, n=2). In contrast to these results, *in vivo* populations did not demonstrate detectable difference in mitochondrial depolarization between CFSE-high and CFSE-low populations (Appendix I Figure 1B, n=2). These early data suggest a potential for increased resistance to apoptotic signaling in CFSE-high cells that may be context dependent and further regulated by the presence of *in vivo* signaling not replicated *in vitro*. It is likely that regulation of apoptotic signaling *in vivo* is more complex and less responsive to any single input than any current *in vitro* model.

In order to understand the role that p35 may have on priming cells to apoptotic stimuli, we repeated the BCL2-BH3 profiling on HCT116 cells expressing shp35 constructs (Appendix I Figure 1C, n=1). In comparison to shGFP controls, both constructs demonstrated increased depolarization of the mitochondrial membrane for almost all peptides explored. These preliminary data indicate that loss of p35 expression increases cell susceptibility to apoptotic signaling.

Although these findings are preliminary, the *in vitro* studies complement the chemotherapy treatment assays and suggest that slow-cycling cells are resistant to apoptotic death signaling. Furthermore, these studies suggest a mechanism

Appendix I Figure 1: BH3 Profiling of slow-cycling cancer cells

HCT116 CFSE pulse/chased spheres, tumors, and shp35 clones were profiled for BH3 family peptide priming and mitochondrial membrane depolarization by JC-1 staining and flow cytometry. (A) *In vitro* CFSE BH3 profiling of CFSE-high (green) and CFSE-low cells (grey). CFSE-high cells demonstrated less mitochondria depolarization to BH3 peptide mimics for BIM, BAD, PUMA, and HRK (n=2) but did not reach statistical significance. (B) *In vivo* CFSE BH3 profiling of CFSE-high (green) and CFSE-low cells (grey). No significant difference was observed between CFSE-high and CFSE-low cells *in vivo* (n=2). (C) *In vitro* CFSE BH3 profiling for HCT116 shGFP (grey), shp35-G6(blue), and shp35-G8(purple) clones. Loss of p35 is associated with increased mitochondria depolarization for the majority of BH3 peptides assessed (n=1).



through which p35 promotes the BCL2 ability to block pro-apoptotic BCL2 BH3 family pore formation and apoptosis. It would be interesting to expand these assays to include HCT116 cells over-expressing p35. If this proposed mechanism is valid, p35 over-expression should further limit mitochondrial membrane depolarization and promote cell survival. Future repetition and expansion of these assays to include inhibitors for both p35 and BCL2 will help to better define interactions between these two proteins.

Appendix II

Complete qPCR Array

	HCT116 <i>In Vitro</i> (n=2)	HCT116 <i>In Vivo</i> (n=3)	2953T <i>In Vivo</i> (n=1)	48116 <i>In Vivo</i> (n=1)	MDA231 <i>In Vivo</i> (n=3)	2597T <i>In Vivo</i> (n=1)
ABL1	2.51	3.47	1.22	0.73	1.75	3.13
ADAR	2.65	0.38	0.64	0.85	0.95	1.74
ANAPC2	2.90	1.58	1.05	1.64	1.23	1.28
ANAPC4	1.21	2.14	0.79	0.74	1.63	1.06
APC	1.98	1.51	0.84	0.60	2.78	1.77
ASCL2	3.03	3.57	0.78	0.92	1.08	1.68
ATM	2.54	0.98	0.74	1.39	0.73	2.80
ATR	2.10	1.76	0.93	0.77	1.19	1.00
AXIN1	3.43	1.89	1.03	0.88	1.22	1.84
BCCIP	1.16	0.82	0.74	0.82	1.58	1.01
BCL2	3.05	3.67	1.89	2.38	5.74	3.43
BMI1	1.52	1.16	0.82	1.03	2.39	1.59
BRCA1	1.72	1.18	0.65	0.64	1.09	1.25
BRCA2	1.56	1.12	0.74	0.59	1.85	2.23
BTRC	2.60	2.53	0.74	0.62	1.52	1.93
CCNA2	1.33	1.65	1.17	2.08	3.79	0.90
CCNB1	0.88	1.50	0.98	1.56	2.18	0.83
CCNB2	0.92	1.32	0.80	1.36	2.13	1.07
CCNC	1.04	1.28	0.89	0.92	1.80	0.99
CCND1	3.76	1.81	1.17	0.74	0.96	1.82
CCND2	3.03	3.26	0.79	1.18	1.77	2.26
CCNE1	2.22	0.48	0.92	0.66	1.35	0.96
CCNF	2.67	0.77	0.71	0.76	50.87	1.58
CCNG2	2.89	0.93	0.79	0.60	4.55	2.80
CCNH	1.38	4.02	1.06	0.94	2.15	2.09
CCNT1	2.23	0.76	0.72	0.66	1.25	1.65
CCNT2	2.80	0.89	1.21	2.01	2.04	2.67
CD133	1.94	1.04	0.84	1.16	0.89	2.69

CD44	2.50	1.22	0.91	1.21	2.05	1.74
CDC16	1.86	0.84	0.92	1.59	1.26	1.82
CDC2	1.59	2.98	1.23	1.38	2.02	1.36
CDC20	1.11	0.72	0.91	1.06	0.93	0.92
CDC34	3.05	1.42	1.18	2.88	5.20	1.87
CDC42	1.58	1.67	1.47	4.30	2.63	1.19
CDK2	1.48	0.45	1.17	0.77	1.50	2.01
CDK4	1.17	1.50	0.86	1.21	2.26	1.38
CDK5R1	2.63	2.39	7.09	3.81	1.79	6.57
CDK6	2.61	3.12	0.92	1.05	3.55	1.71
CDK7	1.71	1.11	0.96	0.75	1.16	1.42
CDK8	1.75	0.81	0.81	0.92	3.27	1.33
CDKN1A	2.65	2.45	1.00	0.77	1.49	2.56
CDKN1B	2.52	1.18	0.97	0.79	2.37	1.36
CDKN2A	1.07	0.96	0.95	0.83	4.93	5.08
CDKN2D	1.66	0.63	0.82	0.94	1.01	1.14
CDKN3	1.11	0.57	1.26	1.29	1.24	1.40
CHEK1	1.70	2.27	0.83	0.66	2.42	1.39
CHEK2	2.22	0.90	1.04	0.89	1.05	2.60
CKS1B	1.03	2.05	1.07	0.96	1.89	1.19
CUL1	1.12	0.68	0.72	0.82	1.13	1.15
CUL2	1.27	2.14	0.91	0.96	1.31	1.30
CUL3	2.40	1.06	0.91	0.81	1.80	2.05
DDX11	3.62	1.28	1.25	1.39	3.83	2.47
DIRAS3	1.20	1.40	0.51	1.09	1.46	0.57
DTX1	2.63	1.59	0.97	0.67	1.17	2.29
E2F4	1.46	1.88	0.82	0.74	1.23	1.08
EP300	2.75	1.83	1.32	2.84	1.56	1.80
FGF1	2.75	1.75	0.74	0.48	3.20	2.41
FGF2	2.70	1.87	1.81	2.01	2.23	2.32
FGF3	2.67	0.81	0.75	0.79	1.17	2.05
FGF4	2.78	1.02	0.84	0.51	1.15	1.90
FRAT1	3.29	1.44	0.89	0.60	1.10	2.05
FZD1	2.03	0.78	0.86	0.61	0.85	1.23

GADD45A	2.21	0.69	0.90	0.65	1.72	1.85
HUS1	2.24	1.18	0.71	0.75	2.50	1.53
JAG1	6.59	0.83	1.58	2.53	2.57	1.69
KNTC1	2.15	1.78	0.99	0.87	1.35	2.02
LGR5	3.16	1.33	0.91	1.10	1.91	3.07
MAD2L1	1.07	1.22	1.10	1.18	1.74	1.19
MAD2L2	1.47	0.97	0.86	0.63	1.31	1.56
MKI67	1.20	1.41	1.03	0.97	1.20	1.33
MYC	3.03	0.88	0.87	0.87	1.47	2.34
MYST1	1.45	1.86	1.18	1.16	2.27	2.09
NBN	1.51	0.84	0.57	0.53	2.03	1.24
NEUROG2	2.86	2.71	1.16	0.70	1.92	2.90
NFATC1	3.70	1.97	0.94	0.63	1.22	2.29
NOTCH1	3.89	1.43	0.74	0.54	2.00	-
NOTCH2	1.15	3.93	0.78	0.70	1.02	1.07
NUMB	2.74	0.79	1.03	0.78	1.12	1.62
OLFM4	3.27	0.93	0.73	0.94	1.31	3.11
PARD6A	3.16	0.79	1.05	2.60	1.94	2.46
PCNA	1.67	1.37	1.26	0.88	1.18	1.41
PPARD	3.10	1.56	1.43	2.37	1.86	1.62
RAD1	1.75	1.29	1.02	0.72	2.34	1.74
RAD17	1.59	0.89	1.08	0.86	1.42	1.99
RAD9A	2.01	0.60	0.87	0.62	1.37	1.51
RB1	1.70	2.01	0.70	0.59	1.81	1.35
RBBP8	1.32	2.51	0.88	0.47	1.67	1.05
SKP2	1.64	1.25	0.88	0.75	1.57	1.33
SOX2	2.71	1.08	1.02	2.57	2.66	1.45
TFDP1	2.35	0.95	0.91	1.31	1.89	0.99
TFDP2	1.73	0.41	0.75	0.82	1.56	1.82
TP53	2.29	0.63	0.68	0.98	0.62	2.01
WNT1	3.18	1.13	0.62	0.36	0.82	1.48

Appendix III

Materials and Methods

Cell Lines and CFSE Labeling

Adherent HCT116 (ATCC CCL-247) and MDA-MB-231 (ATCC HTB-26) cultures were grown in DMEM (Gibco 11995) or RPMI (Gibco 22400) respectively with 10% FBS and 1% Penicillin/Streptomycin.

Sphere cultures were grown in Sphere media consisting of DMEM/F12 (Gibco 11320) with 1X B-27 (Gibco 12587), 15 mM HEPES (Gibco 15630), 1% Penicillin/Streptomycin, 20 ng/ml bFGF (Invitrogen 13256-029), and 10 ng/ml EFG (Sigma E9644). Spheres were digested in alkaline solution (Sphere media with NaOH, pH 11.6) and quenched with acidic solution (Sphere media with HCl, pH 1.7) then filtered through a 40 μ M mesh.

Lentiviruses containing TRCN-shRNA constructs against p35 were purchased from the University of Massachusetts Medical School RNAi Core Facility (RHS4459, TRCN0000006218, and TRCN0000006220). HCT116 cells transduced with shRNA were cultured in Complete DMEM containing 2 μ g/ml puromycin. A pCMV-SPORT6 vector containing the p35 cDNA was purchased from Open Biosystems (MSH1010-58341) and transfected into cells using X-tremegene HD (Roche 06366244001). An empty pCMV-SPORT6 control vector was created by removing the p35 cDNA between EcoRV and Not1 sites, blunting overhangs with Klenow (New England Biolabs

M0210S), and ligating with T4 Ligase (New England Biolabs M0202S). Adherent lines were periodically checked by qPCR to confirm knockdown.

CFSE (carboxyfluorescein diacetate, succinimidyl ester) labeling was conducted with 10 μ M CFSE stock according to manufacturer's protocol for cells in suspension (Molecular Probes C34554).

Mice and Tumor Xenografts

NOD.CB17-Prkdc scid/J mice were purchased from Jackson Laboratories and housed in the UMass Animal Medicine Facilities. NOD-scid IL2 γ null mice were kindly provided by Dr. Dale Greiner of the University of Massachusetts Medical School. All animals were housed in the UMass Animal Medicine Facilities and experiments were conducted under IACUC approval.

Adherent HCT116 (1×10^7) or MDA-MB-231 (7×10^6) CFSE labeled cells were suspended in Matrigel (BD Biosciences 354234) and injected sub-cutaneously into the flank or #3 mammary fat pad, respectively. After two weeks, two to four tumor digests were combined to obtain adequate cell numbers and live sorted.

Primary patient tumor tissue was obtained from the UMass Cancer Center Tissue and Tumor Bank with IRB approval or the Eastern Division of the Cooperative Human Tissue Network (CHTNET) and was exclusively passaged in NOD-scid IL2 γ null mice. 2597T Primary Breast Tumor: Invasive metaplastic carcinoma. Grade 3. ER, PR, HER-2 negative. Patient received neoadjuvant chemotherapy without significant response.

2953T Primary Colon Tumor: Invasive adenocarcinoma with positive lymph nodes. Moderately differentiated, Grade 2.

48116 Primary Colon Tumor: Invasive adenocarcinoma with venous invasion and no positive lymph nodes. Poorly differentiated. No chemotherapy or radiation.

To obtain single cell suspensions, tumors were mechanically and enzymatically (2 mg/ml collagenase) digested, dissociated on a gentleMACs Dissociator (Miltenyi Biotech), and filtered through a 40 μ M mesh and labeled as previously described.

Chemotherapy Enrichment Assays

Normal and shp35 cell lines were cultured in Sphere media for at least one week and passaged once before use. P35-CMV transfected lines were used immediately following three days of transfection. Single cell suspensions of CFSE-labeled cells were plated at 4.0×10^4 cells/ml. One week chased single cell suspensions were re-plated at 4.0×10^4 cells/ml in Sphere media containing either DMSO vehicle control, 2 μ M Oxaliplatin (Sigma 9512), 250 μ M 5-Fluorouracil (Sigma F6627), or FOX (Oxaliplatin and 5-fluorouracil) for three days before being analyzed for CFSE content. Alternately, FOX treated cultures were re-plated in fresh Sphere media containing 10 μ M BrdU (BD Pharmingen 550891) for 3 days.

Mice were injected with 5×10^6 HCT116 CFSE labeled cells into the #3 and #8 mammary fat pads. Twelve days after engraftment (day 0) mice (n=4/condition) were injected IP with 40mg/kg 5FU and 10mg/kg Oxali or DMSO diluted in PBS. Injections were repeated on day 4 and day 8. On day 12, tumors were collected and processed as

described. BrdU pulsed tumors received 1mg BrdU by IP injection on days 14, 15, and 16, and were processed on day 17.

Flow Cytometry

Single cell suspensions derived from sphere cultures were washed in PBS⁺ (PBS with 1% 1M HEPES and 2% FBS). Single cell *in vivo* tumor digests were washed in PBS⁺ and stained with the epithelial positive selection marker EpCAM (eBiosciences 50-9326) and the negative selection markers TER119, CD31, and CD45 (BD Pharmingen 553673, 553373, and 553089). *In vitro* and *in vivo* samples were suspended in PBS and 20% Sphere media with 7AAD (BD Pharmingen 559925). A maximum of 5% of the most CFSE intense-Live/Lineage negative cells were collected. Live cells were sorted into complete Sphere media.

Tumor initiation dilution analysis was performed by first counting live sorted cells and then replating in Sphere media or resuspending in Matrigel before injection into the mammary fat pads of NOD.CB17-Prkdc scid/J mice at indicated dilutions. Spheres were counted and measured using the measure function on Image J software (<http://rsbweb.nih.gov/ij/index.html>) after one week of growth. Dilution cohorts of both CFSE-high and CFSE-low mice were sacrificed and tumors were collected and measured after the first tumor in the cohort reached $\sim 1000\text{mm}^3$. Cohorts without visible tumor growth after 3 months were sacrificed and examined for tumors.

Chemotherapy treated samples and BrdU treated samples were labeled with the viability discriminator Live/Dead Blue (Invitrogen L23105) and fixed in Cytifix buffer

(BD Biosciences 51-2090KZ). BrdU treated samples were stained with anti-BrdU antibody (Roche 11170376001, APC secondary Santa Cruz sc-3818). Final samples were suspended in FACS Buffer (1x PBS, 1mM sodium azide, and 0.05 g/ml BSA). Cell cycle analysis was performed on cytofixed cells in DAPI (Roche 236276).

Cancer stem cell marker analysis was performed on CFSE pulse/chased spheres at 1 week or tumors after two weeks. Spheres/tumors were digested and labeled with Live/Dead Blue as described and then stained with primary antibodies against CD133 (Miltenyi Biotec 293C3), CD44 (Millipore MAB4065), or ALDH (BD 611194) and secondary antibody anti-mouse PE (Santa Cruz Biotec sc-3738).

Side population analysis was performed on CFSE pulse/chased spheres digested and viability labeled as described above. Live cells were incubated at 37 °C for 90 minutes in 5 µg/ml Hoechst 33342 (Invitrogen H1399) with or without 2.5 µM Fumitremorgin C (FTC, Enzo Life Sciences 350-127-C250).

All samples were analyzed and sorted by the UMass Medical School Flow Cytometry Facility on a BD FACS Aria II or on a BD LSRII. The proliferation wizard from the Modfit analysis package was used to generate peaks from HCT116 *in vivo* xenografts at two weeks.

Immunoprecipitation and Western Blot

CDK5, p35, p-BCL2, and IgG antibodies were purchased from Santa Cruz Biotechnology (173, 820, 21864, 2027). PHF-1 antibody was obtained from Peter Davies at Albert Einstein College of Medicine. Tubulin antibody was purchased from

Sigma (T9026). BCL2, Anti-Rabbit HRP, and Anti-Mouse HRP were purchased from Dako (M0887, P0448, and P0260)

Western blot lysates were prepared in Cell Lysis Buffer (Cell Signaling 9803S) with Protease Inhibitor Cocktail (Sigma P-2704). Proteins were run on an acrylamide gel and transferred to an Immobilon-P PVDF (Millipore IPVH00010) membrane.

Membranes were blocked in PBS with 0.1% Tween-20 and 5% Milk.

Immunoprecipitations were performed using the Pierce® Crosslink Immunoprecipitation Kit according to the manufacturer's protocol (26147).

RT-PCR Array Profiling and qPCR

RNA was isolated using the Qiagen RNeasy® Mini Kit (74104) and cDNA was generated following the protocol described for the RT² First Strand Kit (SABiosciences PP4067).

qPCR was performed using Power SYBR Green (Applied Biosystems 4367659) with p35 primers (Fw: AAGAACGCCAAGGACAAGAA, Rv: TCATTGTTGAGGTGCGTGAT) and GAPDH primers (Fw: GAAATCCCATCACCATCTTCCAG, Rv: ATGAGTCCTTCCACGATACCAAAG).

A customized RT² Profiler PCR Array System was purchased from SABiosciences (CAPH09537A) and run on an ABI 9700HT following manufacturer protocol.

Staining

Tumor samples were frozen in OCT compound, sectioned at 6 μm thickness, fixed in 4% paraformaldehyde and stained with H&E stains. Fluorescent stains were mounted with Vectashield containing DAPI (Vector H-1200).

Cells for immunofluorescent staining were grown as adherent cultures on cover slips and fixed for 5 min in 4% paraformaldehyde. Cells were then washed in PBS and blocked in PBS with .1% Triton X-100 and 5% goat serum for 1 hr. Primary antibodies for staining were the same as those used for western blotting. Secondary antibodies used were Anti-mouse Cy3 (Millipore Ap124C) and anti-Rabbit FitC (Jackson ImmnuoResearch 111-096-144).

Rectal tumor samples were obtained from the UMass Cancer Center Tissue and Tumor Bank. Immunohistochemical stains were performed by the UMass Memorial Pathology Department. Primary p35 antibody was purchased from Abgent (AP7743a).

Statistics

Statistical analysis and p-values were calculated using the t-test functions of the GraphPad Prism software.

Appendix IV

Alternative Experiments and Future Directions

The use of CFSE and development of a protocol to positively identify and isolate live slow-cycling cancer cells is a major strength throughout this body of work. This technique has the potential to be universally applicable to cell lines, but this potential was not fully explored here as the majority of assays were performed in only the HCT116 cell line. Expansion of the CFSE protocol and assessment of slow-cycling characteristics in an additional colon tumor line, two breast tumor lines, and additional primary tumor samples would confirm that the phenomena observed are not cell line specific.

Expansion to more cell lines would also allow a more in-depth exploration of the relationship of slow-cycling cells and the CSC phenotype. The use of additional cell lines may suggest a more intersecting relationship between CSCs and slow-cycling cells that is consistent with the work of other researchers that demonstrated a stronger CSC phenotype within slow-cycling cells (40, 62, 71, 72).

The use of qPCR profiling array was a relatively inexpensive, although limiting, way to explore predictable differences in slow-cycling cells and rapidly proliferating cells across multiple cell lines and tumor types. Repeating these arrays to increase the power of the study and to expand to multiple tumor types would greatly support our findings. Alternatively, high throughput deep sequencing techniques to compare the two populations would allow for a more unbiased approach and the identification of potentially thousands more dysregulated transcripts.

While the shp35 and CMV-p35 knockdown and expression studies began to shed light on the importance and role of p35 in tumors, the vectors utilized were not optimal for the studies performed. Recloning of both the over-expression and knockdown vectors into selectable and inducible lenti-viral models would greatly enhance the capabilities of these studies. Selectable lenti-viral vectors would allow for more reliable and uniform transductions and the potential to move these vectors into primary samples more easily. By making the vectors inducible, we gain the ability to better regulate how much protein is expressed based on concentration of induction agent. In this way, it would be possible to better titer over-expression of p35 to more physiologically relevant levels and potentially increase the knockdown levels to greater than 50%. Additionally, inducible vectors would better facilitate understanding the role of p35 in an *in vivo* chemotherapy model by allowing us to mimic p35 inhibition at various stages of chemotherapy (before, during, and after) and test for changes in tumor growth or recurrence.

External events prevented a more in-depth study of the relevant targets for p35. Further exploration of the mechanisms of cell cycle inhibition, specifically localization, binding interactions, and activity states of p27, Rb, and E2F would further define the role of p35 in cell cycle regulation of cancer. Specifically, determining if p35/CDK5 is able to complex with p27 and sequester E2F. Additionally, exploration into the mechanism by which p35 regulates BCL2 would also greatly benefit this project. Determining if p35 can directly bind and regulate BCL2 and/or alter the Erb pathway or PI3K/AKT kinase are important questions in further research into p35 in cancer.

Finally, future work evaluating the role of p35 in tumors should focus on migration regulation and the potential for changes in invasion and metastasis in cancer. p35 is well studied in neuronal precursor regulation of migration. The use of over-expression and knockdown vectors or small molecule inhibitors coupled with migration and invasion assays in Boyden chambers may clarify the role for p35 in metastasis. Additionally, expansion of p35 over-expression and knockdown into cells and primary tumors for the creation of xenografts may lead to differences in invasive potential and the ability to metastasize.

References

1. Massague J. (2004). G1 cell-cycle control and cancer. *Nature* 432:298-306.
2. Harbour JW, RX Luo, A Dei Santi, AA Postigo and DC Dean. (1999). Cdk phosphorylation triggers sequential intramolecular interactions that progressively block Rb functions as cells move through G1. *Cell* 98:859-869.
3. Malumbres M and M Barbacid. (2009). Cell cycle, CDKs and cancer: a changing paradigm. *Nat Rev Cancer* 9:153-166.
4. Park MT and SJ Lee. (2003). Cell cycle and cancer. *J Biochem Mol Biol* 36:60-65.
5. Cheng T, N Rodrigues, H Shen, Y Yang, D Dombkowski, M Sykes and DT Scadden. (2000). Hematopoietic stem cell quiescence maintained by p21cip1/waf1. *Science* 287:1804-1808.
6. Kippin TE, DJ Martens and D van der Kooy. (2005). p21 loss compromises the relative quiescence of forebrain stem cell proliferation leading to exhaustion of their proliferation capacity. *Genes Dev* 19:756-767.
7. Matsumoto A, S Takeishi, T Kanie, E Susaki, I Onoyama, Y Tateishi, K Nakayama and KI Nakayama. (2011). p57 is required for quiescence and maintenance of adult hematopoietic stem cells. *Cell Stem Cell* 9:262-271.
8. Krishnamurthy J, MR Ramsey, KL Ligon, C Torrice, A Koh, S Bonner-Weir and NE Sharpless. (2006). p16INK4a induces an age-dependent decline in islet regenerative potential. *Nature* 443:453-457.
9. Pei XH, F Bai, MD Smith and Y Xiong. (2007). p18Ink4c collaborates with Men1 to constrain lung stem cell expansion and suppress non-small-cell lung cancers. *Cancer Res* 67:3162-3170.
10. Molofsky AV, SG Slutsky, NM Joseph, S He, R Pardal, J Krishnamurthy, NE Sharpless and SJ Morrison. (2006). Increasing p16INK4a expression decreases forebrain progenitors and neurogenesis during ageing. *Nature* 443:448-452.
11. Lalioti V, D Pulido and IV Sandoval. (2010). Cdk5, the multifunctional surveyor. *Cell Cycle* 9:284-311.
12. Paglini G and A Caceres. (2001). The role of the Cdk5--p35 kinase in neuronal development. *Eur J Biochem* 268:1528-1533.
13. Morgan DO. (1995). Principles of CDK regulation. *Nature* 374:131-134.
14. Zhang J, H Li, O Yabut, H Fitzpatrick, G D'Arcangelo and K Herrup. (2010). Cdk5 suppresses the neuronal cell cycle by disrupting the E2F1-DP1 complex. *J Neurosci* 30:5219-5228.
15. Zhang J, H Li and K Herrup. (2010). Cdk5 nuclear localization is p27-dependent in nerve cells: implications for cell cycle suppression and caspase-3 activation. *J Biol Chem* 285:14052-14061.
16. Mao D and PW Hinds. (2010). p35 is required for CDK5 activation in cellular senescence. *J Biol Chem* 285:14671-14680.
17. Watt FM and KB Jensen. (2009). Epidermal stem cell diversity and quiescence. *EMBO Mol Med* 1:260-267.

18. **Reya T, SJ Morrison, MF Clarke and IL Weissman. (2001). Stem cells, cancer, and cancer stem cells. *Nature* 414:105-111.**
19. **Cotsarelis G, TT Sun and RM Lavker. (1990). Label-retaining cells reside in the bulge area of pilosebaceous unit: implications for follicular stem cells, hair cycle, and skin carcinogenesis. *Cell* 61:1329-1337.**
20. **Lyle S, M Christofidou-Solomidou, Y Liu, DE Elder, S Albelda and G Cotsarelis. (1998). The C8/144B monoclonal antibody recognizes cytokeratin 15 and defines the location of human hair follicle stem cells. *J Cell Sci* 111 (Pt 21):3179-3188.**
21. **Clayton E, DP Doupe, AM Klein, DJ Winton, BD Simons and PH Jones. (2007). A single type of progenitor cell maintains normal epidermis. *Nature* 446:185-189.**
22. **Welm BE, SB Tepera, T Venezia, TA Graubert, JM Rosen and MA Goodell. (2002). Sca-1(pos) cells in the mouse mammary gland represent an enriched progenitor cell population. *Dev Biol* 245:42-56.**
23. **Shackleton M, F Vaillant, KJ Simpson, J Stingl, GK Smyth, ML Asselin-Labat, L Wu, GJ Lindeman and JE Visvader. (2006). Generation of a functional mammary gland from a single stem cell. *Nature* 439:84-88.**
24. **Potten CS, M Kellett, SA Roberts, DA Rew and GD Wilson. (1992). Measurement of in vivo proliferation in human colorectal mucosa using bromodeoxyuridine. *Gut* 33:71-78.**
25. **Barker N, JH van Es, J Kuipers, P Kujala, M van den Born, M Cozijnsen, A Haegebarth, J Korving, H Begthel, PJ Peters and H Clevers. (2007). Identification of stem cells in small intestine and colon by marker gene *Lgr5*. *Nature* 449:1003-1007.**
26. **Leong KG, BE Wang, L Johnson and WQ Gao. (2008). Generation of a prostate from a single adult stem cell. *Nature* 456:804-808.**
27. **Uchida N, DW Buck, D He, MJ Reitsma, M Masek, TV Phan, AS Tsukamoto, FH Gage and IL Weissman. (2000). Direct isolation of human central nervous system stem cells. *Proc Natl Acad Sci U S A* 97:14720-14725.**
28. **Osawa M, K Hanada, H Hamada and H Nakauchi. (1996). Long-term lymphohematopoietic reconstitution by a single CD34-low/negative hematopoietic stem cell. *Science* 273:242-245.**
29. **Morrison SJ and IL Weissman. (1994). The long-term repopulating subset of hematopoietic stem cells is deterministic and isolatable by phenotype. *Immunity* 1:661-673.**
30. **Coller HA, L Sang and JM Roberts. (2006). A new description of cellular quiescence. *PLoS Biol* 4:e83.**
31. **Sang L, HA Coller and JM Roberts. (2008). Control of the reversibility of cellular quiescence by the transcriptional repressor *HES1*. *Science* 321:1095-1100.**
32. **Viatour P, TC Somervaille, S Venkatasubrahmanyam, S Kogan, ME McLaughlin, IL Weissman, AJ Butte, E Passegue and J Sage. (2008). Hematopoietic stem cell quiescence is maintained by compound contributions of the retinoblastoma gene family. *Cell Stem Cell* 3:416-428.**

33. Lyle S, M Christofidou-Solomidou, Y Liu, DE Elder, S Albelda and G Cotsarelis. (1999). Human hair follicle bulge cells are biochemically distinct and possess an epithelial stem cell phenotype. *J Invest Dermatol Symp Proc* 4:296-301.
34. Roh C, M Roche, Z Guo, C Photopoulos, Q Tao and S Lyle. (2008). Multipotentiality of a new immortalized epithelial stem cell line derived from human hair follicles. *In Vitro Cell Dev Biol Anim* 44:236-244.
35. Jaks V, N Barker, M Kasper, JH van Es, HJ Snippert, H Clevers and R Toftgard. (2008). *Lgr5* marks cycling, yet long-lived, hair follicle stem cells. *Nat Genet* 40:1291-1299.
36. Potten CS. (1998). Stem cells in gastrointestinal epithelium: numbers, characteristics and death. *Philos Trans R Soc Lond B Biol Sci* 353:821-830.
37. Nishimura S, N Wakabayashi, K Toyoda, K Kashima and S Mitsufuji. (2003). Expression of *Musashi-1* in human normal colon crypt cells: a possible stem cell marker of human colon epithelium. *Dig Dis Sci* 48:1523-1529.
38. Potten CS, C Booth, GL Tudor, D Booth, G Brady, P Hurley, G Ashton, R Clarke, S Sakakibara and H Okano. (2003). Identification of a putative intestinal stem cell and early lineage marker; *musashi-1*. *Differentiation* 71:28-41.
39. Ricci-Vitiani L, E Fabrizio, E Palio and R De Maria. (2009). Colon cancer stem cells. *J Mol Med*.
40. Pece S, D Tosoni, S Confalonieri, G Mazzarol, M Vecchi, S Ronzoni, L Bernard, G Viale, PG Pelicci and PP Di Fiore. (2010). Biological and molecular heterogeneity of breast cancers correlates with their cancer stem cell content. *Cell* 140:62-73.
41. Visvader JE and GJ Lindeman. (2006). Mammary stem cells and mammapoiesis. *Cancer Res* 66:9798-9801.
42. Morshead CM, BA Reynolds, CG Craig, MW McBurney, WA Staines, D Morassutti, S Weiss and D van der Kooy. (1994). Neural stem cells in the adult mammalian forebrain: a relatively quiescent subpopulation of subependymal cells. *Neuron* 13:1071-1082.
43. Tsujimura A, Y Koikawa, S Salm, T Takao, S Coetzee, D Moscatelli, E Shapiro, H Lepor, TT Sun and EL Wilson. (2002). Proximal location of mouse prostate epithelial stem cells: a model of prostatic homeostasis. *J Cell Biol* 157:1257-1265.
44. Teng C, Y Guo, H Zhang, M Ding and H Deng. (2007). Identification and characterization of label-retaining cells in mouse pancreas. *Differentiation* 75:702-712.
45. Society AC. (2012). *Cancer Facts & Figures 2012*. AAC Society, ed.
46. Gill S, CL Loprinzi, DJ Sargent, SD Thome, SR Alberts, DG Haller, J Benedetti, G Francini, LE Shepherd, J Francois Seitz, R Labianca, W Chen, SS Cha, MP Heldebrant and RM Goldberg. (2004). Pooled analysis of fluorouracil-based adjuvant therapy for stage II and III colon cancer: who benefits and by how much? *J Clin Oncol* 22:1797-1806.
47. Hanahan D and RA Weinberg. (2000). The hallmarks of cancer. *Cell* 100:57-70.

48. Dean M. (2006). Cancer stem cells: redefining the paradigm of cancer treatment strategies. *Mol Interv* 6:140-148.
49. Woodward WA, MS Chen, F Behbod and JM Rosen. (2005). On mammary stem cells. *J Cell Sci* 118:3585-3594.
50. Blanpain C and E Fuchs. (2009). Epidermal homeostasis: a balancing act of stem cells in the skin. *Nat Rev Mol Cell Biol* 10:207-217.
51. Kangsamaksin T, HJ Park, CS Trempus and RJ Morris. (2007). A perspective on murine keratinocyte stem cells as targets of chemically induced skin cancer. *Mol Carcinog* 46:579-584.
52. Al-Hajj M, MS Wicha, A Benito-Hernandez, SJ Morrison and MF Clarke. (2003). Prospective identification of tumorigenic breast cancer cells. *Proc Natl Acad Sci U S A* 100:3983-3988.
53. Jordan CT, ML Guzman and M Noble. (2006). Cancer stem cells. *N Engl J Med* 355:1253-1261.
54. Ricci-Vitiani L, A Pagliuca, E Palio, A Zeuner and R De Maria. (2008). Colon cancer stem cells. *Gut* 57:538-548.
55. Visvader JE and GJ Lindeman. (2008). Cancer stem cells in solid tumours: accumulating evidence and unresolved questions. *Nat Rev Cancer* 8:755-768.
56. Bonnet D and JE Dick. (1997). Human acute myeloid leukemia is organized as a hierarchy that originates from a primitive hematopoietic cell. *Nat Med* 3:730-737.
57. Collins AT, PA Berry, C Hyde, MJ Stower and NJ Maitland. (2005). Prospective identification of tumorigenic prostate cancer stem cells. *Cancer Res* 65:10946-10951.
58. Li C, DG Heidt, P Dalerba, CF Burant, L Zhang, V Adsay, M Wicha, MF Clarke and DM Simeone. (2007). Identification of pancreatic cancer stem cells. *Cancer Res* 67:1030-1037.
59. O'Brien CA, A Pollett, S Gallinger and JE Dick. (2007). A human colon cancer cell capable of initiating tumour growth in immunodeficient mice. *Nature* 445:106-110.
60. Ricci-Vitiani L, DG Lombardi, E Pillozzi, M Biffoni, M Todaro, C Peschle and R De Maria. (2007). Identification and expansion of human colon-cancer-initiating cells. *Nature* 445:111-115.
61. Chu P, DJ Clanton, TS Snipas, J Lee, E Mitchell, ML Nguyen, E Hare and RJ Peach. (2009). Characterization of a subpopulation of colon cancer cells with stem cell-like properties. *Int J Cancer* 124:1312-1321.
62. Gao MQ, YP Choi, S Kang, JH Youn and NH Cho. (2010). CD24+ cells from hierarchically organized ovarian cancer are enriched in cancer stem cells. *Oncogene* 29:2672-2680.
63. Singh SK, C Hawkins, ID Clarke, JA Squire, J Bayani, T Hide, RM Henkelman, MD Cusimano and PB Dirks. (2004). Identification of human brain tumour initiating cells. *Nature* 432:396-401.
64. Shmelkov SV, JM Butler, AT Hooper, A Hormigo, J Kushner, T Milde, R St Clair, M Baljevic, I White, DK Jin, A Chadburn, AJ Murphy, DM Valenzuela, NW

- Gale, G Thurston, GD Yancopoulos, M D'Angelica, N Kemeny, D Lyden and S Raffii. (2008). CD133 expression is not restricted to stem cells, and both CD133+ and CD133- metastatic colon cancer cells initiate tumors. *J Clin Invest* 118:2111-2120.
65. Kemper K, MR Sprick, M de Bree, A Scopelliti, L Vermeulen, M Hoek, J Zeilstra, ST Pals, H Mehmet, G Stassi and JP Medema. (2010). The AC133 epitope, but not the CD133 protein, is lost upon cancer stem cell differentiation. *Cancer Res* 70:719-729.
66. Gires O. (2011). Lessons from common markers of tumor-initiating cells in solid cancers. *Cell Mol Life Sci* 68:4009-4022.
67. Diehn M and MF Clarke. (2006). Cancer stem cells and radiotherapy: new insights into tumor radioresistance. *J Natl Cancer Inst* 98:1755-1757.
68. Fillmore CM and C Kuperwasser. (2008). Human breast cancer cell lines contain stem-like cells that self-renew, give rise to phenotypically diverse progeny and survive chemotherapy. *Breast Cancer Res* 10:R25.
69. Minn AJ, Y Kang, I Serganova, GP Gupta, DD Giri, M Doubrovin, V Ponomarev, WL Gerald, R Blasberg and J Massague. (2005). Distinct organ-specific metastatic potential of individual breast cancer cells and primary tumors. *J Clin Invest* 115:44-55.
70. Uchino M, H Kojima, K Wada, M Imada, F Onoda, H Satofuka, T Utsugi and Y Murakami. (2010). Nuclear beta-catenin and CD44 upregulation characterize invasive cell populations in non-aggressive MCF-7 breast cancer cells. *BMC Cancer* 10:414.
71. Roesch A, M Fukunaga-Kalabis, EC Schmidt, SE Zabierowski, PA Brafford, A Vultur, D Basu, P Gimotty, T Vogt and M Herlyn. (2010). A temporarily distinct subpopulation of slow-cycling melanoma cells is required for continuous tumor growth. *Cell* 141:583-594.
72. Dembinski JL and S Krauss. (2009). Characterization and functional analysis of a slow cycling stem cell-like subpopulation in pancreas adenocarcinoma. *Clin Exp Metastasis* 26:611-623.
73. Mani SA, W Guo, MJ Liao, EN Eaton, A Ayyanan, AY Zhou, M Brooks, F Reinhard, CC Zhang, M Shipitsin, LL Campbell, K Polyak, C Brisken, J Yang and RA Weinberg. (2008). The epithelial-mesenchymal transition generates cells with properties of stem cells. *Cell* 133:704-715.
74. Ben-Porath I, MW Thomson, VJ Carey, R Ge, GW Bell, A Regev and RA Weinberg. (2008). An embryonic stem cell-like gene expression signature in poorly differentiated aggressive human tumors. *Nat Genet* 40:499-507.
75. Reya T and H Clevers. (2005). Wnt signalling in stem cells and cancer. *Nature* 434:843-850.
76. Turton NJ, DJ Judah, J Riley, R Davies, D Lipson, JA Styles, AG Smith and TW Gant. (2001). Gene expression and amplification in breast carcinoma cells with intrinsic and acquired doxorubicin resistance. *Oncogene* 20:1300-1306.
77. Qiu W, EB Carson-Walter, H Liu, M Epperly, JS Greenberger, GP Zambetti, L Zhang and J Yu. (2008). PUMA regulates intestinal progenitor cell radiosensitivity and gastrointestinal syndrome. *Cell Stem Cell* 2:576-583.

78. Eyler CE and JN Rich. (2008). Survival of the fittest: cancer stem cells in therapeutic resistance and angiogenesis. *J Clin Oncol* 26:2839-2845.
79. Bao S, Q Wu, RE McLendon, Y Hao, Q Shi, AB Hjelmeland, MW Dewhirst, DD Bigner and JN Rich. (2006). Glioma stem cells promote radioresistance by preferential activation of the DNA damage response. *Nature* 444:756-760.
80. Dekaney CM, AS Gulati, AP Garrison, MA Helmuth and SJ Henning. (2009). Regeneration of intestinal stem/progenitor cells following doxorubicin treatment of mice. *Am J Physiol Gastrointest Liver Physiol* 297:G461-470.
81. Merritt AJ, CS Potten, AJ Watson, DY Loh, K Nakayama and JA Hickman. (1995). Differential expression of bcl-2 in intestinal epithelia. Correlation with attenuation of apoptosis in colonic crypts and the incidence of colonic neoplasia. *J Cell Sci* 108 (Pt 6):2261-2271.
82. Naumov GN, JL Townson, IC MacDonald, SM Wilson, VH Bramwell, AC Groom and AF Chambers. (2003). Ineffectiveness of doxorubicin treatment on solitary dormant mammary carcinoma cells or late-developing metastases. *Breast Cancer Res Treat* 82:199-206.
83. Hambardzumyan D, OJ Becher, MK Rosenblum, PP Pandolfi, K Manova-Todorova and EC Holland. (2008). PI3K pathway regulates survival of cancer stem cells residing in the perivascular niche following radiation in medulloblastoma in vivo. *Genes Dev* 22:436-448.
84. Thames HD, AC Ruifrok, L Milas, N Hunter, KA Mason, NH Terry and RA White. (1996). Accelerated repopulation during fractionated irradiation of a murine ovarian carcinoma: downregulation of apoptosis as a possible mechanism. *Int J Radiat Oncol Biol Phys* 35:951-962.
85. Todaro M, M Perez Alea, A Scopelliti, JP Medema and G Stassi. (2008). IL-4-mediated drug resistance in colon cancer stem cells. *Cell Cycle* 7:309-313.
86. Thomadaki H and A Scorilas. (2006). BCL2 family of apoptosis-related genes: functions and clinical implications in cancer. *Crit Rev Clin Lab Sci* 43:1-67.
87. Ryan JA, JK Brunelle and A Letai. (2010). Heightened mitochondrial priming is the basis for apoptotic hypersensitivity of CD4+ CD8+ thymocytes. *Proc Natl Acad Sci U S A* 107:12895-12900.
88. Cory S and JM Adams. (2002). The Bcl2 family: regulators of the cellular life-or-death switch. *Nat Rev Cancer* 2:647-656.
89. Phillips TM, WH McBride and F Pajonk. (2006). The response of CD24(-/low)/CD44+ breast cancer-initiating cells to radiation. *J Natl Cancer Inst* 98:1777-1785.
90. Perucca P, O Cazzalini, M Madine, M Savio, RA Laskey, V Vannini, E Prosperi and LA Stivala. (2009). Loss of p21 CDKN1A impairs entry to quiescence and activates a DNA damage response in normal fibroblasts induced to quiescence. *Cell Cycle* 8:105-114.
91. Sage J, AL Miller, PA Perez-Mancera, JM Wysocki and T Jacks. (2003). Acute mutation of retinoblastoma gene function is sufficient for cell cycle re-entry. *Nature* 424:223-228.

92. Forsberg EC, E Passegue, SS Prohaska, AJ Wagers, M Koeva, JM Stuart and IL Weissman. (2010). Molecular signatures of quiescent, mobilized and leukemia-initiating hematopoietic stem cells. *PLoS ONE* 5:e8785.
93. Shimojo H, T Ohtsuka and R Kageyama. (2008). Oscillations in notch signaling regulate maintenance of neural progenitors. *Neuron* 58:52-64.
94. Liu S, G Dontu, ID Mantle, S Patel, NS Ahn, KW Jackson, P Suri and MS Wicha. (2006). Hedgehog signaling and Bmi-1 regulate self-renewal of normal and malignant human mammary stem cells. *Cancer Res* 66:6063-6071.
95. Horsley V, AO Aliprantis, L Polak, LH Glimcher and E Fuchs. (2008). NFATc1 balances quiescence and proliferation of skin stem cells. *Cell* 132:299-310.
96. Cheung ZH, K Gong and NY Ip. (2008). Cyclin-dependent kinase 5 supports neuronal survival through phosphorylation of Bcl-2. *J Neurosci* 28:4872-4877.
97. Wang CX, JH Song, DK Song, VW Yong, A Shuaib and C Hao. (2006). Cyclin-dependent kinase-5 prevents neuronal apoptosis through ERK-mediated upregulation of Bcl-2. *Cell Death Differ* 13:1203-1212.
98. Lin S, J Wang, Z Ye, NY Ip and SC Lin. (2008). CDK5 activator p35 downregulates E-cadherin precursor independently of CDK5. *FEBS Lett* 582:1197-1202.
99. Kesavapany S, KF Lau, DM McLoughlin, J Brownlees, S Ackerley, PN Leigh, CE Shaw and CC Miller. (2001). p35/cdk5 binds and phosphorylates beta-catenin and regulates beta-catenin/presenilin-1 interaction. *Eur J Neurosci* 13:241-247.
100. Plattner F, M Angelo and KP Giese. (2006). The roles of cyclin-dependent kinase 5 and glycogen synthase kinase 3 in tau hyperphosphorylation. *J Biol Chem* 281:25457-25465.
101. Bramblett GT, M Goedert, R Jakes, SE Merrick, JQ Trojanowski and VM Lee. (1993). Abnormal tau phosphorylation at Ser396 in Alzheimer's disease recapitulates development and contributes to reduced microtubule binding. *Neuron* 10:1089-1099.
102. Barker N, RA Ridgway, JH van Es, M van de Wetering, H Begthel, M van den Born, E Danenberg, AR Clarke, OJ Sansom and H Clevers. (2009). Crypt stem cells as the cells-of-origin of intestinal cancer. *Nature* 457:608-611.
103. Vermeulen L, EMF De Sousa, M van der Heijden, K Cameron, JH de Jong, T Borovski, JB Tuynman, M Todaro, C Merz, H Rodermond, MR Sprick, K Kemper, DJ Richel, G Stassi and JP Medema. (2010). Wnt activity defines colon cancer stem cells and is regulated by the microenvironment. *Nat Cell Biol* 12:468-476.
104. Lin H, JL Juang and PS Wang. (2004). Involvement of Cdk5/p25 in digoxin-triggered prostate cancer cell apoptosis. *J Biol Chem* 279:29302-29307.
105. Hsu FN, MC Chen, MC Chiang, E Lin, YT Lee, PH Huang, GS Lee and H Lin. (2011). Regulation of androgen receptor and prostate cancer growth by cyclin-dependent kinase 5. *J Biol Chem* 286:33141-33149.
106. Abbas T and A Dutta. (2009). p21 in cancer: intricate networks and multiple activities. *Nat Rev Cancer* 9:400-414.

107. Shen KC, H Heng, Y Wang, S Lu, G Liu, CX Deng, SC Brooks and YA Wang. (2005). ATM and p21 cooperate to suppress aneuploidy and subsequent tumor development. *Cancer Res* 65:8747-8753.
108. Jackson RJ, J Adnane, D Coppola, A Cantor, SM Sebti and WJ Pledger. (2002). Loss of the cell cycle inhibitors p21(Cip1) and p27(Kip1) enhances tumorigenesis in knockout mouse models. *Oncogene* 21:8486-8497.
109. Philipp J, K Vo, KE Gurley, K Seidel and CJ Kemp. (1999). Tumor suppression by p27Kip1 and p21Cip1 during chemically induced skin carcinogenesis. *Oncogene* 18:4689-4698.
110. Andre T, C Boni, M Navarro, J Tabernero, T Hickish, C Topham, A Bonetti, P Clingan, J Bridgewater, F Rivera and A de Gramont. (2009). Improved overall survival with oxaliplatin, fluorouracil, and leucovorin as adjuvant treatment in stage II or III colon cancer in the MOSAIC trial. *J Clin Oncol* 27:3109-3116.
111. Brewster AM, GN Hortobagyi, KR Broglio, SW Kau, CA Santa-Maria, B Arun, AU Buzdar, DJ Booser, V Valero, M Bondy and FJ Esteva. (2008). Residual risk of breast cancer recurrence 5 years after adjuvant therapy. *J Natl Cancer Inst* 100:1179-1183.
112. Jung Y and SJ Lippard. (2007). Direct cellular responses to platinum-induced DNA damage. *Chem Rev* 107:1387-1407.
113. Papamichael D. (1999). The use of thymidylate synthase inhibitors in the treatment of advanced colorectal cancer: current status. *Oncologist* 4:478-487.
114. Selleri S, F Arnaboldi, M Palazzo, U Hussein, A Balsari and C Rumio. (2005). Caveolin-1 is expressed on multipotent cells of hair follicles and might be involved in their resistance to chemotherapy. *Br J Dermatol* 153:506-513.
115. Kusumbe AP and SA Bapat. (2009). Cancer stem cells and aneuploid populations within developing tumors are the major determinants of tumor dormancy. *Cancer Res* 69:9245-9253.
116. Grimshaw MJ, L Cooper, K Papazisis, JA Coleman, HR Bohnenkamp, L Chiapero-Stanke, J Taylor-Papadimitriou and JM Burchell. (2008). Mammosphere culture of metastatic breast cancer cells enriches for tumorigenic breast cancer cells. *Breast Cancer Res* 10:R52.
117. Chikamatsu K, H Ishii, G Takahashi, A Okamoto, M Moriyama, K Sakakura and K Masuyama. (2011). Resistance to apoptosis-inducing stimuli in CD44+ head and neck squamous cell carcinoma cells. *Head Neck*.
118. Harper LJ, DE Costea, L Gammon, B Fazil, A Biddle and IC Mackenzie. (2010). Normal and malignant epithelial cells with stem-like properties have an extended G2 cell cycle phase that is associated with apoptotic resistance. *BMC Cancer* 10:166.
119. Quintana E, M Shackleton, MS Sabel, DR Fullen, TM Johnson and SJ Morrison. (2008). Efficient tumour formation by single human melanoma cells. *Nature* 456:593-598.
120. Moore N, J Houghton and S Lyle. (2011). Slow-Cycling Therapy-Resistant Cancer Cells. *Stem Cells Dev*.

121. Dhariwala FA and MS Rajadhyaksha. (2008). An unusual member of the Cdk family: Cdk5. *Cell Mol Neurobiol* 28:351-369.
122. Lopes JP and P Agostinho. (2011). Cdk5: multitasking between physiological and pathological conditions. *Prog Neurobiol* 94:49-63.
123. Chae T, YT Kwon, R Bronson, P Dikkes, E Li and LH Tsai. (1997). Mice lacking p35, a neuronal specific activator of Cdk5, display cortical lamination defects, seizures, and adult lethality. *Neuron* 18:29-42.
124. Schuman EM and S Murase. (2003). Cadherins and synaptic plasticity: activity-dependent cyclin-dependent kinase 5 regulation of synaptic beta-catenin-cadherin interactions. *Philos Trans R Soc Lond B Biol Sci* 358:749-756.
125. Wrobel G, P Roerig, F Kokocinski, K Neben, M Hahn, G Reifenberger and P Lichter. (2005). Microarray-based gene expression profiling of benign, atypical and anaplastic meningiomas identifies novel genes associated with meningioma progression. *Int J Cancer* 114:249-256.
126. Eggers JP, PM Grandgenett, EC Collisson, ME Lewallen, J Tremayne, PK Singh, BJ Swanson, JM Andersen, TC Caffrey, RR High, M Ouellette and MA Hollingsworth. (2011). Cyclin-dependent kinase 5 is amplified and overexpressed in pancreatic cancer and activated by mutant K-Ras. *Clin Cancer Res* 17:6140-6150.
127. Goodyear S and MC Sharma. (2007). Roscovitine regulates invasive breast cancer cell (MDA-MB231) proliferation and survival through cell cycle regulatory protein cdk5. *Exp Mol Pathol* 82:25-32.
128. Liu JL, XY Wang, BX Huang, F Zhu, RG Zhang and G Wu. (2011). Expression of CDK5/p35 in resected patients with non-small cell lung cancer: relation to prognosis. *Med Oncol* 28:673-678.
129. Li BS, W Ma, H Jaffe, Y Zheng, S Takahashi, L Zhang, AB Kulkarni and HC Pant. (2003). Cyclin-dependent kinase-5 is involved in neuregulin-dependent activation of phosphatidylinositol 3-kinase and Akt activity mediating neuronal survival. *J Biol Chem* 278:35702-35709.
130. Kang JS, CJ Lee, JM Lee, JY Rha, KW Song and MH Park. (2003). Follicular expression of c-Kit/SCF and inhibin-alpha in mouse ovary during development. *J Histochem Cytochem* 51:1447-1458.
131. Lopes JP, CR Oliveira and P Agostinho. (2009). Cdk5 acts as a mediator of neuronal cell cycle re-entry triggered by amyloid-beta and prion peptides. *Cell Cycle* 8:97-104.
132. Zhang J, SA Cicero, L Wang, RR Romito-Digiaco, Y Yang and K Herrup. (2008). Nuclear localization of Cdk5 is a key determinant in the postmitotic state of neurons. *Proc Natl Acad Sci U S A* 105:8772-8777.
133. Zhang J, H Li, T Zhou, J Zhou and K Herrup. (2012). Cdk5 levels oscillate during the neuronal cell cycle: Cdh1 ubiquitination triggers proteasome-dependent degradation during S-phase. *J Biol Chem*.
134. Dalerba P, SJ Dylla, IK Park, R Liu, X Wang, RW Cho, T Hoey, A Gurney, EH Huang, DM Simeone, AA Shelton, G Parmiani, C Castelli and MF Clarke. (2007). Phenotypic characterization of human colorectal cancer stem cells. *Proc Natl Acad Sci U S A* 104:10158-10163.

135. Huang EH, MJ Hynes, T Zhang, C Ginestier, G Dontu, H Appelman, JZ Fields, MS Wicha and BM Boman. (2009). Aldehyde dehydrogenase 1 is a marker for normal and malignant human colonic stem cells (SC) and tracks SC overpopulation during colon tumorigenesis. *Cancer Res* 69:3382-3389.
136. Vermeulen L, M Todaro, F de Sousa Mello, MR Sprick, K Kemper, M Perez Alea, DJ Richel, G Stassi and JP Medema. (2008). Single-cell cloning of colon cancer stem cells reveals a multi-lineage differentiation capacity. *Proc Natl Acad Sci U S A* 105:13427-13432.
137. Nagano O and H Saya. (2004). Mechanism and biological significance of CD44 cleavage. *Cancer Sci* 95:930-935.
138. Zeilstra J, SP Joosten, M Dokter, E Verwiel, M Spaargaren and ST Pals. (2008). Deletion of the WNT target and cancer stem cell marker CD44 in *Apc*(Min/+) mice attenuates intestinal tumorigenesis. *Cancer Res* 68:3655-3661.
139. Wielenga VJ, R Smits, V Korinek, L Smit, M Kielman, R Fodde, H Clevers and ST Pals. (1999). Expression of CD44 in *Apc* and *Tcf* mutant mice implies regulation by the WNT pathway. *Am J Pathol* 154:515-523.
140. Bauer N, AV Fonseca, M Florek, D Freund, J Jaszai, M Bornhauser, CA Fargeas and D Corbeil. (2008). New insights into the cell biology of hematopoietic progenitors by studying prominin-1 (CD133). *Cells Tissues Organs* 188:127-138.
141. Freund D, N Bauer, S Boxberger, S Feldmann, U Steller, G Ehninger, C Werner, M Bornhauser, J Oswald and D Corbeil. (2006). Polarization of human hematopoietic progenitors during contact with multipotent mesenchymal stromal cells: effects on proliferation and clonogenicity. *Stem Cells Dev* 15:815-829.
142. Zhang M, M Shoeb, J Goswamy, P Liu, TL Xiao, D Hogan, GA Campbell and NH Ansari. (2009). Overexpression of aldehyde dehydrogenase 1A1 reduces oxidation-induced toxicity in SH-SY5Y neuroblastoma cells. *J Neurosci Res* 88:686-694.
143. Ma I and AL Allan. (2010). The role of human aldehyde dehydrogenase in normal and cancer stem cells. *Stem Cell Rev* 7:292-306.
144. Szotek PP, R Pieretti-Vanmarcke, PT Masiakos, DM Dinulescu, D Connolly, R Foster, D Dombkowski, F Preffer, DT Maclaughlin and PK Donahoe. (2006). Ovarian cancer side population defines cells with stem cell-like characteristics and Mullerian Inhibiting Substance responsiveness. *Proc Natl Acad Sci U S A* 103:11154-11159.
145. Patrawala L, T Calhoun, R Schneider-Broussard, J Zhou, K Claypool and DG Tang. (2005). Side population is enriched in tumorigenic, stem-like cancer cells, whereas ABCG2+ and ABCG2- cancer cells are similarly tumorigenic. *Cancer Res* 65:6207-6219.
146. Kondo T, T Setoguchi and T Taga. (2004). Persistence of a small subpopulation of cancer stem-like cells in the C6 glioma cell line. *Proc Natl Acad Sci U S A* 101:781-786.
147. Haraguchi N, T Utsunomiya, H Inoue, F Tanaka, K Mimori, GF Barnard and M Mori. (2006). Characterization of a side population of cancer cells from human gastrointestinal system. *Stem Cells* 24:506-513.

148. Moserle L, M Ghisi, A Amadori and S Indraccolo. (2009). Side population and cancer stem cells: therapeutic implications. *Cancer Lett* 288:1-9.
149. Moore N and S Lyle. (2010). Quiescent, slow-cycling stem cell populations in cancer: a review of the evidence and discussion of significance. *J Oncol* 2011.
150. Kai K, O Nagano, E Sugihara, Y Arima, O Sampetrean, T Ishimoto, M Nakanishi, NT Ueno, H Iwase and H Saya. (2009). Maintenance of HCT116 colon cancer cell line conforms to a stochastic model but not a cancer stem cell model. *Cancer Sci*.
151. Yeung TM, SC Gandhi, JL Wilding, R Muschel and WF Bodmer. (2010). Cancer stem cells from colorectal cancer-derived cell lines. *Proc Natl Acad Sci U S A* 107:3722-3727.
152. Smith GH. (2005). Label-retaining epithelial cells in mouse mammary gland divide asymmetrically and retain their template DNA strands. *Development* 132:681-687.
153. Xin HW, DM Hari, JE Mullinax, CM Ambe, T Koizumi, S Ray, AJ Anderson, GW Wiegand, SH Garfield, SS Thorgeirsson and I Avital. (2012). Tumor-initiating label-retaining cancer cells in human gastrointestinal cancers undergo asymmetric cell division. *Stem Cells* 30:591-598.
154. Parish CR. (1999). Fluorescent dyes for lymphocyte migration and proliferation studies. *Immunol Cell Biol* 77:499-508.
155. Shapiro GI. (2006). Cyclin-dependent kinase pathways as targets for cancer treatment. *J Clin Oncol* 24:1770-1783.
156. Senderowicz AM, D Headlee, SF Stinson, RM Lush, N Kalil, L Villalba, K Hill, SM Steinberg, WD Figg, A Tompkins, SG Arbuck and EA Sausville. (1998). Phase I trial of continuous infusion flavopiridol, a novel cyclin-dependent kinase inhibitor, in patients with refractory neoplasms. *J Clin Oncol* 16:2986-2999.
157. Stadler WM, NJ Vogelzang, R Amato, J Sosman, D Taber, D Liebowitz and EE Vokes. (2000). Flavopiridol, a novel cyclin-dependent kinase inhibitor, in metastatic renal cancer: a University of Chicago Phase II Consortium study. *J Clin Oncol* 18:371-375.
158. Schwartz GK, D Ilson, L Saltz, E O'Reilly, W Tong, P Maslak, J Werner, P Perkins, M Stoltz and D Kelsen. (2001). Phase II study of the cyclin-dependent kinase inhibitor flavopiridol administered to patients with advanced gastric carcinoma. *J Clin Oncol* 19:1985-1992.
159. Rathkopf D, MA Dickson, DR Feldman, RD Carvajal, MA Shah, N Wu, R Lefkowitz, M Gonen, LM Cane, HJ Dials, JL Winkelmann, GJ Bosl and GK Schwartz. (2009). Phase I study of flavopiridol with oxaliplatin and fluorouracil/leucovorin in advanced solid tumors. *Clin Cancer Res* 15:7405-7411.
160. Gorlick R, EA Kolb, PJ Houghton, CL Morton, G Neale, ST Keir, H Carol, R Lock, D Phelps, MH Kang, CP Reynolds, JM Maris, C Billups and MA Smith. (2012). Initial testing (stage 1) of the cyclin dependent kinase inhibitor SCH 727965 (dinaciclib) by the pediatric preclinical testing program. *Pediatr Blood Cancer*.
161. Hassan M, H Sallam and Z Hassan. (2011). The Role of Pharmacokinetics and Pharmacodynamics in Early Drug Development with reference to the Cyclin-

dependent Kinase (Cdk) Inhibitor - Roscovitine. Sultan Qaboos Univ Med J 11:165-178.

162. Dickson MA and GK Schwartz. (2009). Development of cell-cycle inhibitors for cancer therapy. Curr Oncol 16:36-43.